The Role of Peroxisomes in Oxidative Stress

De rol van peroxisomen in oxidatieve stress

(met een samenvatting in het Nederlands)

Proefschrift

ter verkrijging van de graad van doctor aan de Universiteit Utrecht op gezag van de Rector Magnificus, Prof.Dr. W. H. Gispen, ingevolge het besluit van het College van Promoties in het openbaar te verdedigen op donderdag 27 september 2001 des namiddags te 2:30 uur

door

Tobias Bas Dansen

geboren op 6 november 1973 te Rotterdam

# Table of contents

List of Abbreviations

BCFA	branched chain fatty acid
BODIPY	4,4-difluoro-4-bora-3a,4a-diaza-s-indacene-3-propionyl
BSA	bovine serum albumin
CCCP	carbonyl m-chlorophenylhydrazone
CHO	chinese hamster ovary
Cu,ZnSOD	copper, zinc superoxidedismutase
Cy3/Cy5	cyanine dye
DBE	Daf-16 binding element
DHAP	dihydroxyacetonephosphate
D-PBE	D-specific peroxisomal bifunctional enzyme
ER	endoplasmic reticulum
FABP	fatty acid binding protein
FAD	flavin adenine dinucleotide
(F)FA	(free) fatty acid
FRET	fluorescence resonance energy transfer
GFP	green fluorescent protein
GPx	glutathione peroxidase
MDR	multidrug resistance
MEF	mouse epithelial fibroblast
MnSOD	manganese superoxidedismutase
NAD	nicotinamide adenine dinucleotide
N-ALD	neonatal adrenoleukodystrophy
NLS	nuclear localization signal
nsLTP	non-specific lipid-tranfer protein (identical to SCP2)
PBD	peroxisome biogenesis disorder
PDK1	$PI(3,4,5)P_3$ dependent kinase
PI3K	phosphatidyl-inositol 3-OH kinase
PI-3P	phosphatidyl-inositol 3-phosphate
PKB	protein kinase B (identical to Rac and Akt)
PMP	peroxisomal membrane protein
PP	peroxisome proliferator
PPAR	peroxisome proliferator activated receptor
PPRE	peroxisome proliferator responsive element
PtdChol	phosphatidylcholine
PtdEtOH	phosphatidylethanolamine
PTEN	phosphatase and tensin homologue on chromosome 10
PTS	peroxisomal targeting sequence
PUFA	poly-unsaturated fatty acid
RCDP	rhizomelic chondrodysplasia punctata
ROS	reactive oxygen species
SCPx/SCP2	sterol carrier protein x/2
SNAFL	semi-naphto-fluorescein
TBARS	total barbituric acid reactive substances
TGN	trans-Golgi network
THCA	trihydroxycholestanoic acid
TLC	thin layer chromatography
VLCFA	very-long-chain fatty acid
ZS	Zellwegers' cerebro-hepato-renal syndrome
4OHT	4-hydroxy-tamoxifen

General Introduction.
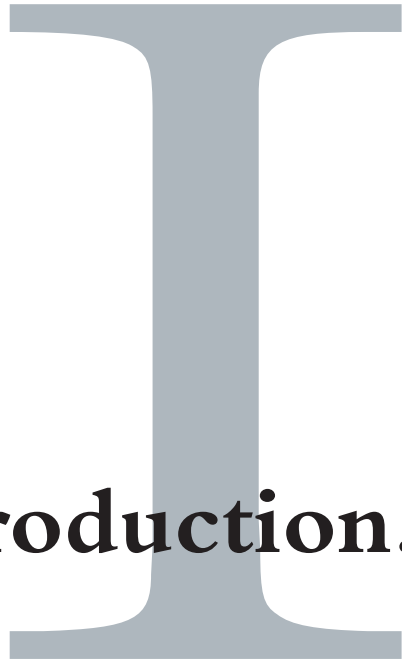
Introduction

Fatty acids play several important roles in the human body. First of all, they are the building blocks of lipids. The membranes, that ensure the compartmentalization of physiological processes in the cell, are made up of lipids. Furthermore, signal molecules and hormones involved in virtually every process in the cell, from proliferation to cell death, can be derived from fatty acids. And last but not unimportantly, fatty acids enable the body to store large amounts of energy in a relatively small mass in the form of triacylglycerols. Fatty acids undergo different metabolic processes before they can be used by the body. Most fatty acids are degraded in the mitochondria, but these organelles can only handle straight chain fatty acids up to sixteen carbon atoms. Longer acyl chains and some other special fatty acids are degraded in the peroxisomes. During the breakdown of fatty acids oxygen is consumed, which may lead to the formation of reactive oxygen species. These highly reactive compounds with at least one oxygen atom that contains an unpaired electron can attack several biomolecules including proteins, lipids and DNA. Reactive oxygen species have been implicated in many processes like carcinogenesis, Alzheimers disease and aging. Peroxisomes have an elaborate anti-oxidant defense system. In this thesis more insight is given in the functioning of the peroxisome and its involvement in the formation and detoxification of reactive oxygen species.

Peroxisomes

The peroxisome was the last true organell to be discovered. It was first described by Rhodin, who identified the new compartment by EM and called it microbody (1). De Duve and Baudhuin performed the biochemical characterization and introduced the name "peroxisome" because of the oxidase and hydrogen peroxide consuming properties of this organelle (2). It took ten more years before it was found that the peroxisome was capable of degrading fatty acids (3). First it was believed that the peroxisome was a redundant organelle: a remainder of a fatty acid degrading compartment from a pre-mitochondrial era. In the early seventies however, Goldfischer discovered that peroxisomes were absent in the liver of Zellweger patients (4). Ten years later Brown and Heymans established that in these patients very-long chain fatty acids accumulated in the plasma (5) and plasmalogens were absent (6). This was the first observation indicating that proper cellular functioning is impossible without peroxisomes. To date, more than twenty inherited peroxisomal disorders, that are often lethal at early age, have been characterized (7-9). The peroxisome is involved in a number of unique enzymatic reactions, including the breakdown of very-long chain and branched chain fatty acids, and cholesterol- and etherphospholipid biosynthesis (10).

Peroxisome Biogenesis
The biogenesis of peroxisomes has been extensively studied and the latest models involve a multistep assembly of the organelle (11, 12): a process that involves at least 23 peroxisome biogenesis proteins, or peroxins (Pexs), see table 1. As shown in figure 1, the first step involves the insertion of Pex3p and Pex16p in a membranous structure that possibly derives form the ER (13), (although this is questioned by other groups (11)). This insertion is possibly facilitated by Pex19p, yielding a peroxisomal membrane protein (PMP) import competent peroxisome. Subsequently a number of PMPs including Pex10p, Pex12p, Pex13p, Pex14p and Pex17p are directed to the PMP-import competent peroxisome, by virtue of Pex19p that

Table 1: The human peroxins and their interactions

| Peroxin	Protein interactions	Notes
Pex1p	Pex6p	AAA ATPase, required for matrix protein import.
Pex2p		C3CH4 zinc-binding integral PMP required for matrix protein import.
Pex3p	Pex19p	Integral PMP required for membrane biogenesis.
Pex4p	Pex22p	E2 ubiquitin-conjugating enzyme required for matrix protein import.
Pex5p	Pex7p, Pex14p, Pex13p, Pex10p, Pex12p, PTS1-proteins	PTS1 receptor, required for both PTS1- and PTS2-mediated import.
Pex6p	Pex1p	AAA ATPase, required for matrix protein import.
Pex7p	Pex5p, Pex14p, Pex13p, PTS2-proteins	PTS2 receptor, required for PTS2-mediated import.
Pex8p	Pex5p	integral PMP required for matrix protein import.
Pex9p	n.d.	integral PMP required for matrix protein import.
Pex10p	Pex12p, Pex5p, Pex19p	C3CH4 zinc-binding integral PMP required for matrix protein import.
Pex11p	Pex19p	PMP involved in peroxisome proliferation.
Pex12p	Pex10p, Pex5p, Pex19p	C3CH4 zinc-binding integral PMP required for matrix protein import.
Pex13p	Pex5p, Pex7p, Pex14p, Pex19p	SH3 containg PMP required for matrix protein import.
Pex14p	Pex5p, Pex7p, Pex13p, Pex17p, Pex19p	PMP required for matrix protein import: the receptor docking site.
Pex15p	n.d.	PMP require for matrix protein import.
Pex16p	Pex19p	Integral PMP required for membrane biogenesis.
Pex17p	Pex14p, Pex19p	PMP required for matrix protein import
Pex18p	Pex7p	Required for PTS2-mediated import
Pex19p	Multiple PMPs	Involved in PMP import
Pex20p	Thiolase	Thiolase import in Y. lipolytica
Pex21p	Pex7p	Required for PTS2-mediated import
Pex22p	Pex4p, Pex19p	PMP required for matrix protein import
Pex23p	n.d.	PMP required for matrix protein import

Table adapted form Sacksteder & Gould (11).

docks onto Pex3p. In this way the matrix–protein import machinery is assembled yielding a matrix–protein import competent peroxisome. In this stadium the peroxisome may either first undergo Pex11p mediated peroxisome division and subsequently import matrix proteins to become a mature peroxisome, or mature first and then divide. This model is depicted in figure 1.
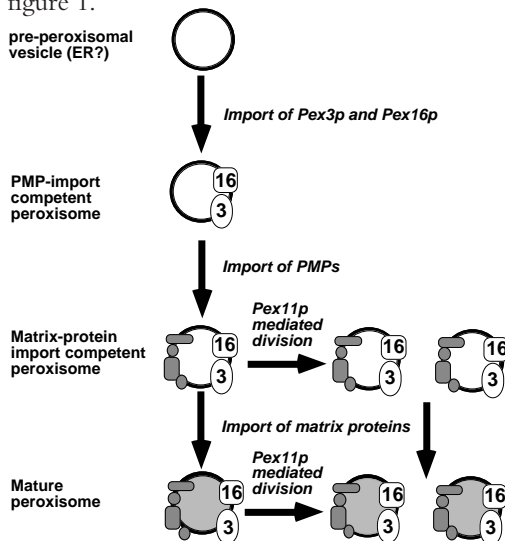
Figure 1: Biogenesis of peroxisomes involves a multistep process. A mebranous structure, which is possibly deriving of or part of the ER is first made PMP import competent by insertion of Pex3p and Pex16p. The other PMPs including a number of peroxins that are part of the matrix-protein import machinery are then transported to the peroxisome most probably by Pex19p which is able to dock onto Pex3p. When the import machinery is present, the peroxisome is matrix protein import competent. The peroxisome matures by the import of the matrix-proteins required for the peroxisomal functions. The peroxisome can divide with help of Pex11p. Figure adapted from Sacksteder, K.A., and Gould, S.J., Annu. Rev. Genet. 2000 34:623-652
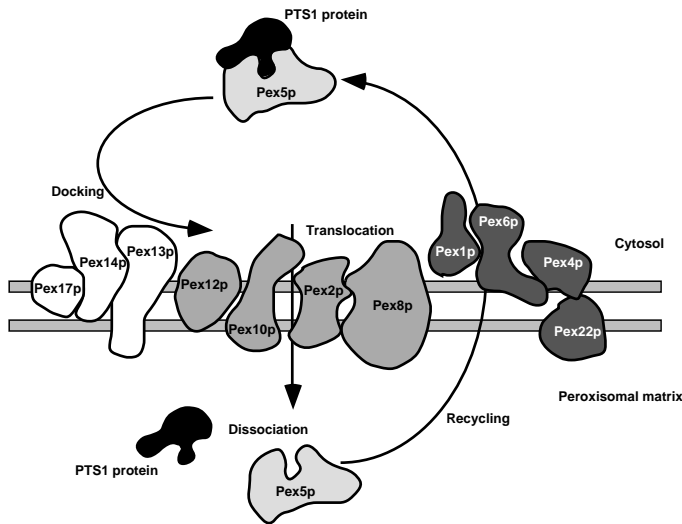
Figure 2: PTS1-mediated Peroxisomal matrix protein import. Peroxisomal matrix-proteins are synthesized in the cytosol. Cytosolic receptors can bind to a peroxisomal targeting signal in these proteins (Pex5p for PTS1 and Pex7p for PTS2). Only the import of PTS1 proteins is depicted. After binding to the receptor, the complex of Pex5p and the protein docks on Pex14p. The complex of Pex5p and the PTS1 protein is sub-sequently translocated over the peroxisomal membrane. Pex2p, Pex10p and Pex12p are thought to be involved in the translocation. Pex8p could be involved in the dissociation of proteins from Pex5p since it has a PTS1, which is not required for the targeting of Pex8p to the membrane of the peroxisome. Pex1p and Pex6p are believed to be involved in recycling of Pex5p to the cytosol, probably with help of Pex4p and Pex22p.

Matrix protein import

Matrix proteins are imported via at least two distinct pathways, depending on the targeting sequence in the protein. The majority of matrix enzymes is imported via a peroxisomal targeting sequence of type 1 (PTS1) which comprises a C-terminal (C/A/S)-(K/R/H)-(L/I) (14). This sequence is recognized by Pex5p which is a cytosolic receptor (15). The PTS1-protein/Pex5p complex docks onto Pex14p (16) and is imported in a folded state (17). Pex5p is then released and shuttled back into the cytosol. A similar mechanism is only found in nucleocytoplasmic protein import (18). The import of complexed folded proteins is remarkable since earlier experiments describe the impermeable nature of the peroxisomal membrane (19, 20). Peroxisomal targeting via PTS2 applies to matrix proteins containing (R/K)-L-XXXXX-(H/Q)-L near the N-terminus (21). This sequence is recognized by Pex7p (22), a cytosolic receptor like Pex5p. PTS2-mediated import is also dependent on Pex5p which binds to the complex of the PTS2 protein and Pex7p. However, PTS1 mediated protein import is independent of Pex7p (11). Figure 2 illustrates peroxisomal matrix protein import.

Peroxisome Biogenesis Disorders

In the peroxisomal biogenesis disorders (PBDs), peroxisomal function is completely or partially lost due to a defect in either the biogenesis of the entire peroxisome or a defect in one or both of the matrix protein import pathways. Most peroxisomal matrix enzymes are instable or inactive in the cytosol resulting in loss of function, stressing the importance of compartmentlization of the peroxisomal processes. Patients with a genetic defect in *pex3*, *pex16* or *pex19* lack detectable peroxisomal membranes completely. The phenotype of these patients is Zellwegers' cerebro-hepato-renal syndrome (ZS). The same phenotype is observed in patients that do have detectable peroxisomal membrane structures (so called ghosts) but due to a genetic defect in the pex-genes encoding parts of the import machinery, cannot import PTS1 and PTS2 proteins. Patients with an isolated defect in PTS2-mediated protein

import have Rhizomelic Chondrodysplasia Punctata (RCDP) type 1. These patients lack the peroxisomal functions that depend on PTS2 proteins, which is the case for amongst others ether-phospholipid biosynthesis and phytanic acid breakdown. Some patients have been characterized with an isolated defect in PTS1-mediated import, displaying a Neonatal-Adrenoleukodystropy (N-ALD) phenotype. There are also a number of peroxisomal disorders that are caused by a genetic defect in one of the matrix enzymes. Depending on the enzyme, the phenotype may be similar to a PBD phenotype. This is the case for acyl-CoA oxidase deficiency (pseudo-ZS) and for defects in dihydroxyacetonephosphate acyltransferase (RCDP type 2) or alkyl-dihydroxyacetone-phosphate synthase (RCDP type 3)
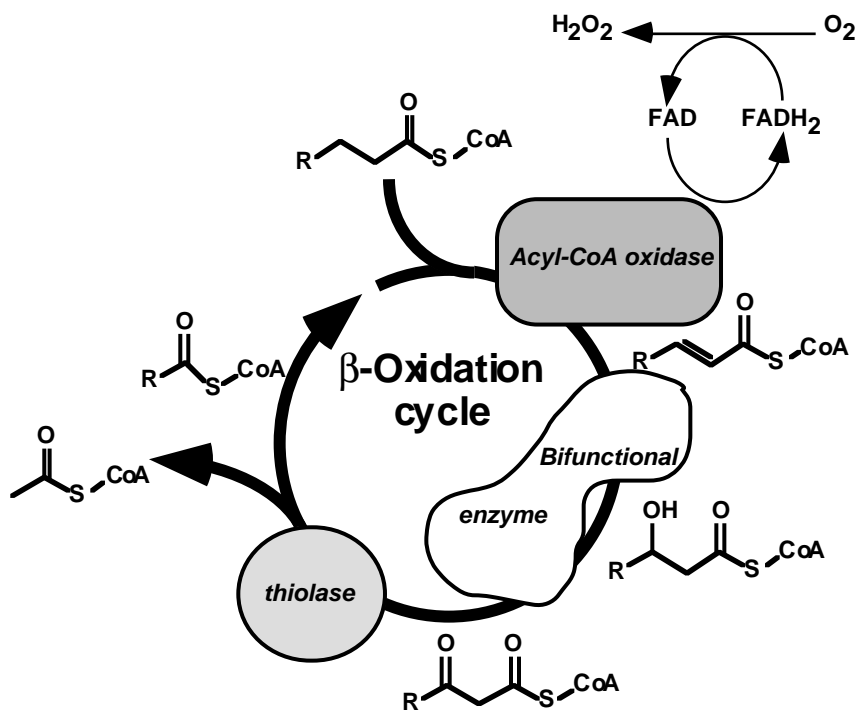

Figure 3: The peroxisomal β-oxidation cycle. During the peroxisomal β-oxidation of fatty acids, two carbon atoms are cleaved off from a fatty acid in a 4 step reaction. In short, Acyl-CoA oxidase introduces a double bond, which is subsequently hydrated and dehydrogenated by the bifunctional enzyme. Thiolase splits of acetyl-CoA and transfers the remainder of the fatty acid to a new CoA molecule. The cycle repeats until the acyl chain becomes too short for acyl-CoA oxidase. Hydrogen peroxide is formed in the oxidase step via FAD which is part of acyl-CoA oxidase.

Peroxisomal fatty acid breakdown

Fatty acids that are degraded in the peroxisome have to be activated first by fatty acyl-CoA synthases to yield fatty-acyl-CoA esters. The degradation of these fatty-acyl-CoA esters in peroxisomes can be divided into three processes. 1) Fatty acid β-oxidation; substrates are oxidized at the β-carbon resulting in a substrate that is two carbon atoms shorter. 2) Fatty acid α-oxidation; substrates that have a methyl group at the γ-position are oxidized at the α-position to yield a substrate with a methyl group at the β-position. 3) The auxiliary β-oxidation; the interconversion of (poly-)unsaturated fatty acids into Δ^2-fatty acids which can be oxidized further by the β-oxidation pathway. The reactions of the β-oxidation are depicted in figure 3. The reactions of the auxiliary β-oxidation are outlined in chapter 2 of this thesis.

Typical substrates for the peroxisomal fatty acid β-oxidation are very-long chain fatty acids (VLCFAs), branched chain fatty acids (BCFAs) and the bile acid intermediates di- and trihydroxycholestanoic acid. Other substrates like poly-unsaturated fatty acids (PUFAs), dicarboxylic acid as well as some prostaglandins, leukotrienes and thromboxans are oxidized in the peroxisome, but it is a matter of discussion whether this happens exclusively in this organelle. BCFAs have their own set of β–oxidation enzymes which are also used for the processing of the bile acid intermediates. These enzymes and their reactions are shown in figure 4.

Unlike the mitochondrial fatty acid β-oxidation, the peroxisomal β-oxidation does not go to completion. This is due to the substrate specificity of the peroxisomal acyl-CoA oxidase. Fatty acyl-CoA esters that cannot be further degraded in the peroxisome are transported to the mitochondria for further processing in a carnitin dependent way. In contrast to the mitochondrial β-oxidation, breakdown of fatty acids in the peroxisome does not contribute to ATP formation. For a review on fatty acid breakdown see Kunau or Wanders *et al.* (23, 24).
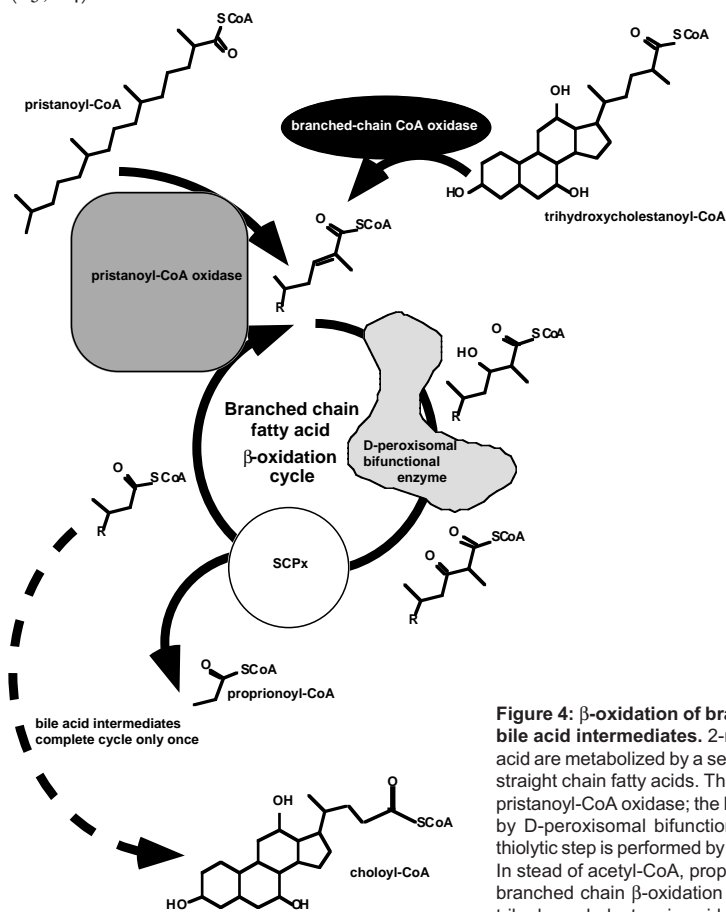
Figure 4: β**-oxidation of branched chain fatty acids and bile acid intermediates.** 2-methyl fatty acids like pristanic acid are metabolized by a separate subset of enzymes than straight chain fatty acids. The double bond is introduced by pristanoyl-CoA oxidase; the hydration and dehydrogenation by D-peroxisomal bifunctional enzyme (D-PBE) and the thiolytic step is performed by sterol-carrier-protein x (SCPx). In stead of acetyl-CoA, proprionyl-CoA is cleaved off in the branched chain β-oxidation cycle. The bile acid precursor trihydroxycholestanoic acid is oxidized by branched-chain CoA oxidase and subsequently proprionyl-CoA is cleaved off by the actions of D-PBE and SCPx. The then formed choloyl-CoA leaves the β-oxidation cycle and is conjugated to glycine or taurine to yield bile acids.

The Sterol Carrier Protein

In 1977 a protein was purified from the membrane-free supernatant of rat and bovine liver (25). This protein of 12 kDa was able to catalyze the transfer of various phospholipids and cholesterol *in vitro* (for a review see Wirtz *et al.* (26, 27)). This wide range of substrate transport led to the name non-specific lipid-transfer protein (nsLTP). In the same time, it was shown by Scallen *et al.* that the sterol carrier protein 2 (SCP2) was able to stimulate a number of reactions in cholesterol metabolism including cholesterol esterification, bile acid formation and hormone synthesis (28). It turned out that nsLTP and SCP2 were the same protein. In this thesis the name SCP2 will be used. It was reported recently that SCP2 could bind fatty acids and especially their CoA esters with much higher affinity than sterols and phospholipids (29). Using antibodies raised against SCP2, a 58 kDa cross reactive protein was found. Later studies showed that this 58 kDa protein contains the entire SCP2 sequence at its C-terminus and was named SCPx (30, 31). Both sterol carrier proteins are encoded by the *scp* gene, which consists of 16 exons. This gene contains two promoters; one upstream of the gene, and a second one within intron 11 (32). When transcribed from the first promoter, mRNAs encoding the full length SCPx are formed, whereas transcription from the second promoter yields the 14 kDa pre-SCP2. SCPx can be cleaved *in vivo* to form a 46 kDa protein and the 12 kDa SCP2. The 46 kDa protein was shown to be a 3-oxoacyl-CoA thiolase, that catalyzes the final steps in the peroxisomal breakdown of branched-chain fatty acids and is involved in formation of bile-acids. Its main substrates are therefore 3-keto-pristanoyl-CoA and 3α,7α,12α-trihydroxy-24-ketocholestanoyl-CoA (24-keto-THC-CoA) (33, 34) (see figure 4). The C-terminus of SCPx/SCP2 contains a PTS1 (AKL). Wouters *et al.* showed that SCP2 interacted with the peroxisomal β-oxidation complex (35). Since the full length SCPx is exclusively found in the peroxisome, the processing into the 46 kDa thiolase and SCP2 must take place in the matrix of this organelle (36). Seedorf *et al.* made an *scp* null mouse which was used to study the *in vivo* function of SCPx/SCP2. These mice showed no defects in their cholesterol homeostasis. Yet, these mice are impaired in the peroxisomal β-oxidation of BCFAs and have impaired bile-acid formation (27, 33). Both these defects can be explained with the absence of SCPx-thiolase activity. The physiological role of SCP2 remains to be established. In this thesis the substrate specificity of SCP2 is discussed. Furthermore, data are presented suggesting a role for SCP2 in the cellular defense against lipid peroxidation by free radicals.

The PI-3-OH-kinase/PKB/Forkhead signalling pathway

Signals a cell senses via receptors at its plasma-membrane have to be transduced to the nucleus to make the cell respond by, for instance, transcription of a gene. In this way, the cell balances its need for proliferation, apoptosis, induction of certain metabolic pathways and so on by several signalling pathways (for a review see (37)). One of these signalling cascades is mediated via phosphatidylinositol-3-OH-kinase (PI3K). This pathway has been implicated in several cellular processes including metabolism, protein translation, cell survival and cell-cycle regulation (38, 39). When receptor tyrosine kinases like the insulin receptor or the platelet derived growth factor receptor bind their ligand, these receptors become autophosphorylated on tyrosine residues creating a docking site. Dependent on the receptor, PI3K can bind to this site either directly or via an adaptor protein, whereupon it becomes activated. Alternatively, PI3K can be activated via Ras, which is activated via receptor tyrosin kinases (40). Active
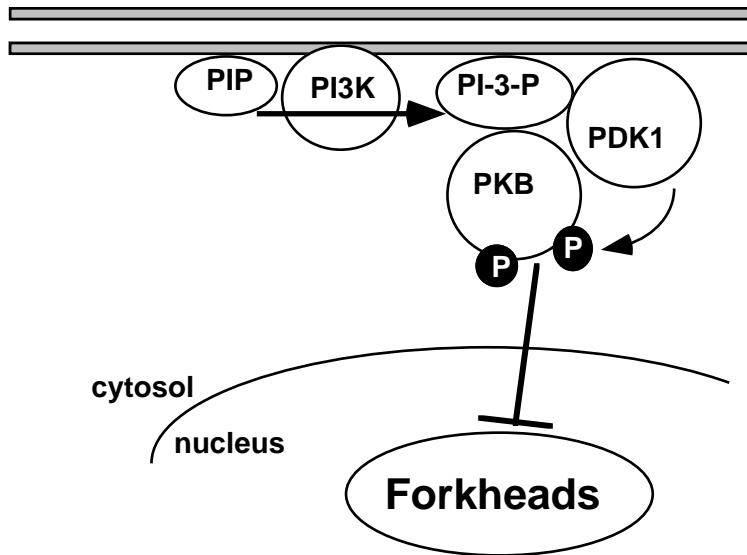
Figure 5: PI3K/PKB/ Forkhead signalling. PI3K, which can be activated by receptor tyrosine kinases mediates the phosphorylation of PIP to PI-3P which can bind proteins to their PH domain. In this way PDK1 and PKB are recruted to the mebrane. There, PDK activates PKB by phosphorylation. Active PKB dissociates form the membrane and phosphorylates Forkhead transcription factors in the nucleus, thereby inactivating them.

PI3K at the plasmamembrane phosphorylates phosphoinositides (PIP) at the 3'OH position forming $PI(3,4)P_2$ and $PI(3,4,5)P_3$. These PI-3Ps are known to act as second messengers in signal transduction. Formation of these 3'OH PI-3Ps leads to (amongst others) the recruitment of phosphokinase B (PKB) to the plasma membrane by binding of these lipid-messengers to the pleckstrin homology (PH) domain of this protein (41, 42). PKB becomes phosphorylated at S473 and T308. The threonine-phosphorylation is catalyzed by the $PI(3,4,5)P_3$ –dependent kinase-1 (PDK1) that is activated via PI3K (43-45). The kinase that performs the serine-phosphorylation still has to be identified. The phosphorylation of PKB can be blocked by PTEN (phosphatase and tensin homologue on chromosome 10), which dephosphorylates the 3-OH PI-3Ps. Deregulation of PTEN has been shown to occur in many cancers, implying a role for PI3K signalling in tumor formation (46). Phosphorylated PKB is released from the plasma membrane and can phosphorylate several targets in the cell. One of these targets is the AFX-like Forkhead transcription factors (47). The regulation of these transcripiton factors via the PI3K pathway was first established in the nematode *C.elegans*. It was discovered that this organism can increase its lifespan by going into a so called Dauer-stage hereby downregulating its metabolism until metabolites are available. During the dauerstage, the worm upregulates protection form external stresses, thereby increasing its lifespan up to ten times. The Dauer formation is dependent on the Daf-16 transcription factor: the *C.elegans* homologue of the forkhead transcription factors. Daf-16 is negatively regulated via Age-1 and Akt, PI3K and PKB homologues respectively (48, 49). It was shown recently that in mammalian cells the daf-16 like forkhead transcription factors AFX, FKHR and FKHR-L1 are also negatively regulated via PI3K and PKB (see figure 5). When these Forkheads become phosphorylated by PKB, they localize mainly in the cytosol where they cannot activate genetranscription. Targets for the Daf-16 like Forkhead transcription factors are the apotosis pro-

moting Bim (50) and FasL (51). Recently it was described that the Forkheads play a role in G1 cell-cycle arrest in some tumor cells (52). In *C.elegans* it was shown that MnSOD and catalase are upregulated via Daf-16, suggesting that the maintenance of the cellular radical balance is important in the increase of the lifespan (53). In this thesis data are presented that over expression of a Daf-16 like forkhead transcription factor in mammalian cells increases MnSOD and catalase protein levels. Furthermore, evidence is presented that SCPx/SCP2 is regulated via Forkheads.

Scope of this thesis

The peroxisome is a cellular site of both generation and degradation of reactive oxygen species. It is not clear to what extent this organelle plays a role in the overall cellular oxidative state. *Chapter 2* reviews these processes. The fragility of the peroxisome makes it difficult to study its physiological processes without disrupting its membrane. In this thesis, a new method is presented to measure biophysical properties in the peroxisome of living cells. This method makes use of fluorescently labelled peptides that cross the plasma membrane by diffusion. The peptide contains a PTS1, and thus is transported and imported into the peroxisome via the matrix-protein import mechanism. Using such a probe we were able to measure the pH of the peroxisomal matrix by fluorescence ratio-imaging (*Chapter 3*). The possibilities which the targeted peptide based fluorescent probes will offer in studying peroxisomes is discussed in *Chapter 4* . *Chapter 5* is giving more details about the synthesis and application of these probes in peroxisome research. *Chapter 6* describes the development of peptide-based probes for other organelles like the Golgi, the ER and the nucleus thereby extending the possibilities of these new class of probes. Sterol Carrier Protein 2 has high binding affinity for fatty acyl-CoA esters as is described in *Chapter 7*. We showed that this protein binds to VLCFA-CoA esters and their enoyl-derivatives. *Chapter 8* describes the regulation of the radical scavenging enzymes MnSOD and catalase by the PI3K/PKB pathway through the daf-16 like Forkhead transcription factors, and in *Chapter 9* we show that SCPx/SCP2 is also regulated by this pathway. In line with the upregulation of the other anti-oxidant enzymes by the Forkheads, we show that SCP2 can protect a fluorescent fatty acid analogue from oxidation by radicals. In *Chapter 10* the findings presented in this thesis are discussed and a model is proposed for the anti-oxidant function of sterol carrier protein, as well as for the possible role of the peroxisome in defense against cellular oxidative stress.

References

(1)   Rhodin, J. (1954) Correlation of ultrastructural organization and function in normal and experimen-tally changed proximal tubule cells of the mouse kidney. *PhD. Thesis, Karolinska Institutet Stockholm, Sweden.*

(2)   de Duve, C., Baudhuin, P. (1966) Peroxisomes (microbodies and related particles). *Physiol. Rev.* **46**,323-357.

(3)   Lazarow, P. B., De Duve, C. (1976) A fatty acyl-CoA oxidizing system in rat liver peroxisomes; enhancement by clofibrate, a hypolipidemic drug. *Proc Natl Acad Sci U S A.* **73**,2043-2046.

(4)   Goldfischer, S., Moore, C.L., Johnson, A.B., Spiro, A.J., Valsamis, M.P., Wisniewski, H.K., Ritch, R.H., Norton, W.T., Rapin, I., Gartner, L.M. (1973) Peroxisomal and mitochondrial defects in the cerebro-hepato-renal syndrome. *Science.* **182**,62-64.

(5)   Brown, F.R., Van Duyn, M.A., Moser, A.B., Schulman, J.D., Rizzo, W.B., Snyder, R.D., Murphy, J.V., Kamoshita, S., Migeon, C.J., Moser, H.W. (1982) Adrenoleukodystrophy: effects of dietary re-striction of very long chain fatty acids and of administration of carnitine and clofibrate on clinical status and plasma fatty acids. *Johns Hopkins Med J.* **151**,164-172.

(6)   Heymans, H.S., Schutgens, R.B., Tan, R., van den Bosch, H., Borst, P. (1983) Severe plasmalogen deficiency in tissues of infants without peroxisomes (Zellweger syndrome). *Nature.* **309**,69-70.

(7)   Wanders, R. J., Tager, J.M. (1998) Lipid metabolism in peroxisomes in relation to human disease. *Mol Aspects Med.* **19**,69-154.

(8)   Wanders, R.J. (1999) Peroxisomal disorders: clinical, biochemical, and molecular aspects. *Neurochem Res.* **24**,565-580.

(9)   Gould, S.J., Valle, D. (2000) Peroxisome biogenesis disorders, genetics and cell biology. *Trends Genet.* **16**,340-345.

(10)   van den Bosch, H., Schutgens, R.B., Wanders, R.J., Tager, J.M. (1992) Biochemistry of peroxisomes. *Annu Rev Biochem.* **61**,157-197.

(11)   Sacksteder, K.A., Gould, S.J. (2000) Genetics of peroxisome biogenesis. *Annu Rev Genet.* **34**,623-652.

(12)   Titorenko, V. I., Rachubinski, R.A. (2001) Dynamics of peroxisome assembly and function. *Trends Cell Biol.* **11**,22-29.

(13)   Titorenko, V.I., Rachubinski, R.A. (1998) The endoplasmic reticulum plays an essential role in per-oxisome biogenesis. *Trends Biochem Sci.* **23**,231-233.

(14)   Gould, S. J., Keller, G.A., Hosken, N., Wilkinson, J., Subramani, S. (1989) A conserved tripeptide sorts proteins to peroxisomes. *J Cell Biol.* **108**,1657-1664.

(15)   Dodt, G., Braverman, N., Wong, C., Moser, A., Moser, H.W., Watkins, P., Valle, D., Gould, S.J. (1995) Mutations in the PTS1 receptor gene, PXR1, define complementation group 2 of the peroxi-some biogenesis disorders. *Nat Genet.* **9**,115-125.

(16)   Schliebs, W., Saidowsky, J., Agianian, B., Dodt, G., Herberg, F.W., Kunau, W.H. (1999) Recombinant human peroxisomal targeting signal receptor PEX5. Structural basis for interaction of PEX5 with PEX14. *J Biol Chem.* **274**,5666-5673.

(17)   Dammai, V., Subramani, S. (2001) The Human Peroxisomal Targeting Signal Receptor, Pex5p, Is Translocated into the Peroxisomal Matrix and Recycled to the Cytosol. *Cell.* **105**,187-196.

(18)   Smith, M.D., Schnell, D.J. (2001) Peroxisomal protein import. the paradigm shifts. *Cell.* **105**,293-296.

(19)   van der Klei, I.J., Veenhuis, M. (1997) Yeast peroxisomes: function and biogenesis of a versatile cell organelle. *Trends Microbiol.* **5**,502-509.

(20)   van Roermund, C.W., Elgersma ,Y., Singh, N., Wanders, R.J., Tabak, H.F. (1995) The membrane of peroxisomes in Saccharomyces cerevisiae is impermeable to NAD(H) and acetyl-CoA under *in vivo* conditions. *EMBO J.* **14**,3480-3486.

(21)   Swinkels, B. W., Gould, S.J., Bodnar, A.G., Rachubinski, R.A., Subramani, S. (1991) A novel, cleav-able peroxisomal targeting signal at the amino-terminus of the rat 3-ketoacyl-CoA thiolase. *EMBO J.* **10**,3255-3262.

(22)   Rehling, P., Marzioch, M., Niesen, F., Wittke, E., Veenhuis, M., Kunau, W.H. (1996) The import receptor for the peroxisomal targeting signal 2 (PTS2) in Saccharomyces cerevisiae is encoded by the PAS7 gene. *EMBO J.* **15**,2901-2913.

(23)   Kunau, W.H., Dommes, V., Schulz, H. (1995) beta-oxidation of fatty acids in mitochondria, peroxisomes, and bacteria: a century of continued progress. *Prog Lipid Res.* **34**,267-342.

(24)   Wanders, R.J., Vreken, P., Ferdinandusse, S., Jansen, G.A., Waterham, H.R., Van Roermund, C.W., Van and Grunsven, E. G. (2001) Peroxisomal fatty acid alpha- and beta-oxidation in humans: enzymology,

peroxisomal metabolite transporters and peroxisomal diseases. *Biochem Soc Trans.* **29**,250-267.

(25)   Bloj, B., Zilversmit, D.B. (1977) Rat liver proteins capable of transferring phosphatidylethanolamine. Purifica
tion and transfer activity for other phospholipids and cholesterol. *J Biol Chem.* **252**,1613-1619.

(26)   Wirtz, K.W. (1997) Phospholipid transfer proteins revisited. *Biochem J.* **324**,353-360.

(27)   Seedorf, U., Ellinghaus, P., Roch Nofer, J. (2000) Sterol carrier protein-2. *Biochim Biophys Acta.* **1486**,45-54.

(28)   Scallen, T.J., Srikantaiah, M.V., Seetharam, B., Hansbury, E., Gavey, K.L. (1974) Proceedings: Sterol carrier protein hypothesis. *Fed Proc.* **33**,1733-1746.

(29)   Frolov, A., Cho, T.H., Billheimer, J.T., Schroeder, F. (1996) Sterol carrier protein-2, a new fatty acyl coenzyme A-binding protein. *J Biol Chem.* **271**,31878-31884.

(30)   Ossendorp, B.C., Van Heusden, G.P., De Beer, A.L., Bos, K., Schouten, G.L., Wirtz, K.W. (1991) Identification of the cDNA clone which encodes the 58-kDa protein containing the amino acid sequence of rat liver non-specific lipid-transfer protein (sterol-carrier protein 2). Homology with rat peroxisomal and mitochondrial 3-oxoacyl-CoA thiolases. *Eur J Biochem.* **201**,233-239.

(31)   Seedorf, U., Assmann, G. (1991) Cloning, expression, and nucleotide sequence of rat liver sterol carrier protein 2 cDNAs. *J Biol Chem.* **266**,630-636.

(32)   Ohba, T., Holt, J.A., Billheimer, J.T., Strauss 3rd, J.F. (1995) Human sterol carrier protein x/sterol carrier protein 2 gene has two promoters. *Biochemistry.* **34**,10660-10668.

(33)   Seedorf, U., Raabe, M., Ellinghaus, P., Kannenberg, F., Fobker, M., Engel, T., Denis, S., Wouters, F., Wirtz, K.W., Wanders, R.J., Maeda, N., Assmann, G. (1998) Defective peroxisomal catabolism of branched fatty acyl coenzyme A in mice lacking the sterol carrier protein-2/sterol carrier protein-x gene function. *Genes Dev.* **12**,1189-1201.

(34)   Wanders, R. J., Denis, S., van Berkel, E., Wouters, F., Wirtz, K.W., Seedorf, U. (1998) Identification of the newly discovered 58 kDa peroxisomal thiolase SCPx as the main thiolase involved in both pristanic acid and trihydroxycholestanoic acid oxidation: implications for peroxisomal beta-oxidation disorders. *J Inherit Metab Dis.* **21**,302-305.

(35)   Wouters, F. S., Bastiaens, P.I., Wirtz, K.W., Jovin, T.M. (1998) FRET microscopy demonstrates molecular association of non-specific lipid transfer protein (nsL-TP) with fatty acid oxidation enzymes in peroxisomes. *EMBO J.* **17**,7179-7189.

(36)   Ossendorp, B. C., Voorhout, W.F., van Amerongen, A., Brunink, F., Batenburg, J.J., Wirtz, K.W. (1996) Tissue-specific distribution of a peroxisomal 46-kDa protein related to the 58-kDa protein (sterol carrier protein x; sterol carrier protein 2/3-oxoacyl-CoA thiolase). *Arch Biochem Biophys.* **334**,251-260.

(37)   Hunter, T. (2000) Signalling—2000 and beyond. *Cell.* **100**,113-127.

(38)   Avruch, J. (1998) Insulin signal transduction through protein kinase cascades. *Mol Cell Biochem.* **182**,3148.

(39)   Blume-Jensen, P., Hunter, T. (2001) Oncogenic kinase signalling. *Nature.* **411**,355-365.

(40)   Rodriguez-Viciana, P., Warne, P.H., Dhand, R., Vanhaesebroeck, B., Gout, I., Fry, M.J., Waterfield, M.D., Downward, J. (1994) Phosphatidylinositol-3-OH kinase as a direct target of Ras. *Nature.* **370**,527-532.

(41)   Burgering, B.M., Coffer, P.J. (1995) Protein kinase B (c-Akt) in phosphatidylinositol-3-OH kinase signal transduction. *Nature.* **376**,599-602.

(42)   Franke, T. F., Yang, S.I., Chan, T.O., Datta, K., Kazlauskas, A., Morrison, D.K., Kaplan, D.R., Tsichlis, P.N. (1995) The protein kinase encoded by the Akt proto-oncogene is a target of the PDGF-activated phosphatidylinositol 3-kinase. *Cell.* **81**,727-736.

(43)   Alessi, D. R., James, S.R., Downes, C.P., Holmes, A.B., Gaffney, P.R., Reese, C.B., Cohen, P. (1997) Characterization of a 3-phosphoinositide-dependent protein kinase which phosphorylates and activates protein kinase Balpha. *Curr Biol.* **7**,261-269.

(44)   Stephens, L., Anderson, K., Stokoe, D., Erdjument-Bromage, H., Painter, G.F., Holmes, A.B., Gaffney, P.R., Reese, C.B., McCormick, F., Tempst, P., Coadwell, J., Hawkins, P.T. (1998) Protein kinase B kinases that mediate phosphatidylinositol 3,4,5-trisphosphate-dependent activation of protein kinase B. *Science.* **279**,710-714.

(45)   Stokoe, D., Stephens, L.R., Copeland, T., Gaffney, P.R., Reese, C.B., Painter, G.F., Holmes, A.B., McCormick, F., Hawkins, P.T. (1997) Dual role of phosphatidylinositol-3,4,5-trisphosphate in the activation of protein kinase B. *Science.* **277**,567-570.

(46)   Simpson, L., Parsons, R. (2001) PTEN: life as a tumor suppressor. *Exp Cell Res.* **264**,29-41.

(47)   Kops, G. J., de Ruiter, N.D., De Vries-Smits, A.M., Powell, D.R., Bos, J.L., Burgering, B.M. (1999)

Direct control of the Forkhead transcription factor AFX by protein kinase B. *Nature.* **398**,630-634.

(48)   Paradis, S., Ruvkun, G. (1998) Caenorhabditis elegans Akt/PKB transduces insulin receptor-like signals from AGE-1 PI3 kinase to the DAF-16 transcription factor. *Genes Dev.* **12**,2499-2498.

(49)   Vanfleteren, J. R., Braeckman, B.P. (1999) Mechanisms of life span determination in Caenorhabditis elegans. *Neurobiol Aging.* **20**,487-502.

(50)   Dijkers, P. F., Medema, R.H., Lammers, J.W., Koenderman, L., Coffer, P.J. (2000) Expression of the pro-apoptotic Bcl-2 family member Bim is regulated by the forkhead transcription factor FKHR-L1. *Curr Biol.* **10**,1201-1204.

(51)   Brunet, A., Bonni, A., Zigmond, M.J., Lin, M.Z., Juo, P., Hu, L.S., Anderson, M.J., Arden, K.C., Blenis, J., Greenberg, M.E. (1999) Akt promotes cell survival by phosphorylating and inhibiting a Forkhead transcription factor. *Cell.* **96**,857-868.

(52)   Medema, R. H., Kops, G.J., Bos, J.L., Burgering, B.M. (2000) AFX-like Forkhead transcription factors mediate cell-cycle regulation by Ras and PKB through p27kip1. *Nature.* **404**,782-787.

(53)   Honda, Y., Honda, S. (1999) The daf-2 gene network for longevity regulates oxidative stress resistance and Mn-superoxide dismutase gene expression in Caenorhabditis elegans. *FASEB J.* **13**,1385-1393.

The peroxisome in oxidative stress.
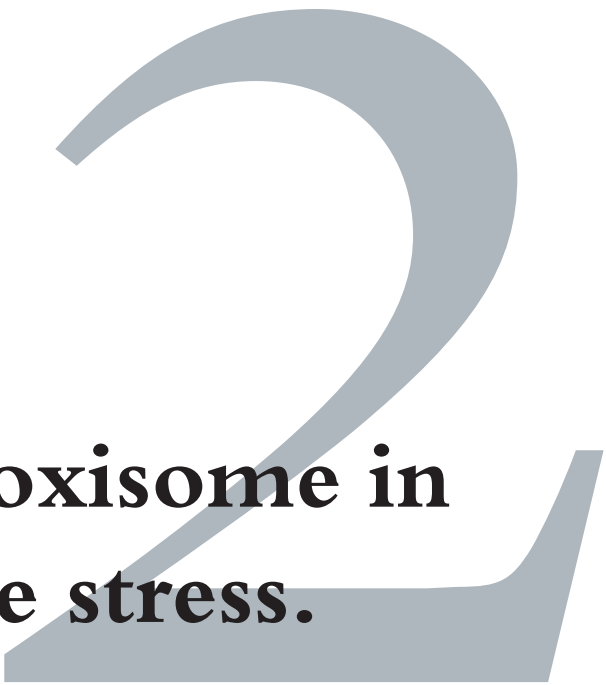
The peroxisome in oxidative stress.

Tobias B. Dansen & Karel W.A. Wirtz.

Institute of Biomembranes, Centre for Biomembranes and Lipid Enzymology, Department of Biochemistry of Lipids, Utrecht University, Padualaan 8, PO Box 80054, 3508 TB Utrecht, The Netherlands. Tel. +31-30-2532856. Fax. +31-30-2533151.

Abstract

Peroxisomes are one of the main sites in the cell where oxygen free radicals are both generated and scavenged. The balance between these two processes is believed to be of great importance for proper functioning of cells and has been implicated in aging and carcinogenesis. We will give an overview of the peroxisomal processes involved in the oxygen radical homeostasis and its implications for the cell.

The peroxisome

The peroxisome is a single membrane-bound organelle present in practically every eukaryotic cell. It is involved in numerous metabolic and biosynthetic pathways, yet these pathways may differ between species. Here we will focus on the peroxisome in the animal cell, although many of the peroxisomal functions described are also present in plant cells. One of the main functions of peroxisomes is the breakdown of those fatty acids that are poor substrates for the mitochondrial β-oxidation, specifically very-long-chain fatty acids (VLCFAs), branched-chain fatty acids (BCFAs) and poly-unsaturated fatty acids (PUFAs). Furthermore, they are involved in etherphospholipid and cholesterol biosynthesis, D-amino acid metabolism, bile acid formation and the detoxification of xenobiotics (1, 2).

Peroxisomal matrix proteins are synthesized on free polyribosomes in the cytosol to be subsequently transported to the peroxisome. Sorting to the peroxisomes takes place by cytosolic receptors that recognize either the peroxisomal targeting signal of type 1 (PTS1) or type 2 (PTS2). The PTS1 comprises a C-terminal tripeptide with the consensus sequence (C/A/S)-(K/R/H)-(L/I) (3). The PTS2 is located near the N-terminus and comprises (R/K)-L-xxxxx-(Q/K)-L. Upon docking onto the import machinery at the peroxisomal membrane the complex of the receptor and the matrix protein is translocated over the membrane in an ATP-dependent manner. The proteins pass through the membrane in a folded state, which is remarkable given that the peroxisomal membrane is impermeable to protons and small solutes(4, 5). For a review on peroxisomal import see Subramani *et al.* (6) .

The importance of the peroxisome for proper functioning of the cell becomes clear from the fact that over twenty human peroxisomal disorders exist in which one or more peroxisomal proteins are absent or dysfunctioning. These inherited disorders may result in death at early age and are generally characterized by an accumulation of VLCFAs and/or

BCFAs and bile acid intermediates in the plasma. The peroxisomal disorders can be divided in three classes. In the first class peroxisomes are absent due to a total inability to import proteins into peroxisomes. In the second class peroxisomes are present, but several enzymes are missing due to an isolated defect in peroxisomal import via either PTS1 or PTS2. The third class comprises the single enzyme disorders. In this group there is no defect in protein import, but peroxisomal function is deregulated because one of the enzymes is missing or destabilized. For a review on peroxisomal disorders see Wanders *et al.* (2, 7).

The peroxisome is a highly dynamic organelle able to move rapidly throughout the cell along microtubuli (8, 9). Depending on the cell type the number of peroxisomes per cell and as well as their shape may vary greatly. The biogenesis of peroxisomes involves either fission of pre-existing organelles or budding from the endoplasmic reticulum. For a review on peroxisome biogenesis see Titorenko *et al.* (10). In rodent liver, the number of peroxisomes is highly increased when activators of the peroxisome proliferator activated receptors (PPARs) like fibrates or free fatty acids are present (11). This response is not observed in human cells, although changes in number and size of peroxisomes have been reported for human hepatoma cells (12).

In this review we will focus on those processes in the peroxisome that affect the delicate free radical balance of the cell. The generation of hydrogen peroxide in the β-oxidation of fatty acids and the formation of radicals derived thereof will be described, as well as the anti-oxidant defense system of the peroxisome. We will also discuss the effects of peroxisome (dys)function on cellular oxidative stress.

Reactive oxygen production in peroxisomes

Hydrogen peroxide-production and the peroxisomal β-oxidation

Hydrogen peroxide in the peroxisome is mainly formed by oxidases that transfer hydrogen from metabolites to molecular oxygen. In liver, about one fifth of the total oxygen consumption is accounted for by peroxisomal oxidase activity (13). For example, about 35% of all hydrogen peroxide formed in rat liver derives from peroxisomal oxidases (14). Processes in which the peroxisomal oxidases are involved include β-oxidation of fatty acids (acyl-CoA oxidase), α-hydroxy acid degradation, urate degradation, polyamine breakdown, D-amino acid metabolism and pipecolic acid oxidation (15). Here we will discuss in more detail the peroxisomal β-oxidation.

The peroxisomal β-oxidation pathway consists of the same reaction steps as the mitochondrial counterpart, yet the enzymes involved are different. In contrast to the mitochondrial β-oxidation, breakdown of fatty acids in the peroxisome does not yield ATP. In order for fatty acids to be degraded in the peroxisome, they are first activated by fatty acyl-CoA synthetases present in the peroxisomal membrane. In the first step of the β-oxidation cycle a double bond is introduced at the β position of the fatty acyl-CoA ester. This step is catalyzed by the FAD-containing acyl-CoA oxidase which transfers hydrogen atoms to molecular oxygen forming hydrogen peroxide (see figure 1a). Subsequently, the enoyl-bond is hydrated and dehydrogenated by the bifunctional enzyme yielding 2-keto-acyl-CoA, which is then cleaved by thiolase. Peroxisomal degradation of fatty acids is incomplete, most probably because of the preference of the acyl-CoA oxidase for long fatty acyl chains. When the chain length becomes too short, the fatty acid is transported to the mitochondria in a carnitin-dependent way to be further degraded.

a

b
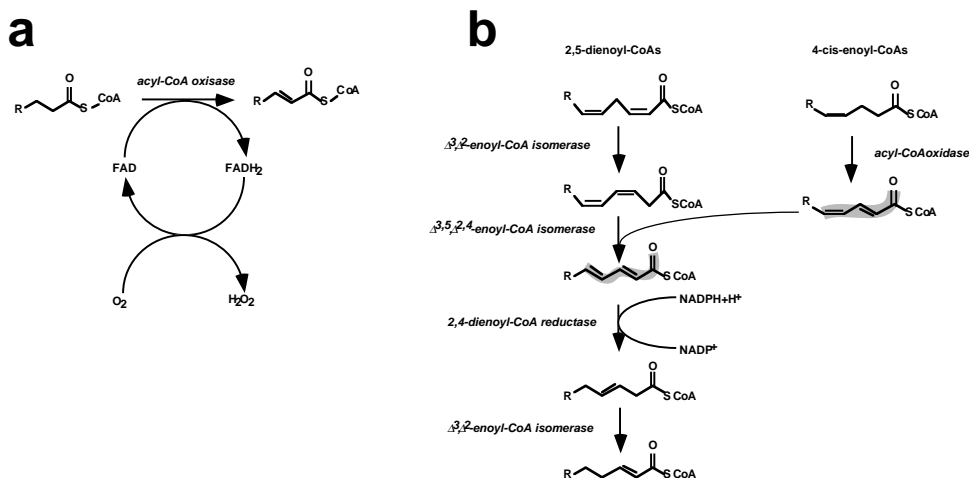
Figure 1:acyl-CoA oxidase and β-oxidation of PUFAs. (a) Acyl-CoA oxidases containing FAD transfer the protons from the β-carbon bond of an activated fatty acid to molecular oxygen via an FADH$_2$ intermediate that is recycled. Hydrogen peroxide is formed in this reaction. Human peroxisomes contain at least three different FAD-containing acyl-CoA oxidases: straight-chain acyl-CoA oxidase, branched-chain acyl-CoA oxidase and pristanoyl-CoA oxidase. **(b)** PUFAs have to be converted to the 2-*trans*-enoyl-CoA form before they can be processed further in the β-oxidation. To this end, a set of isomerases and reductases acts on 4-*cis* and 2,5-dienoyl-CoAs as shown. During this process, intermediates with a conjugated pi-system (shaded) are formed.

In the degradation of PUFAs 2,5-dienoyl-CoA and 4-cis-enoyl-CoA intermediates are formed. These intermediates require the conversion to the 2-*trans* isomers before the β-oxidation cycle can be re-entered (figure 1b). To this end, 4-*cis*-PUFAs are oxidized to 2-*trans*-, 4-*cis* PUFAs by acyl-CoA oxidase. 2,5-dienoyl-CoAs are first converted to 3,5 dienoyl-CoA, subsequently isomerized to 2,4-dienoyl and processed further to a 3-*trans* enoyl-CoA by 2,4-dienoyl-CoA reductase whereupon the 2-*trans* form is produced by enoyl-CoA isomerase. This yields a fatty acyl-CoA that can be hydrated and dehydrogenated by the bifunctional enzyme as in the normal β-oxidation pathway (see figure 1b). During the breakdown of PUFAs, compounds are formed that have a conjugated pi-system. These compounds (i.e. 2,4- and 3,5-dienoyl-CoA)are susceptible to attack by free radicals.

BCFAs have their own set of β-oxidation enzymes that are capable of cleaving 2-methyl-fatty acids like pristanic acid (tetramethylpentadecanoic acid), yielding propionyl-CoA instead of acetyl-CoA. In the reaction cycle branched-chain acyl-CoA oxidase (BrAOX), D-peroxisomal bifunctional enzyme (D-PBE) and Sterol Carrier Protein X (SCPx) are active. These enzymes are also involved in the cleavage of the side chain of the cholesterol derivative 3α,7α,12α-trihydroxy-5β-cholestanoyl-CoA (THCA-CoA) in the bile acid biosynthesis from cholesterol. BCFAs that have a methyl group at the 3-position (like phytanic acid) have to be α-oxidized first by phytanoyl-CoA hydroxylase to meet the criteria for β-oxidation. For a review on peroxisomal β-oxidation see Kunau *et al.* (16).

In short, as a result of hydrogen peroxide formation by the long- and branched-chain fatty acyl-CoA oxidases, oxidative stress is generated during the peroxisomal β-oxidation. During PUFA degradation, intermediates with a conjugated pi-system are formed which may be susceptible towards oxidation by free radicals possibly starting a lipid peroxidation chain reaction. Indeed, there are indications that both in yeast and humans high PUFA levels can lead to substantial lipid peroxidation and formation of conjugated dienes (17, 18). In case fatty

acids, and especially phytanic acid, are not effectively degraded, a constitutive activation of the peroxisome proliferator activated receptor alpha (PPARα) may occur as has been shown in SCPx knock out mice (19). PPARα activation induces increased levels of the peroxisomal (and mitochondrial) β-oxidation enzymes, which can lead to oxidative stress as discussed below.

Transition metal ions

Ions from transition metals like iron and copper are abundant in peroxisomes mainly in a complexed form. It has been shown that certain xenobiotics are capable of releasing iron from proteins like ferritin. Iron complexed to, for instance, ascorbate, histidine or ADP has been shown to induce lipid peroxidation (20) as a result of the formation of hydroxyl radicals in the Fenton reaction (reaction 1) (21).

$$Fe^{3+} + O_2^{\cdot-} \longrightarrow Fe^{2+} + O_2$$
$$Fe^{2+} + H_2O_2 \longrightarrow Fe^{3+} + \cdot OH + OH^- \qquad (1)$$
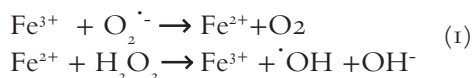
Studies on the induction of lipid peroxidation showed that the scavenging of hydrogen peroxide hardly influenced this reaction whereas the prevention of the formation of the reduced metal ion did lead to inhibition of lipid peroxidation. This indicates that catalase alone is not sufficiently effective to prevent the oxidative damage to the peroxisomal membrane as a result of the Fenton reaction. Indeed, lipid peroxidation events induced by transition metal ions have been reported to occur at the peroxisomal membrane (22). Damage and disruption of the membrane will release the peroxisomal content into the cytosol (23), as a result of which the cell loses essential peroxisomal functions.

Reactive Oxygen detoxification in peroxisomes

Antioxidant enzymes

The peroxisome contains a battery of antioxidant enzymes to prevent oxidative damage by free radicals derived from hydrogen peroxide. Hydrogen peroxide is scavenged by catalase and glutathioneperoxidase. MnSOD and Cu,ZnSOD protect against superoxide anions by converting these into hydrogen peroxide. The latter two enzymes are mainly present in mitochondria and cytosol, but have been reported to be present in peroxisomes as well (24-26). Fatty-acyl hydroperoxides formed upon reaction with hydroxyl radicals are reduced by glutathione peroxidase at the expense of glutathione and by the peroxidase activity of catalase. Glutathione-depending peroxidases are present troughout the cell incuding the peroxisome (26). The various reactions catalyzed by the above enzymes are presented in table 1. For a review on antioxidant enzymes, see Mates *et al.* (27).

Table 1: anti-oxidant enzymes, their substrates, their reactions and their location in the cell.

Enzyme	substrate(s)	reaction	location in the cell
catalase	Hydrogen peroxide, hydroperoxide + H-donor (e.g. EtOH)	$2H_2O_2 \rightarrow 2H_2O + O_2$ $ROOH + AH_2 \rightarrow ROH + A + H_2O$	Peroxisome
Glutathione-peroxidase	Hydrogen peroxide, hydroperoxide	$ROOH + GSH \rightarrow ROH + GSSG + H_2O$	Troughout the cell
MnSOD	superoxide anion	$2O_2^{\cdot-} + 2H^+ \rightarrow H_2O_2 + O_2$	Mitochondrion, peroxisome
Cu,ZnSOD	superoxide anion	$2O_2^{\cdot-} + 2H^+ \rightarrow H_2O_2 + O_2$	Cytosol, Peroxisome

Vitamin C

Free radicals in the matrix can also be scavenged by vitamin C (ascorbate). Furthermore, this anti-oxidant is used as electron acceptor in the alpha-oxidation of phytanic acid catalyzed by phytanoyl-CoA hydroxylase (28). Interestingly, the activity of this enzyme also requires oxygen and iron, thereby possibly contributing to oxidative stress. Ascorbate is also known to recycle oxidized vitamin E, an important anti-oxidant in the protection against lipid peroxidation (29).

Etherphospholipids

Etherphospholipids comprise about 18% of the total phospholipid mass in humans; the ether bond occurs mainly in PtdEtOH and PtdChol (30). In the biosynthesis of etherphospholipds dihydroxyacetonephosphate is acylated by dihydroxyacetone-phosphate acyltransferase to be converted into the alkyl derivative by alkyl-dihydroxyacetonephosphate synthase replacing the acyl-chain with a fatty alcohol. These two enzymes are located in the peroxisome (31). Indeed, patients with a peroxisome biogenesis disorder have very low etherphospholipid levels (32). Since these two enzymes use a different PTS, this deficiency can be explained by a defect in either PTS1- or PTS2-mediated import. Etherphospholipids amongst which plasmalogens (α,β mono-unsaturated etherphospholipids), have been implicated in the defense against oxygen free radicals (33). This defense does not hold only for peroxisomal membranes, but for the entire cell. Plasmalogen-deficient CHO cells with a defect in peroxisomal biogenesis were less resistant to UV-induced oxidative stress, whereas restoration of the plas-
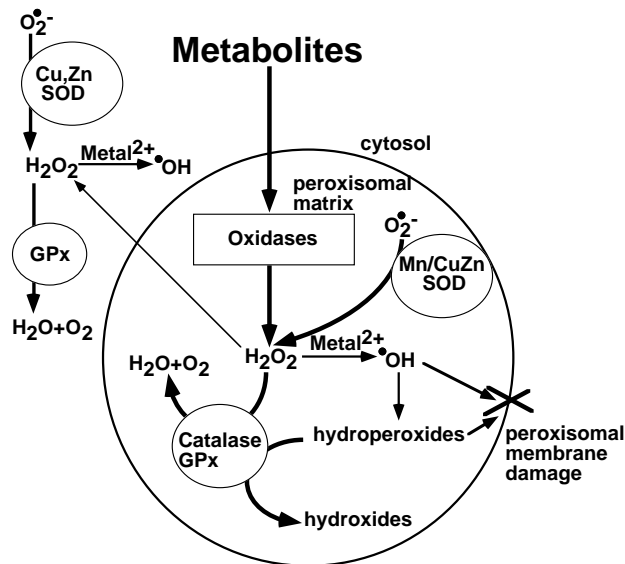
Figure 2:Schematic representation of a number of oxygen radical producing and scavenging pathways in the peroxisome. Hydrogen peroxide is formed by a number of oxidases that degrade metabolites like fatty acids. Hydrogen peroxide is scavenged by catalase and glutathioneperoxidase (GPx) or converted to hydroxyl radicals via the metal-catalyzed Fenton reaction. Some of the hydrogen peroxide may escape to the cytosol, where it is either scavenged by GPx or converted to hydroxyl radicals. The latter can induce lipid peroxidation by attacking unsaturated bonds in fatty acyl-chains. The hydroperoxides formed in this process can be neutralized by catalase and glutathione-peroxidase. Superoxide anions in the peroxisome are scavenged by two superoxide-dismutases.

malogen content could rescue the cells (34). This implied that the higher oxidative stress was not caused by the defect in peroxisomal biogenesis, but by the ensuing deficiency in etherphospholipids. Signalling lipids derived from etherphospholipids, such as platelet activated factor, can also change the radical balance indirectly by the induction of several cellular signalling cascades (35). A number of the oxygen free radical producing and scavenging systems inside the peroxisome and in the cytosol are summarized in Figure 2.

Regulation of radical producing and scavenging enzymes

Most enzymes of the β-oxidation are transcriptionally regulated via the PPARs that upon activation bind to the peroxisome proliferator responsive elements (PPRE) of the DNA. This receptor dimerizes either with itself or with the retinoic acid receptor after binding of ligands (11). These ligands include free fatty acids like phytanic acid (19) and so called peroxisome proliferators like fibrates, plasticizers and pesticides. This means that an inability to degrade fatty acids, as is the case in the peroxisomal biogenesis disorders, results in a continuous activation of the PPARs, and especially the PPARα. This PPAR induces transcription of enzymes involved in the peroxisomal β-oxidation (11), but catalase and GPx are not proportionately induced (15). This may lead to increased hydrogen peroxide concentrations in the peroxisome. The most pronounced effects of peroxisome proliferators are observed in rodents that as a result of continuous activation of PPARα were shown to develop liver tumors. In humans these effects are not observed. In fact, fibrates are used as a drug in the treatment of severe hyperlipidemia (36). On the other hand, an effect of PPARα activation in human hepatoma cells like HepG2 has been reported (37).

Given that hydrogen peroxide may escape from the peroxisomes, it is important for the cell to balance its total anti-oxidant capacity when challenged with peroxisome-related oxidative stress. The regulation of anti-oxidant enzymes is very complex as it involves many signalling pathways. The regulation of these enzymes is thought to be closely related to apoptotic signalling, as the oxidative state of the cell is one of the parameters that determines whether a cell goes into apoptosis or proceeds in the cell-cycle (38). Upregulation of anti-oxidant enzymes can also suppress apoptosis, which has been proposed as one of the mechanisms in carcinogenesis (39). On the other hand, it has been shown that in tumor cells the levels of MnSOD and GPx are diminished whereas the CuZnSOD is unaffected (40). This suggests that both up- and down-regulation of anti-oxidant capacity may lead to carcinogenesis. Clearly, the benefit of radical scavenging is very dependent on the type of tissue. For instance, apoptosis of damaged skin fibroblasts has no detrimental effect because of their rapid regeneration, whereas neuronal cells (that cannot proliferate) prevent oxidative damage by upregulating the anti-oxidant enzymes. In the brain of a Zellweger mouse model, that lacks peroxisomes completely, apoptosis is highly increased (41). It remains to be investigated whether this is an effect of the absence of the anti-oxidant defense by peroxisomes, or results from the fatty acid accumulation in these mice.

Measuring oxidative stress in peroxisomes

So far the evidence that peroxisomes contribute to the oxidative stress in cells is limited. This is due to the fact that most of the standard techniques to measure oxidative stress are only suitable for cell lysates. Recently we developed a new method to measure oxidative stress

(e.g. lipidperoxidation) in peroxisomes in living cells. To this end, we linked a BODIPY derivative to a heptapeptide (acetyl-CKGGAKL-OH) containing a PTS1 (BODIPY-PTS1) (42-44) (see figure 3B). This BODIPY derivative shifts its emission from red to green upon oxidation by hydroxyl radicals (45). The BODIPY-PTS1 crosses the plasma membrane by diffusion whereupon it is targeted to the peroxisomes via the PTS1 on the peptide (43). Using dual wavelength excitation and emission confocal laser scanning microscopy, the formation of the green form of BODIPY can be measured in time. In this way, we determined whether there was an increase in oxidative stress upon incubation of Rat1 fibroblasts with fatty acids. So we showed that incubation of cells with palmitate, which is mainly degraded in mitochondria, did not result in oxidation of the BODIPY-PTS1, but that the breakdown of arachidic acid (C20:0) and phytanic acid did result in peroxisomal oxidative stress (see figure 4; data to be published). This implies that despite the elaborate anti-oxidant defense mechanism of the peroxisome, a level of oxidative stress can be generated sufficient to oxidize biomolecules in peroxisomes.
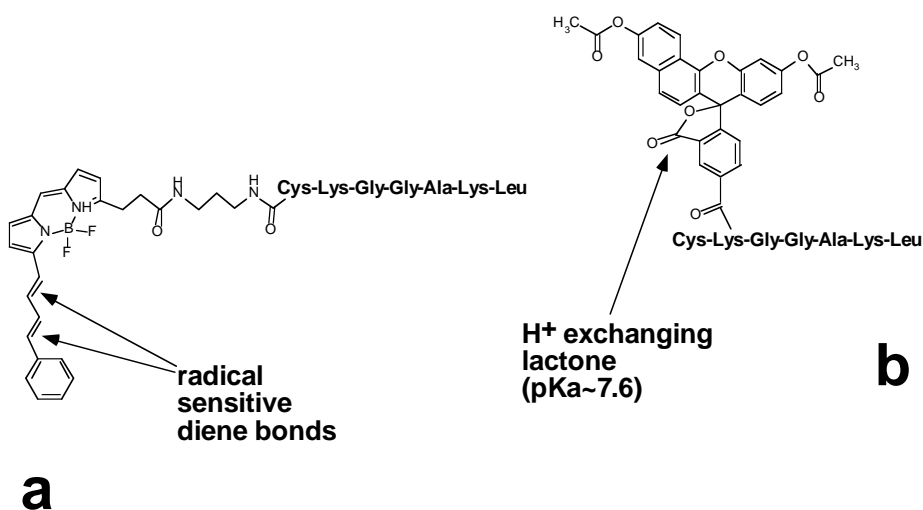
Figure 3: Fluorescent PTS1-probes. Membrane-permeant fluorescent moieties attached to a heptapeptide containing a PTS1 can be targeted to the peroxisomes of living cells. These probes accumulate in peroxisomes within about 15 min after addition to the cell. The radical-sensitive BODIPY-PTS1 (fig **3a**) was designed to measure lipid peroxidation in peroxisomes (see also figure 4). By using the pH-sensitive SNAFL-2-PTS1 (fig **3b**) we were able to measure the pH in the peroxisomal matrix. This probe with a pKa of 7.6 shifts its emission from red to green depending on the pH of its environment.

Importance of the peroxisomal membrane integrity

Recently we have succeeded in targeting the fluorescent pH-sensitive SNAFL-2 to peroxisomes in intact cells by using the same peptide as described above (4, 44). Using this SNAFL-2-PTS1 peptide (figure 3) we established by ratio-imaging that peroxisomes of human fibroblasts have a pH of ±8.2. The concurrent pH-gradient over the peroxisomal membrane was dissipated when an ionophore (CCCP) was added. In fibroblasts of Rhizomelic Chondrodysplasia Punctata (RCDP) patients, which have an isolated defect in the peroxisomal import of proteins carrying a PTS2 sequence, import of SNAFL-2-PTS1 into the peroxisomes appeared normal, yet the pH gradient over the peroxisomal membrane was absent. The observed proton gradient is in line with observations that peroxisomes were impermeable to

small solutes like NAD (5). Most peroxisomal enzymes have a basic pH optimum and a basic isolectric point, which may reflect an adaptation to the alkaline environment. Particularly the peroxidase activity of catalase, which scavenges hydroperoxides derived from lipid peroxidation, is very much dependent on an alkaline pH (46). Hence, it can be speculated that dissipation of the peroxisomal pH-gradient may lead to elevated levels of oxidative stress. The compartmentalization of the peroxisomal fatty acid β-oxidation could contribute in multiple ways to the reduction of oxidative stress. First, the β-oxidation reactions are close to the catalase activity. Second, reactive oxygen species are kept from the cytosol and thirdly at the alkaline pH catalase can effectively neutralize the acylhydroperoxides formed. Since the pH gradient over the peroxisomal membrane in fibroblasts from RCDP patients is diminished, one may wonder whether these fibroblasts have more oxidative stress. Indeed, this has been reported but since the RCDP patient also lacks etherphospholipids, the cause of this increased oxidative stress is not clearly established.

Conclusion

Peroxisomes are of great importance for the detoxification of reactive oxygen species. On the other hand, these radicals are also generated by these organelles. Taking this pivotal role in controlling oxidative stress into account, it may well be that peroxisomes play an important role in processes like apoptosis, aging and carcinogenesis. In applying the new fluorescence techniques described, we hope to be able to gain more insight in this role.
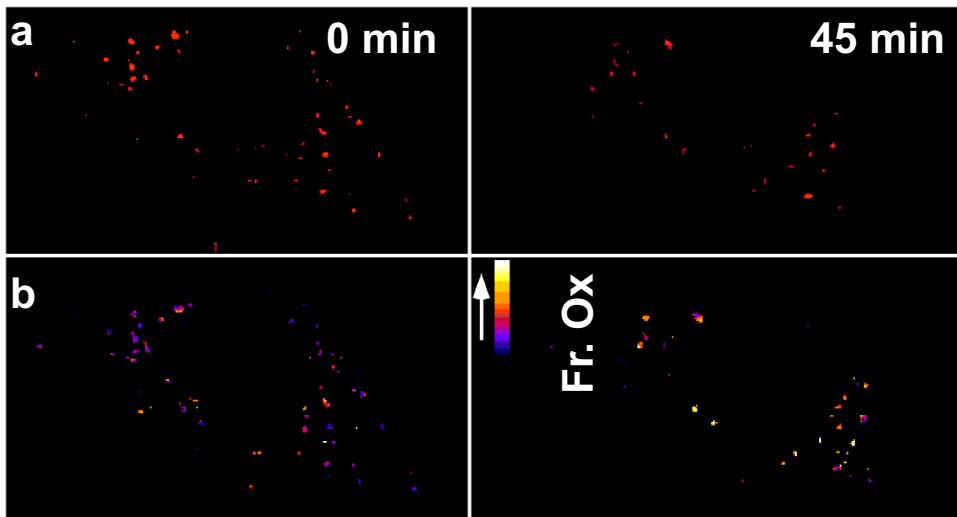

Figure 4: Lipid peroxidation in peroxisomes of living Rat1 fibroblasts after incubation with phytanic acid. Panel A shows the decrease in intensity of the red fluorescence of the BODIPY-PTS1 probe before and after incubation with phytanic acid (10 mM) for 45 min. The green fluorescence, reflecting the oxidized probe increased concomitantly (not shown). Panel B shows a false colour representation of the fraction oxidized probe in the peroxisomes before and after the incubation. This fraction is calculated by dividing the signal of the green BODIPY-PTS1 by the sum of the signals of the oxidized (green) and intact (red) BODIPY-PTS1. It can be clearly seen that a substantial oxidation took place in 45 min. Incubation with palmitic acid (10 mM) did not lead to oxidation of BODIPY-PTS1 (data not shown). Palmitic acid is mainly degraded in mitochondria. A colour-image can be found at the back-cover of this thesis.

References

(1)   van den Bosch, H., Schutgens, R.B., Wanders, R.J., Tager, J.M. (1992) Biochemistry of peroxisomes. *Annu Rev Biochem.* **61**,157-197.

(2)   Wanders, R. J., Tager, J.M. (1998) Lipid metabolism in peroxisomes in relation to human disease. *Mol Aspects Med.* **19**,69-154.

(3)   Gould, S. J., Keller, G.A., Hosken, N., Wilkinson, J., Subramani, S. (1989) A conserved tripeptide sorts proteins to peroxisomes. *J Cell Biol.* **108**,1657-1664.

(4)   Dansen, T. B., Wirtz, K.W.A., Wanders, R.J.A., Pap, E.H.W. (2000) Peroxisomes in human fibroblasts have a basic pH. *Nat Cell Biol.* **2**,51-53.

(5)   van Roermund, C. W., Elgersma ,Y., Singh, N., Wanders, R.J., Tabak, H.F. (1995) The membrane of peroxisomes in Saccharomyces cerevisiae is impermeable to NAD(H) and acetyl-CoA under *in vivo* conditions. *EMBO J.* **14**,3480-3486.

(6)   Subramani, S., Koller, A., Snyder, W.B. (2000) Import of peroxisomal matrix and membrane proteins. *Annu Rev Biochem.* **69**,399-418.

(7)   Wanders, R. J. (1999) Peroxisomal disorders: clinical, biochemical, and molecular aspects. *Neurochem Res.* **24**,565-580.

(8)   Wiemer, E. A., Wenzel, T., Deerinck, T.J., Ellisman, M.H., Subramani, S. (1997) Visualization of the peroxisomal compartment in living mammalian cells: dynamicbehavior and association with microtubules. *J Cell Biol.* **136**,71-80.

(9)   Schrader, M., King, S.J., Stroh, T.A., Schroer, T.A. (2000) Real time imaging reveals a peroxisomal reticulum in living cells. *J Cell Sci.* **113**,3663-3671.

(10)   Titorenko, V. I., Rachubinski, R.A. (2001) Dynamics of peroxisome assembly and function. *Trends Cell Biol.* **11**,22-29.

(11)   Latruffe, N., Malki, M.C., Nicolas-Frances, V., Clemencet, M.C., Jannin, B., Berlot, J.P. (2000) Regulation of the peroxisomal beta-oxidation-dependent pathway by peroxisome proliferator-activated receptor alpha and kinases. *Biochem Pharmacol.* **60**,1027-1032.

(12)   Stier, H., Fahimi, H.D., Van Veldhoven, P.P., Mannaerts, G.P., Volkl, A., Baumgart, E. (1998) Maturation of peroxisomes in differentiating human hepatoblastoma cells (HepG2): possible involvement of the peroxisome proliferator-activated receptor alpha (PPARalpha). *Differentiation.* **64**,55-66.

(13)   Reddy, J. K., Mannaerts, G.P. (1994) Peroxisomal lipid metabolism. *Annu. Rev. Nutr.* **14**,343-370.

(14)   Boveris, A., Oshino, N., Chance, B. (1972) The cellular production of hydrogen peroxide. *Biochem J.* **128**,617-630.

(15)   Yeldandi, A. V., Rao, M.S., Reddy, J.K. (2000) Hydrogen peroxide generation in peroxisome proliferator induced oncogenesis. *Mut Res.* **448**,159-177.

(16)   Kunau, W. H., Dommes, V., Schulz, H. (1995) beta-oxidation of fatty acids in mitochondria, peroxisomes, and bacteria: a century of continued progress. *Prog Lipid Res.* **34**,267-342.

(17)   Jenkinson, A., Franklin, M.F., Wahle, K., Duthie, G.G. (1999) Dietary intakes of polyunsaturated fatty acids and indices of oxidative stress in human volunteers. *Eur J Clin Nutr.* **53**,523-528.

(18)   Howlett, N. G., Avery, S.V. (1997) Induction of lipid peroxidation during heavy metal stress in Saccharomyces cerevisiae and influence of plasma membrane fatty acid unsaturation. *Appl Environ Microbiol.* **63**,2971-2976.

(19)   Ellinghaus, P., Wolfrum, C., Assmann, G., Spener, F., Seedorf, U. (1999) Phytanic acid activates the peroxisome proliferator–activated receptor alpha (PPARalpha) in sterol carrier protein 2-/ sterol carrier protein x-deficient mice. *J Biol Chem.* **274**,2766-2772.

(20)   Ryan, T. P., Aust, S.D.,. (1992) The role of iron in oxygen-mediated toxicities. *Crit Rev Toxicol.* **22**,119-141.

(21)   Stohs, S. J., Bagchi, D. (1995) Oxidative mechanisms in the toxicity of metal ions. *Free radical biology & medicine.* **18**,321-356.

(22)   Bacon, B. R., Britton, R.S. (1989) Hepatic injury in chronic iron overload. Role of lipidperoxidation. *Chem Biol Interact.* **70**,183-226.

(23)   Yokota, S., Oda, T., Fahimi, H.D. (2001) The role of 15-lipoxygenase in disruption of the peroxisomal membrane and in programmed degradation of peroxisomes in normal rat liver. *J Histochem Cytochem.* **49**,613-622.

(24)   Singh, A. K., Dobashi, K., Gupta, M.P., Asayama, K., Singh, I., Orak, J.K. (1999) Manganese superoxide dismutase in rat liver peroxisomes: biochemical and immunochemical evidence. *Mol Cell Biochem.* **197**,7-12.

(25)   Morenom, S., Nardacci, R., Ceru, M.P. (1997) Regional and ultrastructural immunolocalization of copper-zinc superoxide dismutase in rat central nervous system. *J Histochem Cytochem.* **45**,1611-1622.

(26)   Dhaunsi, G. S., Singh, I., Orak, J.K., Singh, A.K. (1994) Antioxidant enzymes in ciprofibrate-induced oxidative stress. *Carcinogenesis.* **15**,1923-1930.

(27)   Mates, J. M. (2000) Effects of antioxidant enzymes in the molecular control of reactive oxygen species toxicology. *Toxicology.* **153**,83-104.

(28)   Croes, K., Foulon, V., Casteels, M., Van Veldhoven, P.P., Mannaerts, G.P. (2000) Phytanoyl-CoA hydroxylase: recognition of 3-methyl-branched acyl-coAs and requirement for GTP or ATP and Mg(2+) in addition to its known hydroxylation cofactors. *J Lipid Res.* **41**,629-636.

(29)   Chan, A. C., Chow, C.K., Chiu, D. (1999) Interaction of antioxidants and their implication in genetic anemia. *Proc Soc Exp Biol Med.* **222**,274-282.

(30)   Nagan, N., Zoeller, R.A. (2001) Plasmaolgens: biosynthesis and functions. *Prog Lipid Res.* **40**,199-229.

(31)   van den Bosch, H., de Vet, E.C. (1997) Alkyl-dihydroxyacetonephosphate synthase. *Biochim Biophys Acta.* **1348**,35-44.

(32)   van den Bosch, H., Schrakamp, G., Hardeman, D., Zomer, A.W., Wanders, R.J., Schutgens, R.B. (1993) Ether lipid synthesis and its deficiency in peroxisomal disorders. *Biochemie.* **75**,183-189.

(33)   Sindelar, P. J., Guan, Z., Dallner, G., Ernster, L. (1999) The protective role of plasmalogens in iron-induced lipid peroxidation. *Free radical Biol Med.* **26**,318-324.

(34)   Zoeller, R. A., Morand, O.H., Raetz, C.R. (1988) A possible role for plasmalogens in protecting animal cells against photosensitized killing. *J Biol Chem.* **263**,11590-11596.

(35)   Prescott, S. M., Zimmerman, G.A., Stafforini, D.M., McIntyre, T.M. (2000) Platelet-activating factor and related lipid mediators. *Annu Rev Biochem.* **69**,419-445.

(36)   Rader, D. J., Haffner, S.M. (1999) Role of fibrates in the management of hypertriglyceridemia. *Am J Cardiol.* **83**,30F-35F.

(37)   Cattley, R. C., DeLuca, J., Elcombe, C., Fenner-Crisp, P., Lake, B.G., Marsman, D.S., Pastoor, T.A., Popp, J.A., Robinson, D.E., Schwetz, B., Tugwood, J., Wahli, W. (1998) Do peroxisome proliferating compounds pose a hepatocarcinogenic hazard to humans? *Regul Toxicol Pharmacol.* **27**,47-60.

(38)   McCormick, F. (1999) Signalling networks that cause cancer. *Trends Cell Biol.* **9**,M53-56.

(39)   Corcoran, G. B., Fix, L., Jones, D.P., Moslen, M.T., Nicotera, P., Oberhammer, F.A., Buttyan, R. (1994) Apoptosis: molecular control point in toxicity. *Toxicol Appl Pharmacol.* **128**,169-181.

(40)   Oberley, L. W., Oberley, T.D. (1988) Role of antioxidant enzymes in cell immortalization and transformation. *Mol Cell Biochem.* **84**,147-153.

(41)   Baes, M., Gressens, P., Baumgart, E., Carmeliet, P., Casteels, M., Fransen, M., Evrard, P., Fahimi, D., Declercq, P.E., Collen, D., van Veldhoven, P.P., Mannaerts, G.P. (1997) A mouse model for Zellweger syndrome. *Nat Genet.* **17**,49-57.

(42)   Dansen, T. B., Pap, E.H.W., Wanders, R.J.A., Wirtz, K.W.A. (2001) Targeted fluorescent probes in peroxisome function. *Histochem J.* **33**,65-69.

(43)   Pap, E. H., Dansen, T.B., van Summeren, R., Wirtz, K.W. (2001) Peptide-based targeting of fluorophores to organelles in living cells. *Exp Cell Res.* **265**,288-293.

(44)   Pap, E. H., Dansen, T.B., Wirtz, K.W. (2001) Peptide-based targeting of fluorophores to peroxisomes in living cells. *Trends Cell Biol.* **11**,10-12.

(45)   Pap, E. H., Drummen, G.P., Winter, V.J., Kooij, T.W., Rijken, P., Wirtz, K.W., Op den Kamp, J.A., Hage, W.J., Post, J.A. (1999) Ratio-fluorescence microscopy of lipid oxidation in living cells using C11-BODIPY(581/591). *FEBS Lett.* **453**,278-282.

(46)   Togo, S. H., Maebuchi, M., Yokota, S., Bun-Ya, M., Kawahara, A., Kamiryo, T. (2000) Immunological detection of alkaline-diaminobenzidine-negativeperoxisomes of the nematode Caenorhabditis elegans purification and unique pH optima of peroxisomal catalase. *Eur J Biochem.* **267**,1307-1312.
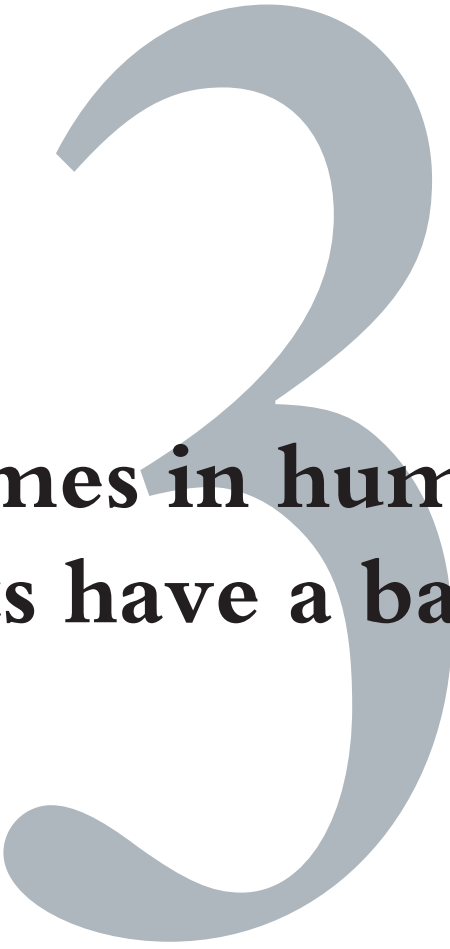
Peroxisomes in human fibroblasts have a basic pH.

Tobias B. Dansen, Karel W.A. Wirtz, Ronald J.A. Wanders & Eward H.W. Pap (2000) *Nature Cell Biology* **2(1),** 51-53.

Peroxisomes in human fibroblasts have a basic pH.

Tobias B. Dansen[1], Karel W. A. Wirtz[1], Ronald J. A. Wanders[2] & Eward H. W. Pap[1]

1.   *Institute of Biomembranes, Centre for Biomembranes and Lipid Enzymology, Department of Biochemistry of Lipids, Utrecht University, Padualaan 8, P.O. box 80054, 3508   TB Utrecht, The Netherlands.*
2.   *Academic Medical Centre, Departments of Clinical Chemistry and Paediatrics, University of Amsterdam, Meibergdreef 9, NL-1105 AZ Amsterdam, The Netherlands.*

Peroxisomes are single membrane-bound organelles found in nearly all eukaryotic cells. These organelles have a central function in lipid metabolism, including the beta-oxidation of very-long and branched chain fatty acids and the biosynthesis of ether phospholipids and cholesterol. Another characteristic of peroxisomes is their ability to degrade hydrogen peroxide by catalase (1, 2). A deficiency in one or more peroxisomal enzymes has been linked to at least twenty (often lethal) disorders (3), showing the key role of this organelle in normal functioning of the human body. Peroxisomes are fragile structures that easily lose their integrity upon isolation (4). This poses a serious problem for studying these organelles *in vitro* and explains why our knowledge about the properties of the peroxisomal membrane including the (pH across it, is limited. *In vivo* peroxisomes have been shown to be closed structures that are impermeable to NAD(H) and NADP(H) implying the existence of NAD(P) redox shuttles (5,6). Here we study the pH in peroxisomes by targeting a pH-sensitive fluorescent reporter group to these organelles in living fibroblasts. We attained specific targeting by conjugating the fluorophore to a membrane-permeable peptide that contains a type I peroxisomal targeting sequence (PTS1; amino acid sequence AKL) (7). Using this peptide probe, we establish that peroxisomes of human fibroblasts have a pH of 8.2 ± 0.3. Fibroblasts from RCDP (rhizomelic form of chondrodysplasia punctata) type 1 patients with severe mutations in PEX7 protein, which result in an isolated defect in PTS2 protein import (8), are still capable of importing the probe into peroxisomes, but have a pH of 6.5 ± 0.3.

        We covalently linked the pH sensitive (5-and 6-) carboxy-SNAFL-2 moiety to the PTS1-containing heptapeptide acetyl-CKGGAKL-COOH at the lysine near the amino-terminus. This peptide-probe (SNAFL-2-PTS1) was rapidly taken up into the cells and a punctate pattern of fluorescence was found, indicative of a peroxisomal localisation. To confirm that these structures are indeed peroxisomes, we used a fixable analogue (BODIPY-PTS1) in co-localization studies with Cy5-labelled antibodies against different peroxisomal proteins (figure 1a-c). The probe was targeted only towards the peroxisomes (figure 1b). Further evidence that the probe was incorporated into peroxisomes came from studies of human
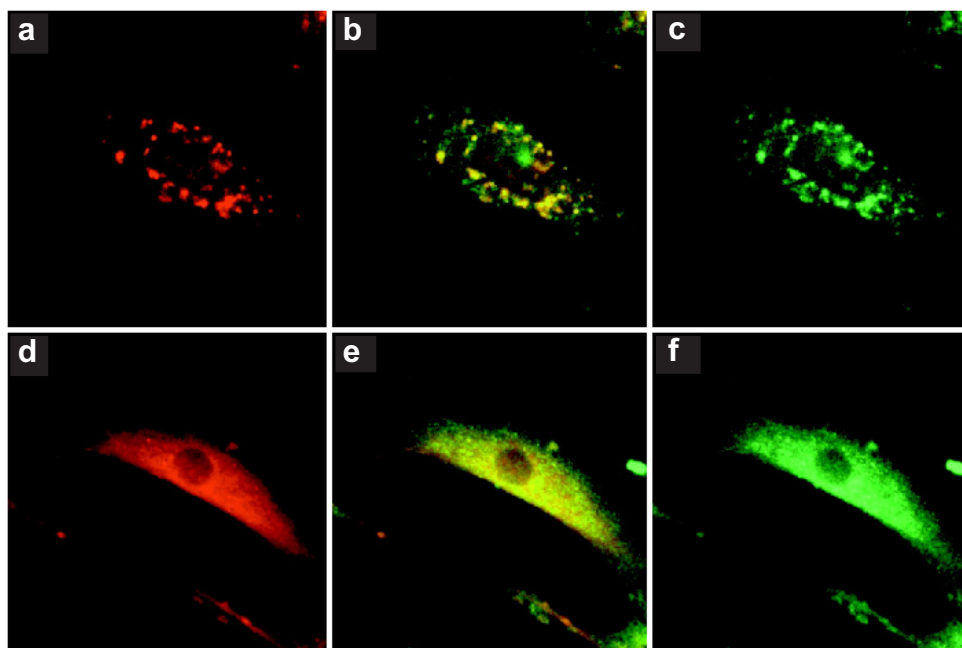
Figure 1. Peroxisomal localisation of BODIPY-PTS1. Incorporation of BODIPY-PTS1 in human fibroblasts (panel **a**). The high intensity structures coincide with that of an anti-nsL-TP-Cy5 staining (panel **c**) as becomes clear in the overlay **(b)**. Fibroblasts from a patient with a general assembly disorder (Zellweger) showed no structures with both the probe (panel **d**) and anti-nsL-TP-Cy5 (panels **e,f**). The same experiment carried out with Cy5-labelled antibodies against acyl-CoA oxidase, catalase and PMP70 gave similar results (data not shown). Colour-image at the back of this thesis.

fibroblasts with defects in peroxisomal import of PTS1-bearing proteins. This probe was not incorporated into peroxisomes in fibroblasts from a patient with mutations in PEX5(9) and an isolated defect in PTS1 protein import. We also failed to detect its incorporation into peroxisomes in cells from a PEX6-deficient patient with Zellweger syndrome who is unable to import PTS1- or PTS2-containing peroxisomal proteins (10). No or few peroxisomal structures were detected in these cells when using either the probe or the Cy5-labelled antibodies (figures 1d-f). ATP depletion, produced by treating cells with deoxyglucose, prevented the translocation of SNAFL-2-PTS1 to peroxisomes (data not shown); the probe remained diffusely distributed throughout the cell. This finding is in agreement with studies that showed that the targeting and incorporation of PTS1-containing proteins into peroxisomes is ATP-dependent (11).

The uptake of SNAFL-2-PTS1 by peroxisomes enables one to determine the pH of these organelles *in situ*. This probe (pKa of 7.7) consists of a basic form with a $\lambda_{em,max}$ of 625 nm and an acidic form with a $\lambda_{em,max}$ of 546 nm. These spectral properties are identical to those of the uncoupled SNAFL-2. By determining the ratio of the red and green fluorescence intensity by confocal laser scanning microscopy, and by comparing this ratio with a pH-calibration curve, the pH can be calculated. Figure 2b shows these ratios for SNAFL-2-PTS1 taken up by human fibroblasts and for unconjugated (5-and 6)-carboxy-SNAFL-2 in the buffer. Figure 2a shows the peroxisomal localization of the probe before addition of (5-and 6)-carboxy-SNAFL-2 to the buffer. The peroxisomal structures in figure 2a coincide with the structures having a lower acid:base ratio than the buffer (figure 2b). From comparison with the pH-calibration series (figure 2c, upper inset) it can be inferred that the pH of the

human fibroblast peroxisome is basic. We carried out identical ratio imaging experiments were carried out with fibroblasts from RCDP type 1 patients. The ratio image (figure 2c) shows no distinct structures although a clear peroxisomal localization of the SNAFL-2-PTS1 probe is observed (lower inset). Thus the pH in the peroxisomes (localization as outlined in figure 2c) is quite similar to that of the cytosol (i.e. pH 7.2).

The dissipation of the pH gradient in the RCDP fibroblasts must be a consequence of their mutations in PEX7 and the resulting defect in PTS2-protein import. RCDP cells are deficient in the known PTS2-targeted proteins alkyl-DHAP (dihydroxyacetone-phosphate) synthase and phytanoyl-CoA alpha hydroxylase and also in the PTS1 protein DHAP acyltransferase (3), the stability of which requires an interaction with alkyl-DHAP synthase (12). To determine whether the basic peroxisomal pH in wild-type cells is related to one of the enzymes deficient in the RCDP type 1 patients, we measured the pH in fibroblasts from patients with an isolated defect in DHAP acyltransferase (RCDP type 2(13)), alkyl-DHAP synthase (RCDP type 3 (14)) or phytanoyl-CoA alpha hydroxylase (Refsum disease (15)). All of these cells had a normal basic pH (data not shown). This indicates that the aberrant peroxisomal pH in RCDP type 1 cells must be due to a deficiency in some other enzyme that is not
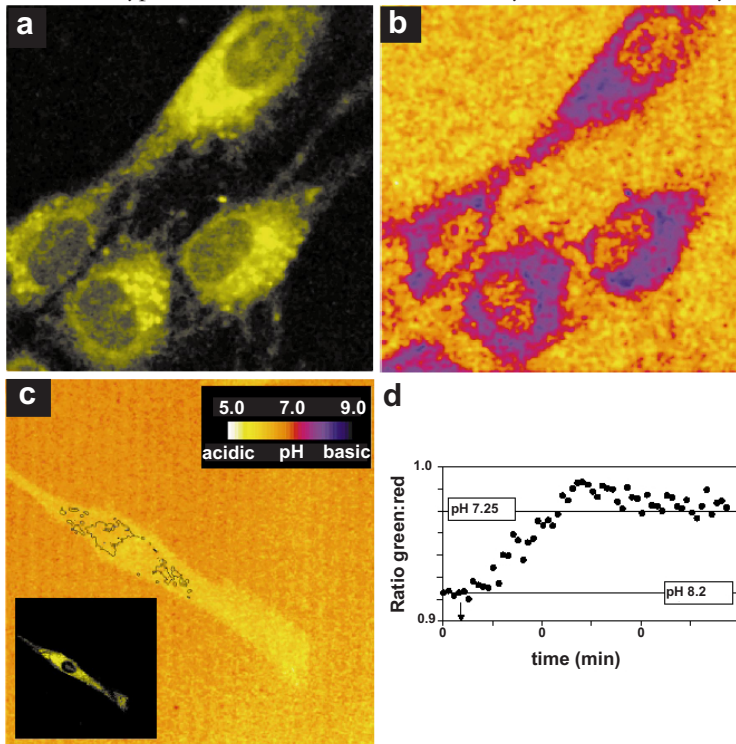
Figure 2. The peroxisomal pH in control and RCDP human fibroblasts. Control human fibroblasts were incubated with the pH-sensitive SNAFL-2-PTS1 (panel **a**). Free SNAFL-2 was added to the PBS++ and the ratio of the acidic and the basic form of the SNAFL-2 moiety both in the cell and in the PBS++ was measured. The peroxisomal structures in panel a coincide with the structures having a basic pH (panel **b**, and colour bar in panel **c**). The peroxisomes in fibroblasts from a patient with RCDP have a pH similar to that of the cytosol (panel **c**). The peroxisomal structures observed in the insert are outlined in black. Time-lapse ratio imaging after addition of the ionophore CCCP to control human fibroblasts was performed (panel **d**). Cells were labelled as described for panel **b**. Ratio images of the acidic over basic form of the SNAFL-2 moiety, both in the peroxisomes and in the PBS+ were taken every 30 sec. CCCP was added after 2 min (see arrow). For each image the acid/base ratio of the peroxisomes was normalised to that of the buffer (set at 1.00). Colour-image at the back of this thesis.

imported, destabilized or deprived of its substrate. The other possibility is that the mutations in PEX7, the PTS2 receptor, give rise to the formation of a transient pore in the peroxisome membrane, allowing protons to leak back into the peroxisome.

The origin of the basic pH in peroxisomes remains to be established. Depletion of ATP by deoxyglucose in human control fibrobalsts labelled with SNAFL-2-PTS1 did not result in a change in peroxisomal pH (data not shown), arguing against the involvement of an ATP-driven proton pump. On the other hand, addition of the uncoupler carbonyl *m*-chlorophenylhydrazone (0.5 μM) resulted in a complete dissipation of the gradient within 10 min (figure 2d). This indicates that the peroxisome membrane is impermeable to protons under normal conditions. The basic pH optimum and basic isoelectric point of most peroxisomal enzymes may reflect the adaptation to the alkalinity of the peroxisome.

Methods

Synthesis of the probes
The pH-sensitive SNAFL-2 was linked to one of the two lysines of the PTS1-peptide by incubating 1 mg acetyl-CKGGAKL-COOH (Ansynth Service BV Roosendaal, The Netherlands) and 0.5 mg carboxy-SNAFL-2-succinimidylester ((5-and 6-)-carboxy-seminaphto-fluoresceine-2 succinimidylester, Molecular Probes) in 0.2 ml bicine buffer (100 mM bicine-NaOH, pH 8.4, 1:1 diluted with *N,N*-dimethylformamide) for 2 h at 37°C in the dark under continuous stirring. The product was precipitated by adding $CHCl_3$ / MeOH (4:1, v/v). Further purification of the peptide carrying the fluorophore on the lysine near the N-terminus was done by TLC and reversed phase HPLC on an Alltech C18 column (econosil, 250 mm). An analogous probe was synthesized containing the fluorophore BODIPY 530/550 IA (Molecular Probes) linked to cysteine group of the same heptapeptide. This probe was suitable for co-localization studies with Cy5-labelled antibodies in fixed cells.

Fluorescently labelled antibodies
Antibodies against the peroxisomal proteins acyl-CoA oxidase, catalase, PMP70, and non-specific lipid-transfer protein (nsL-TP) (purified by Dr. B.C. Ossendorp), were labelled with Cy5-sulfoindocyanine as described in Wouters *et al.* (16).

Tissue culture
Fibroblasts from patients with peroxisomal disorders and human control fibroblasts were cultured in HAM F-10 nutrient mix (Gibco) supplemented with 10% fetal calf serum and Penicillin/streptomycin (1%, Gibco), under a 5% CO_2 - atmosphere. The N-ALD patient with an isolated PTS1 import deficiency (complementation group 2 of the Kennedy Krieger Institute) has been described before (9). The Zellweger patient belonged to complementation group 4 (10). The RCDP patient was of type 1 (complementation group 11 of the Kennedy Krieger Institute) and was described before (8). The patients with dihydroxyacetonephosphate-acyltranserase deficiency (RCDP type 2)(13) and alkyl-dihydroxyacetonephosphate-synthase deficiency (RCDP type 3)(14) were described before.

Labelling of cells and confocal laser scanning microscopy
The medium of cells cultured on coverslips was replaced by enriched phosphate buffered saline (PBS++ :137 mM NaCl, 2.7 mM KCl, 0.5 mM $MgCl_2$, 0.9 mM $CaCl_2$, 1.5 mM

KH$_2$PO$_4$, 8.1 mM Na$_2$HPO$_4$, supplemented with 5 mM glucose, pH 7.25) containing the PTS1-probes at a concentration of ± 5 µg/ml. After 1 h at 37°C the cells were rinsed with fresh PBS++, left for another 15 min and mounted in a temperature controlled lifechamber under the CLSM. Images were taken with a Leica TCSNT confocal laser-scanning system on an inverted microscope DMIRBE (Leica Microsystems, GmbH, Heidelberg, Germany) with an argon-krypton laser as excitation source. The BODIPY-PTS1 was excited with the 488 nm laserline and the emission was detected using a 530/30 bandpass filter. The green and the red fluorescence of SNAFL-2-PTS1 was acquired simultaneously using double wavelength excitation (laserlines 488 nm and the 568 nm) and emission (bandpass filters of 530/30 nm and 600/30 nm). Double labelling experiments were performed, using BODIPY-PTS1 and Cy5-labelled anti-Acyl-CoA oxidase, anti-PMP70, anti-catalase or anti-nsL-TP. After loading with the probe, the cells were fixed and permeabilized in PBS, pH 7.4 containing 3% paraformaldehyde, 0.2 % Triton X-100 and 0.2% glutaric aldehyde EM grade for 1 h at room temperature. The samples were further prepared according to ref. 16. The PTS1-probe in these samples was imaged as described above. The Cy5-labelled antibodies were excited with the 647 nm laserline and their emission was detected using a 665 longpass filter.

pH Measurements

pH-Calibration curves were acquired from free SNAFL-2 and from SNAFL-2-PTS1 diluted in buffers with pHs ranging from 4.0 to 9.0 using a Quantum Master spectrofluorometer (PTI, Surbiton, Surrey, UK). The pH-dependent fluorescence of SNAFL-2 was not affected by its linkage to the PTS1-peptide. Small glass capillaries filled with the calibration samples were used to acquire the pH-calibration curve on the confocal laser-scanning microscope. Images of SNAFL-2-PTS1 in cells were collected using the same microscope settings as were used for the calibration. The ratio of two fluorescence images recorded at 488/530 nm (acidic form of SNAFL2) and 568/600 nm (basic form of SNAFL2) was calculated on a Macintosh PowerPC computer using the NIH image program (W.Rasband). Free SNAFL-2 was added to the buffer as internal reference. The ratio image was filtered 5 times with the 'smooth' option of the NIH-Image program to reduce noise.

ATP-depletion and dissipation of proton gradients

Fibroblasts under the CLSM were treated with PBS+ (PBS++ without glucose) supplemented with 10 mM deoxyglucose for 15 min at 37°C to deplete ATP. Proton gradients were dissipated by addition of the ionophore carbonyl m-chlorophenylhydrazone (0.5 µM) to PBS+

References

(1)   Wanders, R.J., Tager, J.M.(1998) Lipid metabolism in peroxisomes in relation to human disease.*Mol Aspects Med* **19,** 69-154 .

(2)   van den Bosch, H., Schutgens, R.B., Wanders, R.J., Tager, J.M.(1992)Biochemistry of peroxisomes. *Ann Rev Biochem* **61,** 157-197.

(3)   Wanders, R.J.(1999) Peroxisomal disorders: clinical, biochemical, and molecular aspects.*Neurochem Res* **24,** 565-580.

(4)   Subramani, S.(1998) Components involved in peroxisome import, biogenesis, proliferation, turnover, and movement.*Physiol Rev* **78,** 171-188.

(5)   van Roermund, C.W., Elgersma, Y., Singh, N., Wanders, R.J., Tabak, H.F. (1995)The membrane of peroxisomes in Saccharomyces cerevisiae is impermeable to NAD(H) and acetyl-CoA under *in vivo* conditions.*EMBO J* **14,** 3480-3486 .

(6)   Henke, B., Girzalsky, W., Berteaux-Lecellier, V., Erdmann, R.(1998) IDP3 encodes a peroxisomal NADP-dependent isocitrate dehydrogenase required for the beta-oxidation of unsaturated fatty acids. *J Biol Chem* **273,** 3702-3711.

(7)   Gould, S.J., Keller, G.A., Hosken, N., Wilkinson, J., Subramani, S.(1989) A conserved tripeptide sorts proteins to peroxisomes. *J Cell Biol* **108,** 1657-1664.

(8)   Motley, A.M., Hettema, E.H., Hogenhout, E.M., Brites, P., ten Asbroek, A.L., Wijburg, F.A., Baas, F., Heijmans, H.S., Tabak, H.F., Wanders, R.J., Distel, B.(1997) Rhizomelic chondrodysplasia punctata is a peroxisomal protein targeting disease caused by a non-functional PTS2 receptor. *Nat Genet* **15,** 377-380.

(9)   Dodt, G., Braverman, N., Wong, C., Moser, A., Moser, H.W., Watkins, P., Valle, D., Gould, S.J.(1995) Mutations in the PTS1 receptor gene, PXR1, define complementation group 2 of the peroxisome biogenesis disorders. *Nat Genet* **9,** 115-125.

(10)   Yahraus, T., Braverman, N., Dodt, G., Kalish, J.E., Morrell, J.C., Moser, H.W., Valle, D., Gould, S.J. (1996) The peroxisome biogenesis disorder group 4 gene, PXAAA1, encodes a cytoplasmic ATPase required for stability of the PTS1 receptor. *EMBO J* **15,** 2914-2923.

(11)   Dodt, G., Gould, S.J. (1996) Multiple PEX genes are required for proper subcellular distribution and stability of Pex5p, the PTS1 receptor: evidence that PTS1 protein import is mediated by a cycling receptor. *J Cell Biol* **135,** 1763-1774.

(12)   de Vet, E.C., Ijlst, L., Oostheim, W., Wanders, R.J., van den Bosch, H.(1998) Alkyl-dihydroxyacetonephosphate synthase. Fate in peroxisome biogenesis disorders and identification of the point mutation underlying a single enzyme deficiency. *J Biol Chem* **273,** 10296-10301.

(13)   Wanders, R.J., Schumacher, H., Heikoop, J., Schutgens, R.B., Tager, J.M.(1992) Human dihydroxyacetonephosphate acyltransferase deficiency: a new peroxisomal disorder. *J Inherit Metab Dis* **15,**359-391.

(14)   Wanders, R.J., Dekker, C., Hovarth, V.A., Schutgens, R.B., Tager, J.M., Van Laer, P., Lecoutere, D. (1994) Human alkyldihydroxyacetonephosphate synthase deficiency: a new peroxisomal disorder. *J Inherit Metab Dis* **17,** 315-318.

(15)   Mihalik, S.J., Morrell, J.C., Kim, D., Sacksteder, K.A., Watkins, P.A., Gould, S.J. (1997)Identification of PAHX, a Refsum disease gene. *Nat Genet* **17,** 185-189.

(16)   Wouters, F.S., Bastiaens, P.I., Wirtz, K.W., Jovin, T.M.(1998) FRET microscopy demonstrates molecular association of non-specific lipid transfer protein (nsL-TP) with fatty acid oxidation enzymes in peroxisomes. *EMBO J* **17,** 7179-7189.

Peptide–based targeting of fluorophores to peroxisomes in living cells.

Eward H.W. Pap, Tobias B. Dansen & Karel W.A. Wirtz (2001)

Peptide–based targeting of fluorophores to peroxisomes in living cells.

Eward H.W. Pap, Tobias B. Dansen & Karel W.A. Wirtz

Biochemistry of Lipids Dept, Utrecht University, PO Box 80.054, 3508 TB Utrecht, The Netherlands.

Peptides carrying different fluorophores can be designed to incorporate spontaneously into living cells when added to the medium. By incorporating the peroxisome-targeting sequence PTS1, the peptide is recognized by the protein-import machinery of peroxisomes and, as a result, can accumulate in these organelles. Depending on the cell type, an inhibitor of the multidrug-resistance protein might be required to ensure strong accumulation. In this update, we discuss the potential of these peptide-linked fluorophores in solving issues related to organelle function and dynamics.

Fluorescent peptides form a new generation of analytical tools to visualize intracellular processes and molecular interactions at the level of single cells. The peptide-based reporters combine the sensitivity of fluorescence detection with the information specificity of amino acid sequences. Recently, we reported that a membrane-permeable PTS1–peptide carrying fluorophores could be targeted to peroxisomes in intact cells (1). By using this fluorescent peptide, the morphology and dynamics of peroxisomes can be studied. In addition, the functional integrity of the peroxisomal protein-import machineries can be evaluated in mutant cells and in cells of patients. The accumulation of the fluorescent PTS1–peptide in peroxisomes occurs within minutes, whereas the staining of peroxisomes by immunolocalization or by PTS1-targeted green-fluorescent protein (GFP) constructs takes several hours. Moreover, the peptide can deliver parameter-sensitive fluorophores (such as pH or calcium probes) for exploring the local environment of these organelles. The uptake of short unstructured peptides has been observed before and is mainly determined by net charge and by other physico-chemical properties such as hydrophobicity (2). For large peptides (more than 20 amino acid residues) to cross the membrane, distinct tertiary structures derived from, for example, the TAT-domain from HIV (3,4) or from the antennapedia homeodomain of Drosophila (5,6) are of primary importance.

Specific accumulation of the PTS1–peptide in peroxisomes.

Proteins destined for the peroxisomes are synthesized on free ribosomes in the cytosol. They accumulate in this organelle by interaction with receptors that facilitate active import. Two main types of peroxisomal targeting signal (PTS) have been identified that reside either at the C-terminus (PTS1) or near the N-terminus (PTS2) of the protein. PTS1 comprises a tripep-

tide (A/S/C)-(K/R/H)-L and is found in most peroxisomal matrix proteins (7). We recently demonstrated that specific targeting of fluorophores to peroxisomes can be achieved by use of the membrane–permeable peptide CKGGAKL containing the PTS1 motif (see Fig. 1). To minimize the charge of this PTS1–peptide, its N-terminus was acetylated. The fluorophores boron dipyromethene difluoride (BODIPY) or carboxy-seminaphtho-fluorescein (SNAFL) were covalently coupled to a single cysteine residue or to a lysine residue in the peptide. These fluorophores are uncharged and hydrophobic, thereby enhancing the affinity of the ensuing peptides for the cell membrane. To circumvent interference of the fluorophore with the site of recognition of the organelle-specific peptide, one or two glycine residues were positioned between the cysteine residue and the targeting motif.

When added to the growth medium of cultured cells, the fluorescent PTS1-peptide was rapidly internalized at room temperature. Typically, the fluorescence was visible in the cell after 5 min or less. Since uptake was also apparent at 10°C, it appears that endocytosis is most likely not involved. Thus, we have to assume that the SNAFL and BODIPY-labelled peptides are sufficiently hydrophobic to be able to pass through the membrane directly themselves. The PTS1–peptide is taken up by rat-1 fibroblasts and is concentrated in small 'grain-like' organelles (Fig. 1a). Complete colocalization with antibodies against the peroxisomal
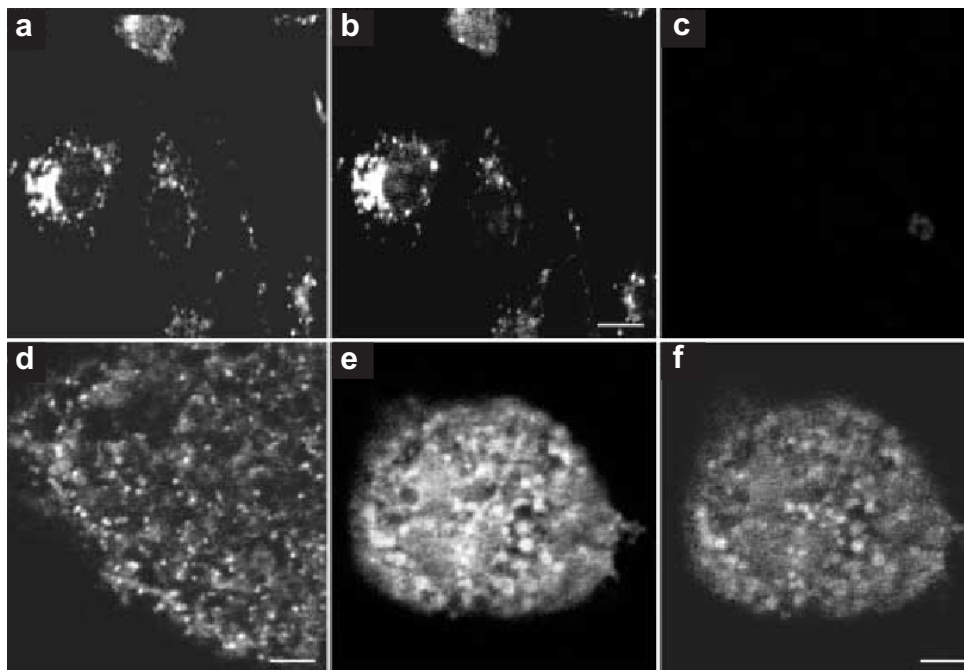
Fig. 1. Localization in rat-1 fibroblasts of the fluorescent PTS1–peptide (a) and the peroxisomal marker acyl-coenzyme A oxidase (stained with a Cy5-labelled antibody) **(b)**. In untreated HepG2 hepatoma cells, no labelling of peroxisomes by the fluorescent PTS1–peptide is observed **(c)**. Counterstaining of the same cell with antibodies against non specific lipid transfer protein (nsLTP) conjugated to Cy5 demonstrates that peroxisomes are abundantly present **(d)**. Peroxisomal localization of BODIPY[581/591]–PTS1 in HepG2 hepatoma cells that have been treated with 5 μm verapamil is shown in **(e)**. The structures labelling with high intensity coincide with those revealed by antibodies against nsLTP-Cy5 (f). Thus the lack of labelling in **(c)** might be attributable to the activity of multidrug-resistance (MDR) transporters that are known to be inhibited by verapamil. Bars, 10 μm **(b)**, 5 μm **(d)** and 10 μm **(f)**.

acyl–coenzyme A oxidase indicates that these organelles are peroxisomes (Fig. 1b). A similar distribution of the PTS1–peptide has been observed in human fibroblasts (1). In that study, it was established that the import of the PTS1–peptide into peroxisomes is ATP dependent. In contrast to this distinct peroxisomal localization, the PTS1–peptide remained distributed diffusely throughout the cytoplasm of fibroblasts from Zellweger patients who suffer from impaired PTS1-dependent protein import. The PTS1-peptide was also used to carry the pH-sensitive fluorophore SNAFL to peroxisomes. Upon accumulation in this organelle, the peptide–probe reported a basic pH (1).
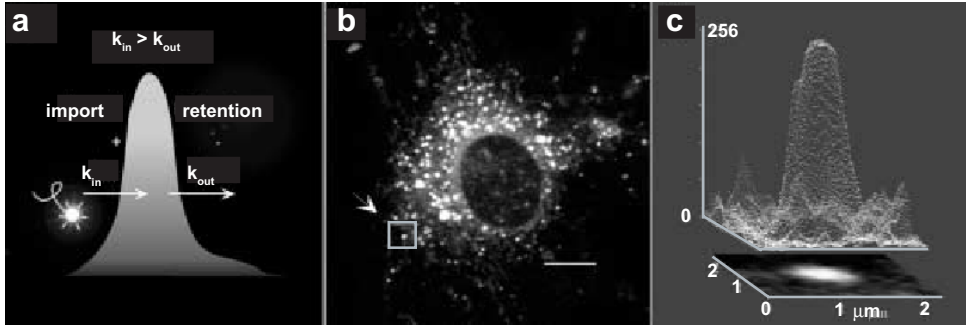
Fig. 2. (a) The concentration of fluorescent peptides in each cellular organelle is determined by their relative rates of entry and extrusion. Accumulation of the peptide takes place when k_{in} exceeds k_{out}. This can be achieved by active import or by retention of a peptide.**(b)** A rat-1 fibroblast after labelling with the fluorescent PTS1-peptide. Bar, 10 μm. **(c)**Presented is a surface plot of the fluorescence intensity of the peroxisomal structure thatis marked with an arrow in panel **(b)**.

Recognition of fluorescent PTS1–peptide by multidrug-resistance proteins

As indicated by several laboratories, a complicating factor for peptide internalization can be the activity of energy-dependent transporters in the plasma membrane (8–10) . Rapid extrusion of peptides by transporters of the ATP-binding cassette family (e.g. multidrug-resistance (Mdr) proteins) was observed. Consistent with the high levels of Mdr proteins in HepG2 hepatoma cells (11), the PTS1–peptide did not accumulate in these cells (Fig. 1c). By counterstaining with a Cy5-labelled antibody against the peroxisomal non-specific lipid transfer protein (nsLTP), we confirmed that peroxisomes are abundant in these cells (Fig. 1d). As shown in Fig. 1e, in the presence of the Mdr-reversing agent verapamil, the PTS1–peptide is internalized efficiently. This demonstrates that, in the absence of verapamil, the export of the PTS1–peptide is at least as efficient as its uptake by HepG2 hepatoma cells.

Membrane permeability versus accumulation

It is remarkable that a peptide that passes through the plasma membrane does accumulate in a specific organelle. After all, it could be expected that, as a consequence of its membrane permeability, the peptide will leak continuously across the organellar membrane. However, given that accumulation of peptides occurs, we have to assume that the rate of entry is greater than the rate of exit ($k_{in} > k_{out}$; Fig. 2a). For the PTS1–peptide accumulating in the peroxisomes (Fig. 2b), this condition is satisfied by active import exceeding passive export. A surface plot of the fluorescence distribution, as shown in Fig. 2c, indicates that the PTS1–peptide gradient over the peroxisomal membrane can be steep. The fluorescence intensity at the centre of the peroxisome has a value of 256, whereas the average surrounding fluorescence intensity corre-

sponds to a value of 8.This indicates that the active import results in a more than 30-fold increase of the PTS1–peptide concentration over the peroxisomal membrane.

The future

The fluorescent PTS1–peptide is one of a series of organelle-specific peptides to be developed. Studies on membrane-permeable peptides carrying signal sequences that are recognized by receptors on the endoplasmic reticulum and the trans-Golgi network are currently in progress. With the advance of this new generation of bioactive reporter molecules, the biogenesis, morphology and dynamics of single organelles will be increasingly visualized with spatio-temporal resolution in living cells (see chapter 6).

Acknowledgements

References

(1) Dansen, T. B., Wirtz, K.W.A., Wanders, R.J.A., Pap, E.H.W. (2000) Peroxisomes in human fibroblasts have a basic pH. *Nat Cell Biol.* **2,**51-53.

(2) Allentoff, A.J., Mandiyan, S., Liang, H., Yuryev, A., Vlattas, I., Duelfer, T., Sytwu, I.I., Wennogle, L.P. (1999) Understanding the cellular uptake of phosphopeptides.*Cell Biochem. Biophys.* **31,**129-140.

(3) Vives, E., Brodin, P., Lebleu, B. (1997) A truncated HIV-1 Tat protein basic domain rapidly translocates through the plasma membrane and accumulates in the cell nucleus. *J. Biol. Chem.* **272,**16010-16017.

(4) Schwarze, S.R., Hruska, K.A., Dowdy, S.F. (2000) Protein transduction: unrestricted delivery into all cells? *Trends Cell Biol.* **10,**290-295.

(5) Perez, F., Joliot, A., Bloch-Gallego, E., Zahraoui, A., Triller, A., Prochiantz, A. (1992) Antennapedia homeobox as a signal for the cellular internalization and nuclear addressing of a small exogenous peptide. *J. Cell Sci.* **102,**717-722.

(6) Prochiantz, A. (1996) Getting hydrophilic compounds into cells: lessons from homeopeptides.*Curr. Opin. Neurobiol.* **6,**629-634.

(7) Gould, S.J., Keller, G.A., Hosken, N., Wilkinson, J., Subramani, S.(1989) A conserved tripeptide sorts proteins to peroxisomes. *J Cell Biol* **108,** 1657-1664.

(8) Oehlke, J., Beyermann, M., Wiesner, B., Melzig, M., Berger, H., Krause, E., Bienert, M. (1997) Evidence for extensive and non-specific translocation of oligopeptides across plasma membranes of mammalian cells. *Biochim. Biophys. Acta* **1330,**50-60.

(9) Sarkadi, B., Muller, M., Homolya, L., Hollo, Z., Seprodi, J., Germann, U.A., Gottesman, M.M., Price, E.M., Boucher, R.C. (1994) Interaction of bioactive hydrophobic peptides with the human multidrug transporter. *FASEB J.* **8,**766-770.

(10) Sharma, R.C., Inoue, S., Roitelman, J., Schimke, R.T., Simoni, R.D. (1992) Peptide transport by the multidrug resistance pump. *J. Biol. Chem.* **267,**5731-5734.

(11) Roelofsen, H., Vos, T.A., Schippers, I.J., Kuipers, F., Koning, H., Moshage, H., Jansen, P.L., Muller, M. (1997) Increased levels of the multidrug resistance protein in lateral membranes of proliferating hepatocyte-derived cells. *Gastroenterology* **112,**511-521.
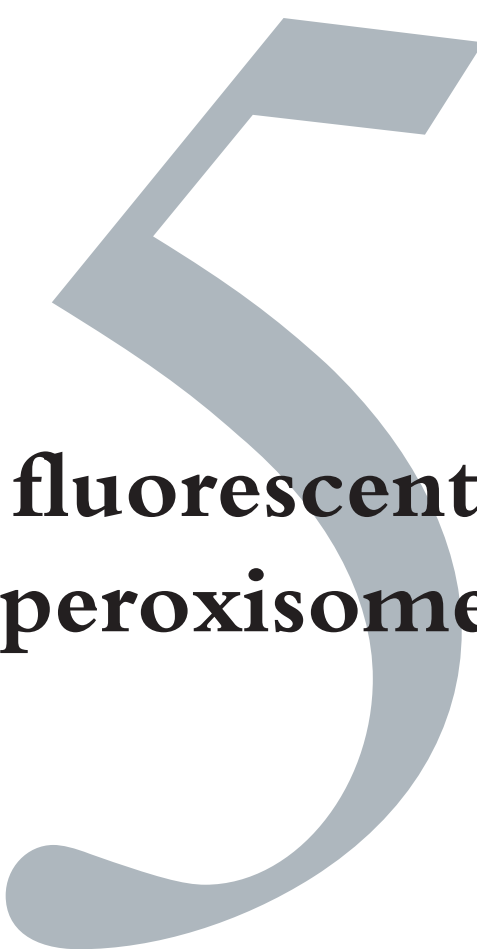
Targeted fluorescent probes in peroxisome function.

Tobias B. Dansen, Eward H.W. Pap, Ronald J.A. Wanders & Karel W.A. Wirtz (2001) *The Histochemical Journal* **33(2),**65-69.

review
Targeted fluorescent probes in peroxisome function.

Tobias B. Dansen[1], Eward H.W. Pap[1], Ronald J.A. Wanders[2] & Karel W.A. Wirtz[1]

1.   *Institute of Biomembranes, Centre for Biomembranes and Lipid Enzymology, Department of Biochemistry of Lipids, Utrecht University, Padualaan 8, PO Box 80054, 3508 TB Utrecht, The Netherlands.*
2.   *Academic Medical Centre, Departments of Clinical Chemistry and Pediatrics, University of Amsterdam, Meibergdreef 9, NL-1105 AZ Amsterdam, The Netherlands.*

Summary

Fluorescent peptides form a new generation of analytical tools to visualize intracellular processes and molecular interactions at the level of single cells. The peptide-based reporters combine the sensitivity of fluorescence detection with the information specificity of amino acid sequences. Recently we have succeeded in targeting a fluorescent heptapeptide (acetyl-CKGGAKL) carrying a peroxisomal targeting signal (PTS1) to peroxisomes in intact cells. The fluorophores conjugated to the PTS1-peptide were fluorescein, BODIPY and the pH-sensitive SNAFL-2. When added to the cells these fluorescent peptides were internalized at 37°C and typically visible in the cell after 15 min or less. Cells lacking an active peroxisomal protein import system as in the case of Zellweger syndrome were stained diffusely throughout the cell. Uptake of the peptide probes was not inhibited at 4°C or when the cells were depleted of ATP; yet under these conditions translocation to peroxisomes was blocked. This indicates that the uptake by cells is diffusion-driven and not an active process. Using the SNAFL-2-PTS1 peptide we established by ratio-imaging that peroxisomes of human fibroblasts have a pH of 8.2. The concurrent pH gradient over the peroxisomal membrane was dissipated when an ionophore (CCCP) was added. In fibroblasts of RCDP patients with defects in the peroxisomal import of proteins carrying a PTS2 sequence, import of the PTS1-peptide probe into peroxisomes appeared normal, but these peroxisomes have a pH of 6.8 equal to that of the cytosol. Coupling different fluorophores to the PTS1-peptide offers the possibility to determine in time and space as to how peroxisomes function in living cells.

Introduction

Since the discovery of the peroxisome (1) and the first biochemical studies by De Duve and Baudhuin (2) much progress has been made in understanding the properties of this organelle.

Most of the knowledge on peroxisomes has been gathered by electron microscopy and other cytochemical techniques, by protein characterization on isolated organelles, or with the help of DNA techniques. By use of these approaches, the morphology and composition of the peroxisome as well as many of the factors required for biogenesis of peroxisomes has been subject of intensive study during the last decade (3). The peroxisome bound by a single membrane, is a fragile organelle that easily loses its integrity upon isolation (4). Therefore, despite our extensive knowledge about the biochemical properties of the peroxisome, relatively little is known about its biophysical properties and its *in vivo* functioning. This, however, can be remedied by having available a non-invasive method that is applicable in living cells. Recently constructs of green fluorescent protein (or derivatives) carrying a build-in peroxisomal targeting sequence, were used to measure peroxisome dynamics in cells (5,6). Here we discuss fluorescent peptide probes that by being membrane-permeable, can be targeted to peroxisomes in the living cell. By using these fluorescent peptides, the morphology,
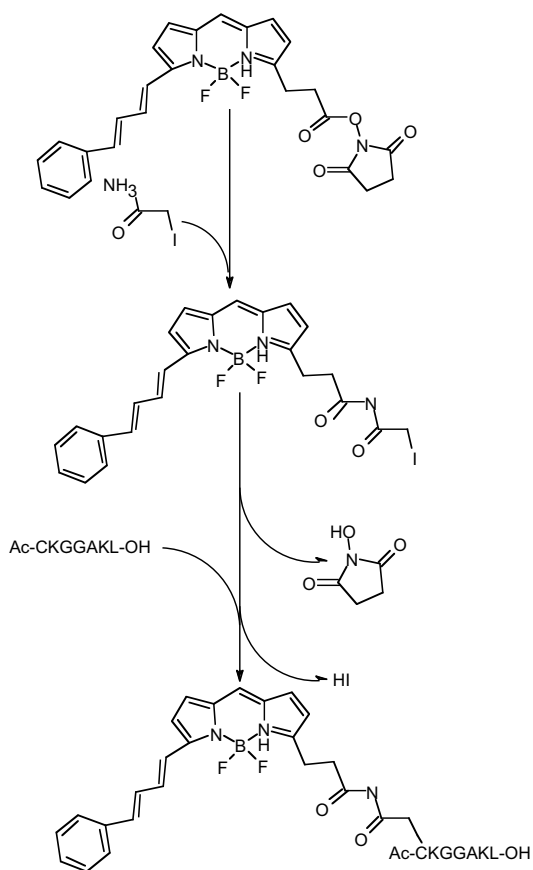
Figure 1. The coupling of a fluorescent probe to a peptide carrying a peroxisomal targeting signal. A BODIPY-succinimidylester is first linked to iodoacetamide. The apolar iodoacetamide-linked BODIPY is separated from the excess iodoacetamide by extraction with chloroform /methanol (1:2 v/v). Then this moiety is linked to the cysteine residue of the heptapeptide CKGGAKL that contains a PTS1 at the C-terminus (underlined). In some instances the iodoacetamide-linked form of fluorophores is commercially available. Alternatively, succinimidylester derivatives of fluorophores can be linked directly to the amino-group of lysine-residues.

Figure 2. Thin layer chromatogram of the reaction product of fluorescein-iodoacetamide and the heptapeptide CKGGAKL. Lane **A** shows the free fluorophore and lane **B** the reaction mixture (the lower spot is the peptide-linked fluorophore). Samples containing approximately 0.02 μg of fluorescein were applied to TLC (Silicagel DC-Fertig, Merck) and run with the eluens chloroform/methanol/water/ammonia (16/10/1/1 v/v/v/v). Spots were visualized by transmitted UV light.

biophysical properties and dynamics of peroxisomes can be studied. In addition, the functional integrity of the peroxisomal protein import machineries can be evaluated in mutant cells and in cells of patients.

Probe design

Proteins are targeted to the peroxisomal matrix by two distinct pathways that make use of either a peroxisomal targeting signal type 1 (PTS1) or type 2 (PTS2) (7). Most peroxisomal matrix proteins carry a PTS1 which comprises a C-terminal tripeptide with the consensus sequence (C/A/S)-(K/R/H)-(L/I)-COOH (8). The PTS2 is more complex located near the N-terminus with the consensus sequence (R/K)-L-X_5-(Q/K)-L .The peptide probe used in the present study is targeted towards the peroxisomes by way of a PTS1. Given that the peptide–probe is added to intact cells it should be able to pass the plasma membrane prior to getting to the peroxisomes. We have achieved this goal by designing the heptapeptide acetyl-CKGGAKL carrying one positive charge and AKL as the PTS1 The positive charge of the N-terminus is blocked by acetylation thereby enhancing the apolar character of the peptide. For the purpose of targeting it is of importance that the C-terminus is indeed a free carboxyl group. It is to be noted that most companies synthesizing peptides have a choice option for this C-terminus. Moreover, the peptide contained two glycine residues located between the PTS1 and the amino acid residues Cys and Lys both of which are suitable sites of coupling for the fluorescent moiety (see figure 1). This spacer prevents the possible steric hindrance of the PTS1 by the fluorescent group. Fluorescent derivatives are commercially available that are reactive towards lysine or cysteine residues. So succinimidyl–esters of fluorescent groups can be linked to the lysine residue and the iodoacetamide and maleimide derivatives to the thiol group of cysteine. It is also possible to convert a fluorescent group that is available as a succinimidyl ester, to a thiol-reactive derivative by linking it first to the amide group of iodoacetamide (see figure 1). For a complete introduction into peptide labelling we refer to the Handbook of Fluorescent Probes, chapter 1 and 2 (Haugland , 1996).

The coupling of the fluorescent groups to peptides was routinely checked by TLC using chloroform/methanol/acetic acid/water (25:15:3:2, v/v) as solvent. By illuminating he TLC-plate with UV, the fluorescently labelled product and the free fluorophore may be visualized (fig. 2). As can be expected, the mobility of the fluorophore linked to the peptide is much less than that of the unreacted group. In the reaction mixture the fluorophores are present in a two-fold molar excess so to assure an optimal yield of the labelled peptide. The peptide-probes are purified by precipitation with chloroform/methanol (3:1, v/v). In practice, purification by precipitation is sufficient (>90% pure). HPLC can be used if a completely homogeneous product is required.

Fluorescent moieties are usually lipophilic most probably facilitating the rapid uptake of the peptide conjugates by living cells. An enormous variety of fluorescent probes is commercially available, amongst which a large number that change spectral properties depending on their environment, or upon reaction with, for instance, calcium or reactive oxygen species.

### Loading of cells with the probes

Cells grown on coverslips are placed in a temperature-controlled holder in an inverted confocal
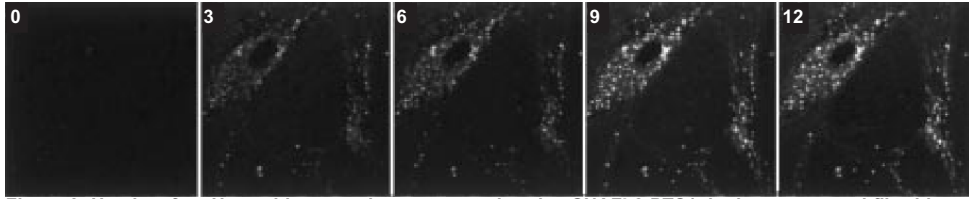
Figure 3. Uptake of a pH-sensitive peroxisome targeted probe, SNAFL2-PTS1, by human control fibroblasts. The probe was added in PBS+ and taken up at 37˚C. The probe localizes to punctated structures within 10 min. Time in min is indicated after addition of the probe.

scanning laser microscope. The medium (DMEM Bicarbonate supplemented with 10% fetal calf serum) is replaced with phosphate–buffered saline supplemented with calcium (0.9 mM), magnesium (0.5 mM) and glucose (5 mM) to keep the cells in good condition during the measurements carried out at 37°C. The probe, dissolved in 50% ethanol, is added to this buffer to a final concentration of ~0.05 μg/ml. Loading of the cells in culture medium is possible but requires more probe because of its binding to components of the calf serum. Uptake of the probe by fibroblasts takes place within 10 min (figure 3). After 20 min, the cells are washed with fresh buffer and the probe present in the cytosol is allowed to translocate to the peroxisomes. The punctate staining is observed in all cells and has an uniform intensity, except in cells that are dying or clearly damaged. We observed that the probe crosses the plasma membrane at 4°C and under conditions where ATP is depleted with deoxyglucose (9,10). However, the staining remains distributed diffusely throughout the cell. This implies that the probes crosses the plasma membrane by diffusion rather than by endocytosis and that the translocation to and/or import into the peroxisome are energy- and temperature–dependent. Cells loaded with probe at 4°C and subsequently warmed to 37°C yielded the punctated structures characteristic for peroxisomes. The amount of probe taken up at 4°C and 37°C in the cells appears to be comparable, although this is difficult to estimate because of the different localization of the probe at these temperatures.

Incubation of human hepatoma cells (HepG2) with the probe failed to give peroxisomal
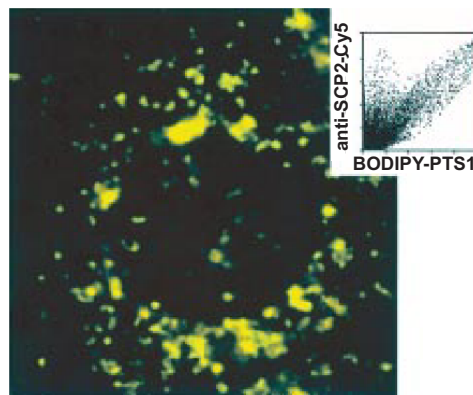
Figure 4. Colocalization of a peroxisome targeted probe (BODIPY-PTS1) and the Cy5-labelled peroxisome-specific antibody against the non-specific lipid transfer protein (anti-SCP2 Cy5). The fluorescence of the probe is given in red and that of the fluorescent antibody in green. Overlapping structures appear in yellow. The staining of the probe coincides mostly with that of the antibody. Some structures labelled with antibody show no label with the probe. This can be due to loss of probe during the fixation, or heterogeneity in import-competence of peroxisomes as described before. There are no structures that show only the probe, confirming its unique peroxisomal localization. The image represents an area of approximately 25x25 μm. The inset shows a correlation plot of the intensities of the two fluorescent labels indicating a nice co-localization. Colour-image at the back of this thesis.

labelling. However, when verapamil was added to inhibit the multi-drug resistance protein (mdr), the peroxisomes did become labelled. This indicates that the peptide-probe is recognized by the mdr which is overexpressed in the hepatoma cells and known to eject cationic lipophilic molecules (10,11).

Localization of the targeted fluorophores

It is very important to confirm that the probe indeed ends up in peroxisomes. For instance, it is possible that coupling of the fluorophore to the peptide may interfere with its recognition by the peroxisome import machinery. Another complication could be the accumulation in lipid-droplets, mitochondria or other compartments involved in the storage and degradation of xenobiotics. By immunolocalization with fluorescent antibodies the peroxisomal localization of the probe was established (figure 4). Since small peptides are difficult to fix we had to use glutaraldehyde as a crosslinker so as to prevent loss of the probe during fixation. Another problem is that not all peroxisomes are necessarily loaded with the probe. This might be due to a non-uniform protein-import competency of peroxisomes (12). As a negative control for peroxisomal staining we used fibroblasts from patients with generalized peroxisome biogenesis disorders (figure 5) (9). Patients with Zellweger's cerebro hepato-renal syndrome (ZS) completely lack peroxisomal import by both PTS1 and PTS2. An isolated loss of import of PTS1 proteins leads to neonatal adrenoleukodystrophy (N-ALD) whereas the inability to
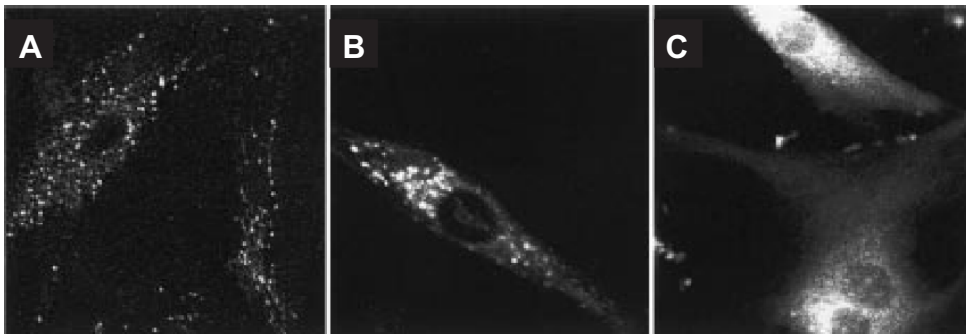
Figure 5. Localization of the PTS1-SNAFL2 probe in patient cells. Localization of the probe in fibroblasts from (**A**) human controls, (**B**) an RCDP patient and (**C**) a Zellweger patient. The probe localizes in peroxisomes in the control and the RCDP patient. A diffuse cytosolic staining is observed in the Zellweger patient.

import PTS2 proteins leads to the rhizomelic form of chondrodysplasia punctata (RCDP) (3). Fibroblasts from a ZS (fig5c) and N-ALD patient (data not shown) gave a uniform cytosolic staining upon loading with the probe confirming its specificity for peroxisomes. This staining is comparable to that observed when the cells are loaded in absence of ATP. The fibroblasts from RCDP patients did accumulate the probe in peroxisomes as expected (fig 5b).

Applications

The applications of the peptide probes described in this paper are numerous. For instance, the screening of fibroblasts for a peroxisome biogenesis disorder is possible. It can also be a useful tool for the elucidation of peroxisome biogenesis and breakdown. Biophysical data can be obtained when fluorophores are used that have function-specific spectral characteristics.

Using a fluorescent pH–dependent ratio probe linked to a PTS1–peptide (PTS1–SNAFL2) we discovered that the peroxisomal membrane is impermeable to protons and that the matrix of the peroxisome is alkaline (pH 8.2). Furthermore we established that the peroxisomes in fibroblasts from a patient with a generalized PTS2 import disorder (RCDP type1) had a neutral pH. RCDP type1 patients lack the PTS2 proteins alkyl–DHAP–synthase and phytanoyl–CoA hydroxylase whilst the PTS1 protein DHAP–acyltransferase is unstable (13). We measured the pH in peroxisomes in fibroblasts from three other patients: an RCDP type 2 patient lacking only the DHAP–acyltransferase, an RCDP type 3 patient defective in alkyl–DHAP–synthase and a Refsum patient with an isolated defect in phytanoyl–CoA hydroxylase. The peroxisomes of all these patients had a normal alkaline pH. In this way we established that the dissipated pH–gradient in the RCDP patient must be due to some other PTS2 protein that is missing, destabilized or deprived of its substrate (9).

Concluding remarks

The application of the pH–sensitive peptide–probe is one example of measuring a biophysical parameter of peroxisomes in living cells. More recently we have developed another probe that monitors the oxidative stress in the peroxisome. Furthermore, membrane–permeable peptide–probes have been synthesized with targeting or retention signals for other organelles including Golgi, endoplasmic reticulum and the nucleus (14). The availability of these fluorescently–labelled targeted peptides enables one to measure several processes at the sub-cellular level by light microscopic techniques.

References

(1)   Rhodin, J. (1954) Correlation of ultrastructural organization and function in normal and experimentally changed proximal tubule cells of the mouse kidney *PhD. Thesis* , *Karolinska Institutet Stockholm, Sweden.*

(2)   de Duve, C., Baudhuin, P. (1966) Peroxisomes (microbodies and related particles). *Physiol. Rev.* **46**, 323-357.

(3)   Gould, S.J., Valle, D. (2000) Peroxisome biogenesis disorders, genetics and cell biology. *Trends Genet.***16**, 340-345.

(4)   Subramani, S. (1998) Components involved in peroxisome import, biogenesis, proliferation, turnover, and movement. *Physiol. Rev.***78**, 171-188.

(5)   Huber, C., Saffrich, R., Anton, M., Passreiter, M., Ansorge, W., Gorgas, K., Just, W. (1997) A heterotrimeric G protein-phospholipase A2 signalling cascade is involved in the regulation of peroxisomal motility in CHO cells. *J. Cell Sci.* **110**, 2955-2968.

(6)   Schrader, M., Wodopia, R., Fahimi, H.D. (1999) Induction of tubular peroxisomes by UV irradiation and reactive oxygen species in HepG2 cells. *J. Histochem. Cytochem.* **47**, 1141-1148.

(7)   Hettema, E.H., Distel, B., Tabak, H.F. (1999) Import of proteins into peroxisomes. *Biochi. Biophy. Acta* **1451**, 17-34.

(8)   Gould, S.J., Keller, G.A., Hosken, N., Wilkinson, J., Subramani, S. (1989) A conserved tripeptide sorts proteins to peroxisomes. *J Cell Biol.* **108**, 1657-1664.

(9)   Dansen, T.B., Wirtz, K.W.A., Wanders, R.J.A., Pap, E.H.W. (2000) Peroxisomes in human fibroblasts have a basic pH. *Nature Cell Biol.* **2**, 51-53.

(10)   Pap, E.H.W., Dansen, T.B., Wirtz, K.W.A. (2001) Peptide-based targeting of fluorophores to peroxisomes in living cells. *Trends Cell Biol.* **11**, 10-12.

(11)   Roelofsen, H., Vos, T.A., Schippers, I.J., Kuipers, F., Koning, H., Moshage, Jansen, P.L., Muller, M. (1997) Increased levels of multidrug resistance protein in lateral membranes of proliferating hepatocyte derived cells. *Gastroenterology* **112,** 511-521.

(12)   Völkl, A., Mohr, H., and Fahimi, H.D. (1999) Peroxisome subpopulations of the rat liver: isolation by immune free flow electrophoresis. *J. Histochem. Cytochem.* **47,** 1111-1117.

(13)   Wanders, R.J. (1999) Peroxisomal disorders: clinical, biochemical, and molecular aspects. *Neurochem. Res.* **24**, 565-580.

(14)   Pap, E.H.W., Dansen, T.B., van Summeren, R., Wirtz, K.W.A. (2001) Peptide-based targeting of fluorophores to organelles in living cells. *Exp Cell Res.* **265,** 288-293.

Peptide–based targeting of fluorophores to organelles in living cells.

**Eward H.W. Pap, Tobias B. Dansen, Ruben van Summeren &
Karel W.A. Wirtz (2001)** *Experimental Cell Research* **265,**288-293.

Peptide-based targeting of fluorophores to organelles in living cells.

Eward H.W. Pap, Tobias B. Dansen, Ruben van Summeren & Karel W.A. Wirtz.

Institute of Biomembranes, Department of Biochemistry of Lipids, Utrecht University, P.O. Box 80.054, 3508 TB Utrecht, The Netherlands .

Abstract

Peptides carrying organelle specific import- or retention sequences can target the fluorophore BODIPY$^{581/591}$ to the nucleus, peroxisomes, endoplasmic reticulum (ER) or the trans-Golgi network (TGN). The peroxisomal peptide contains the PTS1 sequence AKL. For targeting to the ER or TGN the peptides carry the retention sequences KDEL and SDYQRL, respectively. A peptide carrying the nuclear leader sequence of the simian virus SV40 large tumor antigen, KKKRK, was used to direct the fluorophore to the nucleus. The fluorescent peptides for peroxisomes, ER and the TGN spontaneously incorporate into living fibroblasts at 37° C and accumulate in their target organelles within minutes. The uptake is still significant at 4° C indicating that endocytosis is not required for internalization. The highly charged nuclear peptide (net charge +4) does not spontaneously internalize. However, by transient permeabilization of the plasma membrane, this fluorescent peptide could accumulate in the nucleus. These fluorescent peptides open new opportunities to follow various aspects of specific organelles such as their morphology, biogenesis, dynamics, degradation and their internal parameters (pH, redox).

Introduction

Fluorescently labelled peptides form a new class of analytical tools to visualize intracellular processes and molecular interactions at the level of single cells. The peptide-based reporters combine the sensitivity of fluorescence detection with the information specificity of amino acid sequences. Fluorescently labelled peptide-hormones have been used to detect the binding of hormones to receptors at the cellular surface (1) and their subsequent internalization and routing to acidic intracellular compartments (2). A number of fluorescent substrates have been developed to detect the activity of proteases (3). Fluorescently labelled heptapeptides mimicking the carboxy-terminal sequence of N-ras, were reversibly acylated in cultured mammalian fibroblasts (4). A fluorescent substrate of protein kinase A was used to detect the activation of this enzyme by L-glutamate in cultured hippocampal neurons (5).

Here we report on the expansion of this technology with membrane-permeant

fluorescent peptides that accumulate specifically in cellular organelles. Targeting of these peptides to the organelles uses the protein sorting machinery that directs newly synthesized proteins to their distinct destination. Proteins predestined for the peroxisomes and nucleus are synthesized on ribosomes in the cytosol. They accumulate in their target organelles by interaction with receptors that facilitate active import. Conversely, proteins that are synthesized on ER-bound ribosomes are co-translationally translocated into the lumen of this organelle. Dependent on the presence of a retention signal (e.g. KDEL) they are retained in the ER or are targeted to other compartments of the endocytic pathway such as the Golgi apparatus (see for overview ref.6). Tyrosine-containing motifs play an important role in intracellular protein trafficking as well. For instance, the sequence SXYQRL is a retention signal for proteins residing in the TGN (7,8).

In the present paper, we have investigated whether sequences that are recognized by organelle-specific protein-sorting machineries, could be used to target the fluorophore BODIPY[581/591] to the peroxisomes, nucleus, ER and TGN in intact cells. By a similar approach, we have recently determined the pH in peroxisomes using a peptide carrying a peroxisomal targeting sequence (PTS) and a pH sensitive fluorophore (9).

Materials and Methods

Chemicals

All peptides (> 95% pure) were obtained from Ansynth Service BV Roosendaal, The Netherlands. All fluorophores used were obtained from Molecular Probes (Eugene, OR, USA. All other chemicals used were obtained from Sigma (St. Louis, MO, USA) or Merck (Darmstadt, Germany).

Fluorescent labelling of the peptides

An iodacetamide derivative of C2-BODIPY[581/591] was synthesized and coupled to the sulfur-atom of a single cysteine-residue in the peptides. The fluorophore was coupled to iodoacetamide by adding 50 μl of 200 mM iodoacetamide in bicine buffer (50 mM, pH 8.5) to 50 μl of a 15 mM C2-BODIPY[581/591] SE solution in THF. The reaction was carried out under subdued light for one hour. After the reaction, the excess iodoacetamide was removed by acidic extraction. For this purpose 200 μl chloroform, 100 μl water and 5 μl acetic acid were added and the mixture was vortexed and the water phase was removed. The extraction was repeated four times. The product in the chloroform phase was dried under a stream of nitrogen. Next, a five times molar excess of BODIPY-Iodacetamide in tetrahydrofuran was added to 5 μg of peptide dissolved in 100 μl 0.1 M TRIS (pH 7.4). The reducing agent Tris-(2-carboxyethyl)phosphine (0.1 mM) was added to prevent the formation of disulfide bonds. The mixture was stirred for 24 h at room temperature in the dark. Subsequently the reaction mixture was extracted as describe above. With this extraction the unreacted dye partitioned in the chloroform phase and the labelled peptide in the water phase. The extraction was repeated three times. The purity of the fluorescent products was about 95% as verified by thin layer chromatography on silica 60 plates using the eluent: chloroform : methanol : acetic acid : water (25 : 15 : 3 : 2 v/v). Alternatively to the labelling on the cysteine, the TGN peptide was also labelled at the N-terminus by incubating the peptide with a ten-fold excess of C2-BODIPY[581/591] succinimidyl ester in bicine buffer (20 mM Bicine, pH 8.4) for 1 h at room temperature.

Labelling of the cells

Prior to use, rat-1 fibroblasts were grown at least 24 h on glass coverslips (25-mm diameter, Fisher) to 80% confluence in DMEM containing 10% fetal bovine serum, 20 units/ml penicillin, and 20 µg/ml streptomycin under 5% CO_2. Cells were placed in the temperature-controlled cover slip holder of the microscope set at 37°C. The cells were rinsed with enriched phosphate-buffered saline (PBS^{++}: 137 mM NaCl, 2.7 mM KCl, 0.5 mM $MgCl_2$, 0.9 mM $CaCl_2$, 1.5 mM KH_2PO_4, 8.1 mM Na_2HPO_4, supplemented with 5 mM glucose, $pH_{37°C}$ 7.4) and then incubated with PBS^{++} containing the fluorescent peptides (± 5 µg/ml) for up to 30 min. After uptake of the peptides, the cells were washed with fresh PBS^{++}. Similar uptake experiments were carried out at 4°C. To examine the functionality of the NLS-peptide, the plasma membrane of the rat-1 fibroblasts was punctured with glass beads (10). To this end, the fluorescent NLS-peptide was added to the culture medium at a concentration of ± 15 µg/ml. Then glass beads (Ø 106 µ, Sigma) were sprinkled onto the cells and removed after 5 min by washing. After the treatment, the cells remained adherent and well-spread. They were used immediately for microscopic examination.

Colocalisation with organelle-specific markers.

The subcellular localization of the TGN-peptide was determined using NBD-ceramide as a marker for the *trans* Golgi network. After loading with the TGN-peptide, the cells were exposed for 15 min to PBS^{++} containing 0.1 µM NBD-ceramide. Subsequently, the cells were washed with fresh PBS^{++}. As an ER-marker, concanavalin A was used. The distribution of the KDEL-peptide in the cells was imaged. Subsequently, while mounted under the microscope, the cells were fixed and permeabilized using 4% paraformaldehyde in PBS containing 0.1% triton X100 for 15 min at room temperature. Excess fixative was scavenged with 100 mM glycine for 2 times 10 min. The cells were blocked with 5% bovine serum in PBS with 0.1% serum albumin for 20 min at room temperature, washed and incubated with tetramethylrhodamine-labelled concanavalin A. After 20 min the excess of concanavalin A was removed by washing three times with PBS and images were taken.

Confocal Laser Scanning microscopy

Images were taken with a Leica TCSNT confocal laser-scanning system on an inverted microscope DMIRBE (Leica Microsystems, GmbH, Heidelberg, Germany) with an argon-krypton laser as excitation source. The green or red fluorescence of labelled peptides was acquired using the 488 and 568 nm laserlines for excitation and the emission bandpass filters 530/30 and 590/30 for detection, respectively. Adobe Photoshop (Mountain View, CA) was used to assemble and label the images.

Table 1. Amino acid sequence and net charge of the peptides carrying C2-BODIPY[581/591]

Designation of peptide	Amino acid sequence*	Net charge
PTS1 (peroxisomal)	Ac-*C*KGG*AKL*	+1
NLS (nuclear)	Ac-*VVV*KKKRK*VV*C	+4
KDEL(endoplasmic reticulum)	Ac-*CFF*KDEL	-2
TGN (*trans*-Golgi network)	GA*SDYQRL*G*C*	0

* The underlined residues indicate the import or retention sequence; the cysteine residue in italic is coupled to the fluorophore.

Results

Design of organelle-specific fluorescent peptides.

The boron dipyrromethene difluorid fluorophore C2-BODIPY$^{581/591}$ exhibits a bright red fluorescence with wavelength of maximal excitation and emission of 581/591 nm, respectively. It is uncharged and has a preference for the cell membrane (its calculated octanol : water partition coefficient (Log-P) corresponds to ±3). Administration of the free fluorophore to the growth medium of rat-1 fibroblasts leads to a rapid incorporation into the cells. Typically the fluorescence was visible after 1 min or less. The distribution of the probe is diffuse and no distinct selectivity for any subcellular site was observed (data not shown).

To evaluate whether C2-BODIPY$^{581/591}$ can be targeted to various cellular organelles, we have coupled the probe to four different carrier-peptides with known import or retention sequences (table 1). A single cysteine residue was present in all peptides used so as to ensure a site of coupling for the thiol-reactive derivative of the fluorophore. To circumvent interference of the fluorophore with the site of recognition, one to three (mostly hydroophobic) amino acid residues were positioned between the cysteine residue and the targeting motif. For targeting of C2-BODIPY$^{581/591}$ to peroxisomes, we have used the peptide CKGGAKL (table 1). The tripeptide AKL is representative for the peroxisomal targeting signal-1 (PTS1) and is located at the carboxy-terminus of most peroxisomal matrix proteins (11). For targeting of C2-BODIPY$^{581/591}$ to the nucleus, we used the classical localization signal (NLS) composed of four to five consecutive basic amino acids (reviewed in ref. 12). Here we tested the NLS peptide VVVKKKRKVVC derived from the nuclear leader sequence of the simian virus SV40 large tumour antigen (13). The acetylated form of this peptide has four net positive charges (table 1). The carboxyl-terminal KDEL peptide is an important retrieval signal of lumenal ER proteins that have escaped to the Golgi apparatus and other post-ER compartments (14). The KDEL receptor is concentrated in the intermediate compartment, as well as in the Golgi stack (15). After binding to this receptor, the proteins are transported to the ER by way of retrograde vesicle-flow. In order to target C2-BODIPY$^{581/591}$ to the ER, we designed the peptide CFFKDEL containing this ER retention motif (table 1)

Tyrosine-containing motifs play an important role in the internalization of integral membrane proteins at the cell surface and their subsequent targeting to the TGN. They are present in cytosolic domains of the integral membrane proteins and have been shown to interact with the medium chain subunits of adaptor complexes such as AP-2 that are associated with clathrin coated vesicles (16). In order to target C2-BODIPY$^{581/591}$ to the TGN, the fluorophore was coupled to a peptide GASDYQRLGC containing the motif SDYQRL of the integral membrane protein TGN38 (7,8). This protein cycles between the TGN and the plasma membrane but is predominantly found in the TGN. As an alternative to labelling at the cysteine residue, the TGN peptide was also labelled at the amino-terminus using the succinimidyl ester derivative of C2-BODIPY$^{581/591}$.

Targeting of fluorescent peptides to cellular organelles.

The uptake of the PTS1, KDEL and TGN-peptides by rat-1 fibroblasts from the medium is a rapid process. The first indication that the peptides are targeted to the organelles is already visible after 1 min (figure 1). After 16 min of incubation, targeting of all three peptides is complete. Distinct targeting remains clearly visible after the cells were washed to remove the
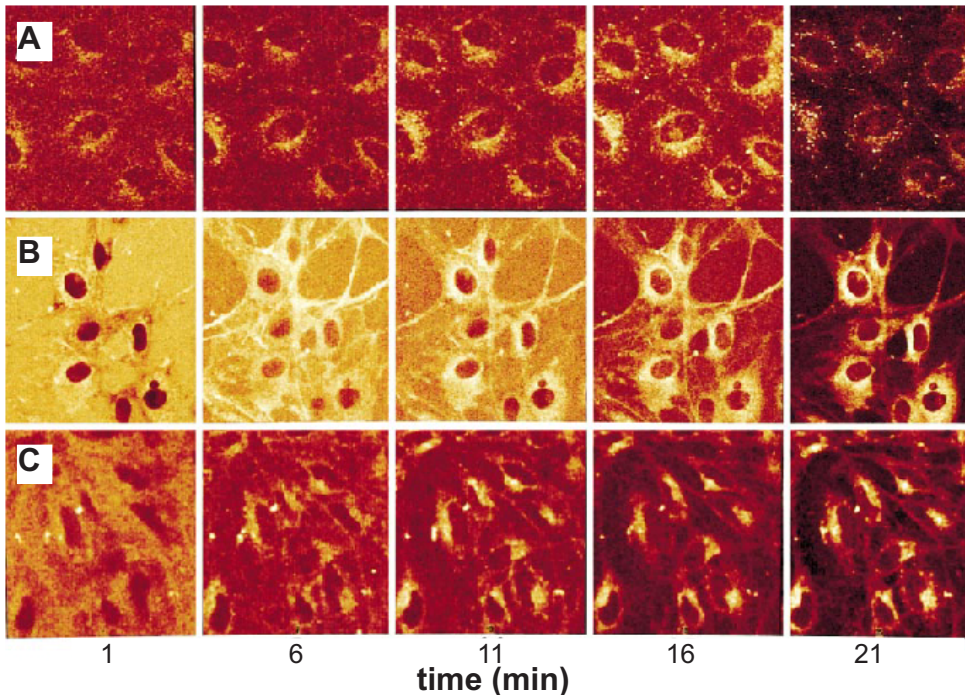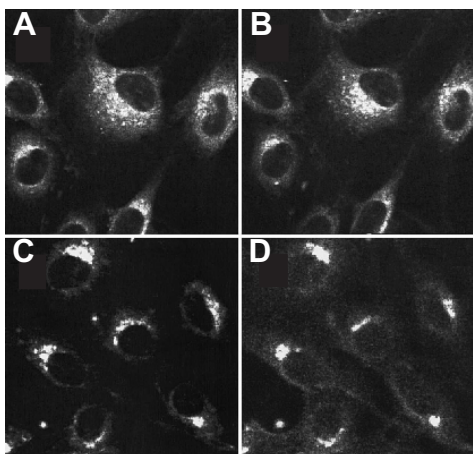
Figure 1. Time series of the uptake of the fluorescent PTS1-peptide (**a**), the KDEL-peptide (**b**) and the TGN-peptide (**c**) by living rat-1 fibroblasts at 37°C. The time between two acquisitions is approximately 5 min. After 16 min of uptake, the cells were washed with PBS⁺⁺ and further incubated for 5min (last frame of each series).
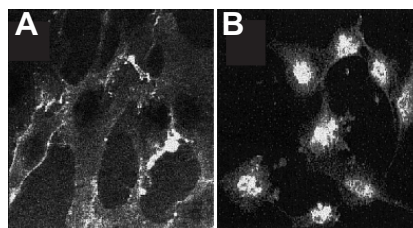
excess probe from the medium and incubated for another 5 min (figure 1, last frame).

The PTS1-peptide is concentrated in small grain-like organelles after 11 min of loading (figure 1A). As shown in a previous study with rat-1 fibroblasts (17) this punctated staining completely co-localized with antibodies against the peroxisomal acyl-coA oxidase indicating that the PTS1-peptide is indeed accumulated in peroxisomes. A similar punctated distribution of the PTS1-peptide has been observed in human fibroblasts (9). Initially, the KDEL-peptide is distributed throughout the cell but after 11 min of loading it concentrates within a large perinuclear compartment (figure 1B). This compartment was identified as ER by labelling the cells after fixation and permeabilization with the ER-marker concanavalin A (figure 2 A, B). Identification of the site of localization has also been performed with an antibody against the KDEL receptor. The data confirmed that the bulk of this receptor is localized in the Golgi apparatus (7,8). We presume that there is a continuous transport of the KDEL-peptide-receptor complex from the Golgi to the ER where the peptide is then released. This would imply that the capacity of the KDEL-receptors is sufficient to result in a net import of the KDEL-peptide in the ER.

As shown in Figure 1 C, the TGN-peptide accumulates in structures close to the nucleus. These structures are already visible after 6 min of loading to become very distinct within 16 min. From the extensive colocalisation with 7-nitrobenz-2-oxa-1,3-diazole-ceramide (NBD-ceramide), a well-known marker of TGN, we infer that the bulk of the TGN-peptide accumulates within the TGN (figure 2 C, D). In addition, a fraction of this peptide is present in structures close to the TGN in which the NBD-ceramide is absent. These may represent

Figure 3. Accumulation of the fluorescent NLS-peptide in the nuclei of rat-1 fibroblasts. Addition of the peptide leads to its accumulation at the membrane surface (**A**). Upon punctation of the plasma membrane by small glass beads, the NLS peptide accumulated in the nucleus (**B**).

Figure 2. Co-localization in rat-1 fibroblasts of the fluorescent KDEL-peptide (**A**) and the ER-marker concanavalin A (**B**) and of the TGN-peptide (**C**) and the TGN marker NBD-ceramide (**D**). After 15 min of uptake of the peptides, the cells were washed with PBS⁺⁺ and incubated with the markers as described in 'Materials and Methods'.

endocytic vesicles that cycle from the plasma membrane to the TGN as was observed for the membrane protein TGN38 (8). We have also tested the TGN–peptide with the fluorescent label attached to the amino–terminus. This peptide was also rapidly taken up by the cells and targeted to the TGN (data not shown).

The NLS–peptide carrying four positive charges was not internalized, yet concentrated at the cellular surface (figure 3A). When the plasma membrane of these cells was punctured by the impact of glass beads, the NLS–peptide was found to accumulate almost instantaneously
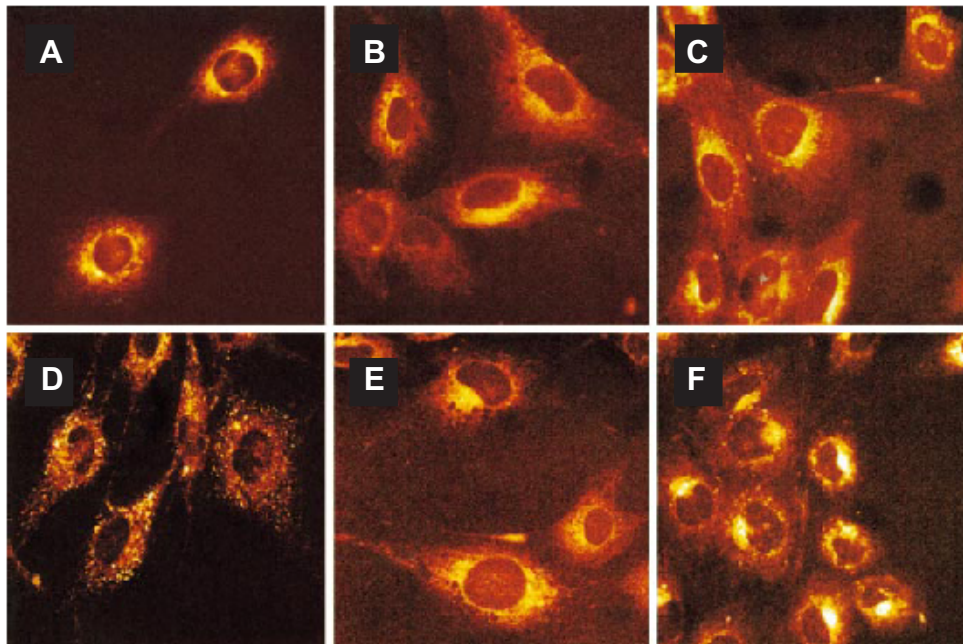
Figure 4. Uptake of the PTS1 (**A**), KDEL (**B**) and TGN (**C**) peptide by rat-1 fibroblasts at 4 °C. After 15 min of uptake the cells were washed with cold PBS⁺⁺ and images taken. Upon raising the temperature to 37 °C images of the PTS1 (**D**), KDEL (**E**) and TGN (**F**) peptide were taken after 30 min.

in the nucleus (figure 3 B). The charged amino acid residues required to target the peptide to the nucleus most likely prevent the peptide from crossing the plasma membrane (12).

Effect of temperature.

The way the fluorescent PTS1-, KDEL- and TGN- peptides enter the cells is still a matter of investigation. To assess whether endocytosis is involved, the uptake of these peptides was determined at 4°C. Internalization by way of coated vesicles and endosomes is blocked at this temperature (18). After 15 min of loading, the cells were washed with cold medium and images were taken. Under these conditions, the PTS1-, KDEL- and TGN- peptides are effectively internalized (figure 4 A, B and C). This implies that endocytosis is not required for the uptake. On the other hand, it appears that at this low temperature all three peptides are localized in structures adjacent to the nucleus and did not yet reach their target organelles. Targeting was attained by subsequently increasing the temperature to 37° C resulting in the accumulation of the peptides in peroxisomes, the ER and the TGN, respectively (Figure 4D, E and F).

Discussion

Here we demonstrate that C2-BODIPY$^{581/591}$ added to intact rat-1 fibroblasts, can be targeted to four different organelles (i.e. peroxisomes, endoplasmic reticulum, the Golgi system and nuclei) provided the probe is coupled to peptides carrying specific import or retention sequences. In agreement with its distinct hydrophobicity, the unconjugated form is rapidly taken up by intact cells and distributes diffusely among the subcellular organelles. Similarly, the probe conjugated to the PTS1-, TGN- and KDEL peptides is effectively taken up by the cells indicating that the peptide moieties do not prevent the conjugates from crossing the plasma membrane. As shown in other studies (19) the uptake of small peptides (4- to 11-aminoacid residues) from the medium can be extensive and is mainly determined by net charge and by other physicochemical properties like hydrophobicity. In fact, several groups have shown that the efficacy of peptide-uptake can be enhanced by their acylation (20,21). In line with this, the C2-BODIPY$^{581/591}$-labelled PTS1-, TGN- and KDEL peptides are presumably sufficiently hydrophobic so as to be able to pass the membrane. These peptides have net charges varying between +2 and −1 (Table 1). On the other hand, the C2-BODIPY$^{581/591}$-labelled NLS-peptide carrying a net charge of +4 is membrane-impermeable. In this case, it appears that the hydrophobicity of the fluorescent moiety is not sufficient to overcome the excess positive charge of the conjugate. Routinely, the uptake of the peptides was carried out at 37°C. An effective uptake of the PTS1-, TGN- and KDEL peptides was also observed at 4°C. This strongly suggests that endocytosis is not involved in the cellular uptake of the peptides. Our observations are in agreement with other studies demonstrating that peptides are effectively internalized at low temperatures by passive diffusion (22,23).

Accumulation of the PTS1-peptide into peroxisomes is an ATP-dependent process involving the protein-import machinery specific for the PTS1 targeting signal (9,11). A complicating factor may be the rapid extrusion of the PTS1-peptide by the multidrug-resistant (MDR) proteins. So it was observed that in the case of HepG2 hepatoma cells accumulation into peroxisomes was effective provided the MDR-reversing agent verapamil was present (17). In the case of the KDEL-peptide we assume that after passage through the plasma membrane, this peptide interacts with the KDEL-receptor which is predominantly located in

the Golgi stack and in the intermediate compartment. This receptor can then be reached either by endocytosis or by passive diffusion. From these post-ER compartments, the peptide will be delivered to the ER by retrograde transport. Accumulation of the KDEL-peptide in the ER implies that its import surpasses export. After the TGN-peptide has crossed the plasma membrane its import into the TGN requires that it first interacts with adaptor proteins on the cytoplasmic side of the plasma membrane or endosomes (16). In case of the endosomes, the interaction sites of the adaptor proteins are most likely accessible to the peptide from the cytosol. The TGN-peptide internalized at 4°C, will accumulate in the TGN at 37°C. This suggests that the uptake and transport to the TGN are two independent events. It is to be noted that the peptides taken up at 4°C appear to be associated with structures particularly abundant around the nucleus (Figure 4). However, this association appears to be reversible as an increase of the temperature to 37°C resulted in each peptide accumulating in its organelle proper. The identity of these structures remains to be elucidated.

The rapid translocation of fluorescent organelle-specific peptides across the plasma membrane offers the opportunity to image organelle-specific functions in living cells with time- and spatial resolution. So it was observed that upon addition of Brefeldin A to cells loaded with the TGN-peptide the TGN extended as tubules throughout the cytoplasm after 30 min of treatment. After 60 min the TGN-peptide accumulated into large vesicles that are distributed throughout the whole cell (unpublished observations). Similarly, exposure of the cells to the ionophore monensin for 30 min completely disrupted the TGN morphology resulting in the accumulation of the TGN peptide in large vesicles. These observations agree with previous studies using antibodies against TGN38 (24,24). In addition, the peptides can be used as diagnostic tools to evaluate the functional integrity of protein import or retention machineries in mutant cells and in cells of patients. Finally, the exact sequence requirements for import or retention could rapidly be determined with libraries of fluorescent peptides.

Acknowledgement.

References

(1)   Gadella, T.W.J. and Jovin, T.M. (1995) Oligomerization of epidermal growth factor receptors on A431 cells studied by time-resolved fluorescence imaging microscopy. A stereochemical model for tyrosine kinase receptor activation. *J. Cell Biol.*, **129**, 1543-1558.

(2)   Carraway, K.L.d. and Cerione, R.A. (1993) Fluorescent-labelled growth factor molecules serve as probes for receptor binding and endocytosis. *Biochemistry*, **32,** 12039-12045

(3)   Packard, B.Z., Toptygin, D.D., Komoriya, A. and Brand, L. (1996) Profluorescent protease substrates: intramolecular dimers described by the exciton model. *Proc. Natl. Acad. Sci. USA.*, **93**, 11640-11645.

(4)   Schroeder, H., Leventis, R., Rex, S., Schelhaas, M., Nägele, E., Waldmann, H. and Silvius, J.R. (1997) S-Acylation and plasma membrane targeting of the farnesylated carboxyl-terminal peptide of N-ras in mammalian fibroblasts.*Biochemistry*, **36,** 13102-13109.

(5)   Higashi, H., Sato, K., Ohtake, A., Omori, A., Yoshida, S. and Kudo, Y. (1997) Imaging of cAMP-dependent protein kinase activity in living neural cells using a novel fluorescent substrate. *FEBS Lett.*, **414**, 55-60.

(6)   Nilsson, T. and Warren, G. (1994) Retention and retrieval in the endoplasmic reticulum and the Golgi apparatus. *Current Opin. Cell Biol.*, **6**, 517-521.

(7)   Bos, K., Wraight, C. and Stanley, K.K. (1993) TGN38 is maintained in the trans-Golgi network by a tyrosine-containing motif in the cytoplasmic domain. *EMBO J.*, **12**, 2219-2228.

(8)   Humphrey, J.S., Peters, P.J., Yuan, L.C. and Bonifacino, J.S. (1993) Localization of TGN38 to the trans-Golgi network: involvement of a cytoplasmic tyrosine-containing sequence. *J. Cell Biol.*, **120**, 1123-1135.

(9)   Dansen, T.B., Wirtz, K.W., Wanders, R.J. and Pap, E.H. (2000) Peroxisomes in human fibroblasts have a basic pH. *Nat. Cell Biol.*, **2(1)**, 51-53.

(10)   McNeil, P.L. and Warder, E. (1987) Glass beads load macromolecules into living cells. *J. Cell Sci.*, **88**, 669-678.

(11)   Gould, S.J., Keller, G.A., Hosken, N., Wilkinson, J. and Subramani, S. (1989) A conserved tripeptide sorts proteins to peroxisomes. *J. Cell Biol.*, **108**, 1657-1664.

(12)   Hicks, G.R. and Raikhel, N.V. (1995) Nuclear localization signal binding proteins in higher plant nuclei. *Annu. Rev. Cell Dev. Biol.*, **11**, 155-188.

(13)   Kalderon, D., Roberts, B.L., Richardson, W.D. and Smith, A.E. (1984) A short amino acid sequence able to specify nuclear location. *Cell*, **39**, 499-509.

(14)   Munro, S. and Pelham, H.R. (1987) A C-terminal signal prevents secretion of luminal ER proteins. *Cell*, **48**, 899-907.

(15)   Griffiths, G., Ericsson, M., Krijnse-Locker, J., Nilsson, T., Goud, B., Söling, H.D., Tang, B.L., Wong, S.H. and Hong, W. (1994) Localization of the Lys, Asp, Glu, Leu tetrapeptide receptor to the Golgi complex and the intermediate compartment in mammalian cells. *J. Cell Biol.*, **127**, 1557-1574.

(16)   Owen, D.J. and Evans, P.R. (1998) A structural explanation for the recognition of tyrosine-based endocytotic signals. *Science*, **282**, 1327-1332.

(17)   Pap, E.W.H., Dansen, T.B. and Wirtz, K.W.A. (2001) Peptide-based targeting of fluorophores to peroxisomes in living cells. *Trends Cell Biol.,* **11**, 10-12

(18)   Kuismanen, E. and Saraste, J. (1989) Low temperature-induced transport blocks as tools to manipulate membrane traffic. *Meth. Cell Biol.*, **32**, 257-274.

(19)   Oehlke, J., Beyermann, M., Wiesner, B., Melzig, M., Berger, H., Krause, E. and Bienert, M. (1997) Evidence for extensive and non-specific translocation of oligopeptides across plasma membranes of mammalian cells. *Biochim. Biophys. Acta*, **1330**, 50-60.

(20)   Eichholtz, T., de Bont, D.B., de Widt, J., Liskamp, R.M. and Ploegh, H.L. (1993) A myristoylated pseudosubstrate peptide, a novel protein kinase C inhibitor. *J. Biol. Chem.*, **268**, 1982-1986.

(21)   Harris, T.E., Persaud, S.J. and Jones, P.M. (1997) Pseudosubstrate inhibition of cyclic AMP-dependent protein kinase in intact pancreatic islets: effects on cyclic   AMP-dependent and glucose-dependent insulin secretion. *Biochem. Biophys. Res Comm.*, **232**, 648-651.

(22)   Allentoff, A.J., Mandiyan, S., Liang, H., Yuryev, A., Vlattas, I., Duelfer, T., Sytwu, I.I. and Wennogle, L.P. (1999) Understanding the cellular uptake of phosphopeptides. *Cell Biochem. Biophys.*, **31**, 129-140.

(23)   Oehlke, J., Scheller, A., Wiesner, B., Krause, E., Beyermann, M., Klauschenz, E., Melzig, M. and Bienert, M. (1998) Cellular uptake of an alpha-helical amphipathic model peptide with the potential to deliver polar compounds into the cell interior non-endocytically. *Biochim Biophys Acta*, **1414**, 127-

139.

(24)   Ladinsky, M.S. and Howell, K.E. (1992) The trans-Golgi network can be dissected structurally and functionally from the cisternae of the Golgi complex by brefeldin A. *Eur. J. Cell Biol.*, **59**, 92-105.

(25)   Reaves, B., Horn, M. and Banting, G. (1993) TGN38/41 recycles between the cell surface and the TGN: brefeldin A affects its rate of return to the TGN. *Mol. Biol. Cell*, **4**, 93-105.
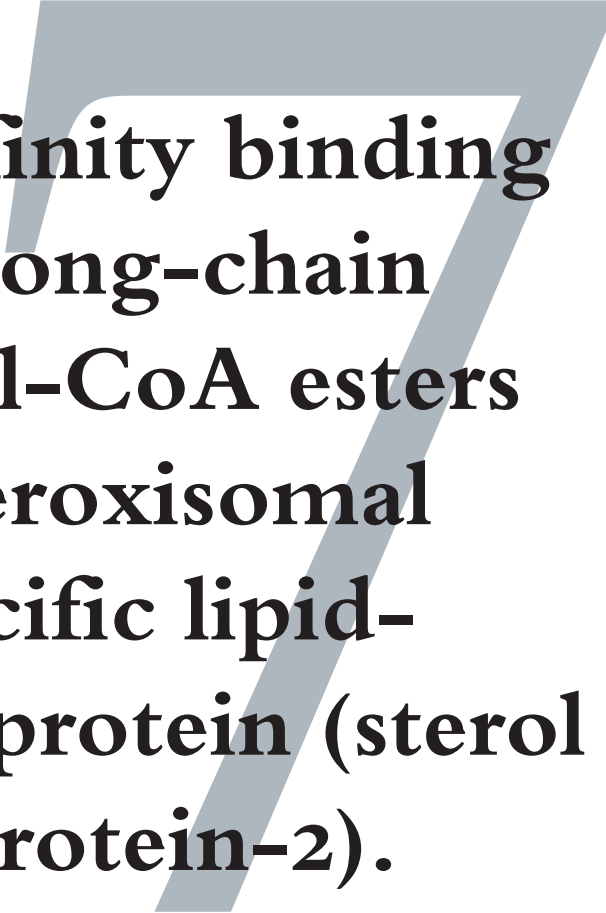
High-affinity binding of very-long-chain fatty acyl-CoA esters to the peroxisomal non-specific lipid-transfer protein (sterol carrier protein-2).

Tobias B. Dansen, Jan Westerman, Fred S. Wouters, Ronald J.A. Wanders, Arie van Hoek, Theodorus W.J. Gadella Jr. & Karel W.A. Wirtz (2001) *Biochemical Journal* **339,**193-199.

High affinity binding of very long chain fatty acyl–CoA esters to the peroxisomal non–specific lipid transfer protein (sterol carrier protein–2)

Tobias B. Dansen[1], Jan Westerman[1], Fred S. Wouters[1], Ronald J.A. Wanders[2], Arie van Hoek[3], Theodorus W.J. Gadella Jr[3], & Karel W.A. Wirtz[1]

1.   *Centre for Biomembranes and Lipid Enzymology, Institute of Biomembranes, Utrecht University, Padualaan 8, 3584 CH Utrecht, The Netherlands.*
2.   *Departments of Clinical Chemistry and Pediatrics, Academical Medical Centre, University of Amsterdam, Meibergdreef 9, 1105 AZ Amsterdam, The Netherlands.*
3.   *MicroSpectroscopy Center, Department of Biomolecular Sciences, Wageningen Agricultural University, Dreijenlaan 3, 6703 HA Wageningen, The Netherlands.*

Abstract

Binding of fluorescent fatty acids to bovine liver non-specific lipid transfer protein (nsL-TP) was assessed by measuring fluorescence resonance energy transfer (FRET) between the single tryptophan residue of nsL-TP and the fluorophore. Upon addition of pyrene dodecanoic acid (Pyr-C12) and cis-parinaric acid to nsL-TP, FRET was observed indicating that these fatty acids were accommodated in the lipid binding site closely positioned to the tryptophan residue. Substantial binding was only observed when these fatty acids were presented in the monomeric form complexed to β-cyclodextrin. As shown by time-resolved fluorescence measurements, translocation of Pyr-C12 from the Pyr-C12/β-cyclodextrin complex to nsL-TP changed dramatically the direct molecular environment of the pyrene moiety: i.e. the fluorescence lifetime of the directly excited pyrene increased at least by 25% and a distinct rotational correlation time of 7 ns was observed. In order to evaluate the affinity of nsL-TP for intermediates of the β-oxidation pathway, a binding assay was developed based on the ability of fatty acyl derivatives to displace Pyr-C12 from the lipid binding site as reflected by the reduction of FRET. Palmitoyl-CoA and palmitenoyl-CoA were found to bind readily to nsL-TP whereas 3-hydroxypalmitoyl-CoA and 3-ketopalmitoyl-CoA bound poorly. The highest affinities were observed for the very long chain fatty acyl-CoA esters (C24:0-CoA, C26:0-CoA) and their enoyl derivatives (C24:1-CoA, C26:1-CoA). Binding of unesterified palmitic acid and lignoceroic acid (C24:0) was negligible.

Introduction

Mammalian nsL-TP is a small (14 kDa), basic (IEP=8.5) protein which *in vitro* is able to mediate the transfer of a great variety of lipids between membranes (1). Originally, this protein was discovered for its ability to transport phosphatidylethanolamine (2,3). Independently, nsL-TP was identified as a protein (sterol carrier protein-2, SCP2) capable of stimulating cholesterol synthesis *in vitro* (4). In line with this activity, nsL-TP effectively stimulates the transfer of cholesterol between membranes (3). These diverse transfer activities may be inherent to nsL-TP having a low affinity lipid binding site interacting with the membrane (5). The physiologically relevant ligand of nsL-TP has been a matter of extensive research. Binding of fluorescently labelled phospholipids has been observed (6,7). As for its ability to bind sterols, conflicting reports exist (5,8,9). Recently, nsL-TP was shown to bind fatty acids and fatty acyl-CoA esters (10,11).

The nsL-TP is synthesized on free cytosolic polyribosomes as a precursor protein (pre-nsL-TP) which by virtue of its C-terminal AKL tripeptide is transported to peroxisomes (12, 13). The peroxisomal localization of nsL-TP was confirmed by immunogold labelling (14,15,16). Recently, evidence was provided in support of nsL-TP being involved in peroxisomal fatty acid oxidation. So it was shown that nsL-TP constitutes the C-terminal part of the peroxisomal 58 kDa protein (SCPx) which expresses branched chain 3-ketoacyl-CoA thiolase and lipid transfer activity (17-19). By FRET experiments *in situ* using BALB/c 3T3 fibroblasts, nsL-TP was shown to be associated with the enzymes of the peroxisomal β-oxidation pathway (20). Knock-out mice lacking nsL-TP and SCPx showed an increased expression of mitochondrial and peroxisomal β-oxidation enzymes (21).

In the study by Frolov *et al.* (11) fluorescent fatty acyl analogues were used, binding of which to nsL-TP induced a change in the fluorescent characteristics of the lipid. In the present study, we make use of a novel fatty acid binding assay which is based on fluorescence resonance energy transfer (FRET) between the tryptophan (the donor) in nsL-TP and a fluorescent fatty acid (the acceptor) bound to nsL-TP. The latter assay has as a major advantage that the binding of naturally occurring fatty acyl species as well as that of other lipids can be estimated directly by measuring their ability to displace the fluorescent fatty acid (Pyr-C12) from the lipid binding site. The efficiency of displacement as reflected by a decrease of FRET, is taken as a measure of the affinity of nsL-TP for the non-fluorescent fatty acids. Making use of this assay we have shown that nsL-TP has a high binding affinity for the CoA esters of very long chain fatty acids.

Materials and methods

Materials

Palmitic acid, the corresponding CoA-esters and β-cyclodextrin were from Sigma (St. Louis, MO, USA). Pyrene dodecanoic acid (Pyr-C12) and *cis*-parinaric were from Molecular Probes (Eugene, OR, USA). The β-oxidation intermediates α,β-unsaturated, 3-hydroxy and 3-ketopalmitoyl-CoA were synthesized enzymatically from palmitoyl-CoA using acyl-CoA oxidase, crotonase and 3-hydroxyacyl-CoA dehydrogenase (all obtained from Sigma), essentially using the method described by Seubert *et al.* (22). The acyl-CoA esters were purified by HPLC using a reverse phase C18-column (Supercosil SPLC-18-DB, 250 mm x 10 mm,

Supelco, Bellefonte, PA, USA) using a gradient of acetonitrile (40-50% v/v) in 16.9 mM sodium phosphate, pH 6.9. Acyl–CoA esters were stored at 4°C in 20 mM MES–NaOH, pH 6.0 in which they were stable for extended periods of time. Lignoceroyl–CoA (C24:0-CoA) was obtained from Sigma. Cerotoyl–CoA (C26:0-CoA) was prepared by the method of Rasmussen (23). The product was purified by HPLC on a Supelco SPLC-8-DB column using a linear gradient of acetonitrile (58-70% v/v) in 16,9 mM sodium phosphate pH 6.9. Lignocerenoyl and cerotenoyl CoA esters (C24:1-CoA, C26:1-CoA) were prepared by incubation of the corresponding saturated fatty acyl–CoA esters (100μM) with acyl–CoA oxidase (Sigma) (7.5 and 22.5 units, respectively) for 1 hr at 37°C in 50 mM Tris pH 8.0, containing 1 μM FAD. The reaction was stopped by adding HCl to a final concentration of 0.5 M. After cooling on ice for 1 hr, the products were sedimented by centrifugation for 10 min at 4000 rpm at 4°C. The pellet was taken up in 20 mM MES buffer pH 6.0 and the products were purified on HPLC using the same conditions as for the cerotoyl–CoA ester. Recombinant rat pre-nsL-TP was overexpressed and purified as described by Ossendorp *et al.* (24). Bovine nsL-TP was purified according to a modification of the procedure by (25). Chicken egg-white lysozyme was from Sigma (St. Louis, MO, USA).

Preparation of fatty acid substrates

Pyr-C12 or *cis*-parinaric acid was diluted from a methanol stock solution to 75 μM in 17.5 mM β-cyclodextrin in PBS, vortexed for 1 min and sonicated for 15 min in a Branson ultrasonic waterbath. The molar excess of β-cyclodextrin (230-fold) was determined by titrating self-quenched Pyr-C12 micelles with β-cyclodextrin until no further increase in fluorescence intensity was observed. Under these conditions, Pyr-C12 is taken up as monomer in the β-cyclodextrin (26). This solution was diluted ten times in PBS to obtain the working solution. Non-fluorescent fatty acids from methanol and the fatty acyl–CoA esters from a 20 mM MES, pH 6.0, stock solution were prepared in a similar way. The concentrations of the fluorescent fatty acids were determined by measuring the absorbance in methanol (ε_{341} of 44 mM^{-1}cm^{-1} for Pyr-C12, ε_{303} of 76 mM^{-1}cm^{-1} for *cis*-parinaric acid) and of the fatty acyl–CoA esters were by measuring the absorbance in 100 mM MES, pH 6.0 (ε_{269} of 16 mM^{-1}cm^{-1}).

Steady-state fluorescence measurements

Measurements were performed on a SLM–Aminco SPF-500C spectrofluorimeter equipped with a thermostatted cuvette holder and a magnetic stirring device. Tryptophan was excited at 280 nm (band width 4 nm) and the emission measured from 300 to 550 nm (band width 10 nm) to obtain spectra or set at 378 nm (Pyr-C12), 415 nm (*cis*-parinaric acid) or 335 nm (tryptophan) for single-point measurements (averaged for 2 sec). All measurements were performed at 25°C under continuous stirring.

Time-resolved fluorescence measurements

Time-resolved fluorescence measurements were carried out using a time-correlated photon counting set-up as partly described earlier (27). The frequency doubled output of a mode-locked continuous wave Nd:YLF laser was used for the synchronously pumping of a cavity-dumped DCM dye laser (repetition rate 475 kHz). A LiJO$_3$ crystal was used for frequency doubling of the output of the dye laser, to get excitation pulses at 340 nm wavelength. The pulse duration was around 4 ps FWHM and the pulse energy in the tens of pJ range.

Fluid samples were in 1.0 cm3 and 1 cm light path fused silica cuvettes, placed in a thermostated holder. The sample holder was placed in a housing, containing as few detection optics as possible to yield maximum detection efficiency. Filters, used for wavelength selection of emission, were an interference filter (Schott IL 381.7 nm, 10.1 nm FWHM, Mainz, Germany), combined with an extra cut-off filter (Schott model KV 370).

Detection electronics were time-correlated single photon counting modules. The start signal for the time-to-amplitude converter (TAC) was generated by exciting a fast PIN photodiode with the 680 nm wavelength light left from the frequency doubling set-up (28). Single fluorescence photon responses from a proximity focused microchannel plate photomultiplier were amplified by a wide-band amplifier and used as a stop signal for the TAC. The output pulses of the TAC were analyzed by an analogue-to-digital converter (ADC). The output of the ADC was gathered in the 1024 channels of a multichannel analyzer.

Pyrene fluorescence was sampled during 10 cycles of 10 seconds in alternating parallel and perpendicular directions. A maximum frequency of fluorescence photons of 23 kHz (≈5% of 475 kHz) in the parallel direction was chosen to prevent pile-up distortion (27). Also other instrumental sources of data distortion were minimized (29) to below the noise level of normal photon statistics. After measuring the fluorescence of the sample, the background emission of a sample with identical composition but excluding Pyr-C12, was measured for 2 cycles of 10 seconds and used for background subtraction.

For obtaining a dynamic instrumental response as a reference for deconvolution, 1,4-bis[2-(5-phenyloxazolyl)]benzene (POPOP) (Eastman Kodak, Rochester, NY) in ethanol (exhibiting a single exponential fluorescence decay with τ=1.35 ns) was measured for 3 cycles of 10 seconds as a reference compound. Data analysis was performed on a workstation (Silicon Graphics model Indy Studio), using the maximum entropy (30) method.
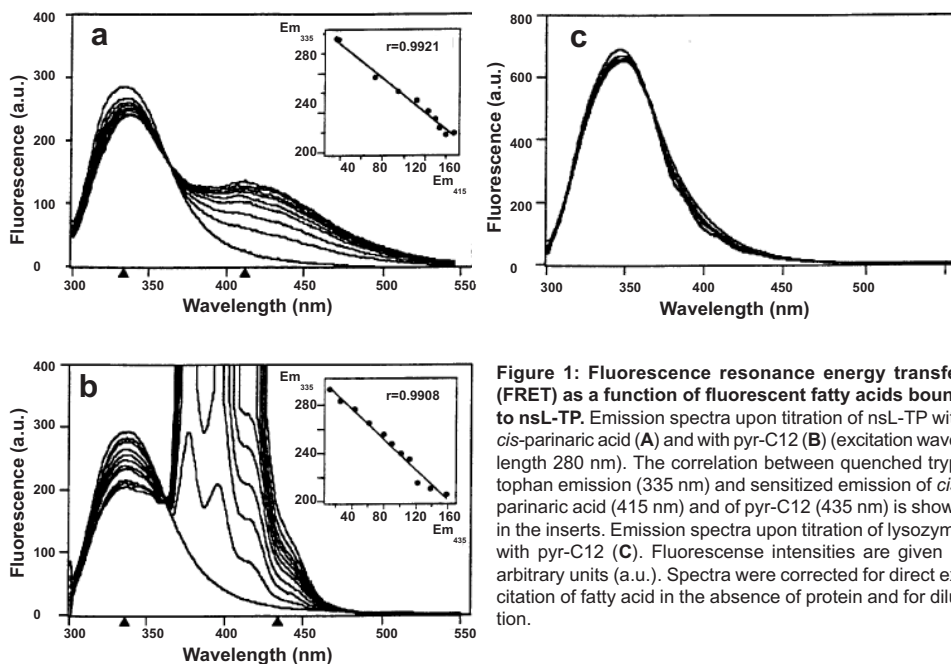
Binding of fluorescent fatty acids

Increasing amounts of fluorescent fatty acid in β-cyclodextrin were added to nsL-TP (0.5 μM) or pre-nsL-TP (0.5 μM) in 1 ml of PBS. As a measure for binding, the emission of Pyr-C12 (378 nm) or of *cis*-parinaric acid (415 nm) was determined upon excitation of tryptophan (280 nm). In case of FRET, the excitation of tryptophan (donor) gives rise to sensitized emission of the fluorescent fatty acid (acceptor), provided that binding of fatty acids has occurred. Emissions were corrected both for direct excitation of the fluorescent fatty acid at 280 nm in the absence of protein and for dilution. Given the low affinity of β-cyclodextrin for fatty acids (230-fold molar excess needed), this compound exerts a minimal effect on the binding of the different fatty acyl compounds to nsL-TP.

Since FRET between tryptophan and Pyr-C12 or *cis*-parinaric acid results in quenching of the tryptophan fluorescence, this quenching can also be used as a measure for fatty acid binding according to:

$$E = 1 - \frac{F_{DA}}{F_D}$$

where E is the energy transfer efficiency, F_{DA} is the fluorescence intensity of the donor (tryptophan) in the presence of acceptor (fluorescent fatty acid) and F_D is the fluorescence intensity of the donor in the absence of acceptor. In this case the fluorescent fatty acids were added to nsL-TP (0.5 μM) to enable accurate tryptophan fluorescence determination.

Figure 1: Fluorescence resonance energy transfer (FRET) as a function of fluorescent fatty acids bound to nsL-TP. Emission spectra upon titration of nsL-TP with *cis*-parinaric acid (**A**) and with pyr-C12 (**B**) (excitation wavelength 280 nm). The correlation between quenched tryptophan emission (335 nm) and sensitized emission of *cis*-parinaric acid (415 nm) and of pyr-C12 (435 nm) is shown in the inserts. Emission spectra upon titration of lysozyme with pyr-C12 (**C**). Fluorescense intensities are given in arbitrary units (a.u.). Spectra were corrected for direct excitation of fatty acid in the absence of protein and for dilution.

Binding of non-fluorescent fatty acids

Protein (0.6 µM nsL-TP or 0.5 µM pre–nsL-TP in PBS) was preincubated with Pyr–C12 (1.7 µM) for 5 min at 25°C followed by the titration with increasing amounts of non-fluorescent fatty acid substrates. The efficiency of competition was determined by measuring the decrease in Pyr–C12 (sensitized) fluorescence emission. After correction for direct excitation of Pyr–C12 (280 nm in the absence of protein) and for dilution, the decrease in fluorescence emission was normalized relative to the small decrease (max. 25%) which was observed with blank titrations (addition of cyclodextrin without competitor). The displacement of Pyr–C12 from nsL-TP by the fatty acid substrates was analyzed by fitting the normalized fluorescence decrease to a hyperbolic function

Results

Binding of fluorescent fatty acids

Upon addition of *cis*-parinaric acid or Pyr–C12 to nsL-TP, the emission of tryptophan (donor) at 338 nm is decreased (Figs. 1A,B). Concomitantly, a sensitized emission of *cis*-parinaric acid (Fig. 1A) and Pyr–C12 (Fig. 1B) is observed indicative of FRET. In agreement with this, a high correlation is observed between the increase in *cis*-parinaric acid emission (inset Fig. 1A) or pyrene emission (inset Fig. 1B) and the decrease in tryptophan emission. The occurrence of FRET demonstrates a very close proximity of pyrene or parinaric acid and the single Trp residue of nsL-TP indicating that these fatty acids are bound to nsL-TP. As shown in Fig 1B, the increase in Pyr-C12 fluorescence intensity is much more pronounced than the decrease in tryptophan emission. In addition to FRET, the increased pyrene fluorescence in the presence of nsL-TP is caused by an increased quantum yield (or fluorescence

lifetime) of Pyr-C12 as compared to Pyr-C12 complexed to cyclodextrin (see below). To investigate the significance of the Pyr-C12 binding to nsL-TP, Pyr-C12 was also added to lysozyme. Lysozyme has a similar isoelectric point and size (IEP=9, Mw=14.3 kDa) as compared to nsL-TP (IEP=8.5, Mw=14 kDa). As is apparent from figure 1C, the intrinsic Trp fluorescence of lysozyme is unaffected by the presence of Pyr-C12, and clearly, no sensitized Pyr-C12 emission can be detected.

Fig. 2 shows the spectra of pyrene-sensitized emission upon titration of nsL-TP (0.5 µM) with Pyr-C12. As shown in Fig. 2 (insert), binding of Pyr-C12 to nsL-TP is saturable yielding a Kd of 0.24 µM . For comparison, the Kd of *cis*-parinaric acid is 0.18 µM (Frolov *et al.*, 1996). Under comparable conditions, pre-nsL-TP (0.5 µM) gave a similar titration curve indicating that the presequence does not affect the affinity for Pyr-C12.

As shown in Fig. 3, fast binding kinetics were observed when Pyr-C12 was offered to nsL-TP in monomeric form, *i.e.* solubilized in β-cyclodextrin (trace A). Equilibration was complete within 1 min. If Pyr-C12 was added directly to nsL-TP without prior complexation
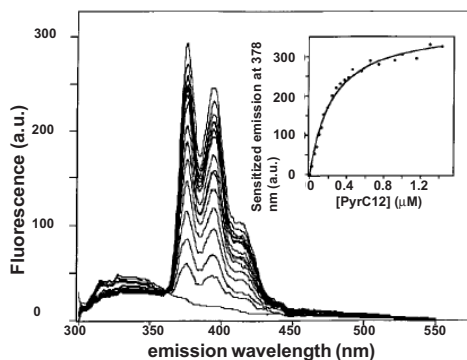
Figure 2: Sensitized emission spectra of pyr-C12 bound to nsL-TP. The increase of pyrene fluorescence emission (378 nm) as a function of the pyr-C12 concentration added to nsL-TP is shown in the insert (excitation wavelength 280 nm). Spectra were corrected for direct excitation of pyr-C12 in the absence of protein and for dilution.
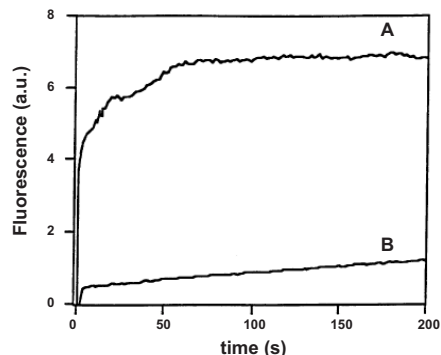
Figure 3: Binding velocity of pyr-C12 to nsL-TP. Time-dependent binding of pyr-C12 to nsL-TP as measured by sensitized emission at 378 nm (excitation wavelength 280 nm). Curve **A**) pyr-C12 associated with β-cyclodextrin; curve **B**) pyr-C12 in buffer.

to β-cyclodextrin binding was much slower (trace B). This observation underlines the importance of presenting the fatty acids and fatty-acyl-CoA esters to be tested in monomeric form so as to eliminate the effect of different substrate solubilities on the interaction with nsL-TP. Since the increase in Pyr-C12-fluorescence emission is much larger than the decrease in tryptophan emission, the pyrene emission was used for estimating the affinities of the fatty acyl substrates in the displacement binding assay (see below).

Time resolved fluorescence analysis of Pyr-C12 binding

To obtain additional information on how Pyr-C12 is accommodated in nsL-TP, time-resolved fluorescence measurements were carried on the Pyr-C12-nsL-TP complex. In figure 4, the results of the experiments are shown, and in Table I, the parameters describing the best fits to the experimental data are listed. From figure 4C, it is inferred that upon addition of nsL-TP to a solution of Pyr-C12-cyclodextrin complex, the pyrene fluorescence decays much slower (compare curves 1 and 2) reflecting an increase of the pyrene average fluorescence

lifetime from 111.9 to 139.6 ns (see Table I). This indicates a substantial change of the molecular environment of the pyrene moiety when Pyr-C12 is bound to nsL-TP. The anisotropy decay (figure 4D) reveals that in contrast to Pyr-C12 bound to cyclodextrin (curve 1), Pyr-C12 bound to nsL-TP shows a distinct anisotropy decay with a rotational correlation time of 6.9 ns (see table I). This correlation time closely resembles that of DPH-PC bound to nsL-TP (5) or of parinaric acid bound to recombinant nsL-TP (32) as found in earlier studies. In addition to this nsL-TP-related rotational mobility, there is also a very fast anisotropy decay (sub-nanosecond timescale) of pyrene analyzed as 0.1-0.15 ns (see table I). This fast decay could represent free rotational motion of pyrene. Despite the excellent fits to the data ($\chi 2$ close to 1.0), the slow timescale of the time-resolved experiments (0.609 ns/channel, necessary for accurate determination of the long pyrene lifetime) prohibits analysis of this fast depolarization process with reasonable accuracy .

Addition of palmitoyl-CoA (1.5 μM final concentration) to the Pyr-C12-nsL-TP complex clearly reduces the Pyr-C12 fluorescence lifetime (curve 3, figure 4C) to 126.3 ns (see table I) and also diminishes the initial anisotropy of the component with a rotational correlation time of 7.6 ns to 0.032. Subsequent addition of a 4-fold excess of palmitoyl-CoA over Pyr-C12 further reduced the fluorescence lifetime (to 120.9 ns) and the initial anisotropy of the slow rotating component to 0.014. It is of note that under these conditions the fluorescence and the anisotropy decay were still slower than the control situation without nsL-TP (compare curves 1 and 4), reflecting incomplete competition by palmitoyl-CoA (see figure 5).

Binding of non-fluorescent fatty acids

The displacement of Pyr-C12 bound to nsL-TP by non-fluorescent fatty acid derivatives is taken as a measure for the affinity of nsL-TP for that particular compound. As shown in Fig. 5, the addition of the VLCFA-CoA esters to nsL-TP pre-equilibrated with Pyr-C12, nearly completely eliminates the sensitized pyrene fluorescence. In fact, given the amount of nsL-TP present (0.6 μM) it appears that at low concentrations (< 0.5 μM) C26:0-CoA and C24:1-CoA bind completely (data not shown). Addition of the unesterified lignoceric acid (C24:0) has virtually no effect on the pyrene emission indicating that nsL-TP has a great preference for the CoA ester. This was also observed for palmitic acid. As for palmitoyl-CoA, the displacement is less efficient over the concentration range tested. The relative decrease in the normalized fluorescence (Fig. 5) correlates very well with the results of the time-resolved fluorescence experiments (see Fig. 4), thereby strongly validating the correctness of the competition binding assay.

Using this assay, different fatty acyl compounds were tested for binding to nsL-TP and its precursor pre-nsL-TP and their IC_{50}-values determined. As shown in Table 2, palmitoyl-CoA has about a 10-fold higher affinity for nsL-TP as compared to palmitic acid. The introduction of a double bond in palmitoyl-CoA (C16:1-CoA) does not affect the binding affinity. However, a significant (about 5-fold) decrease in the affinity is observed when a 3-hydroxy- and a 3-keto-group are introduced into the palmitoyl-CoA. Given that peroxisomes are the intracellular sites of VLCFA degradation (33) we have also assessed the affinity of nsL-TP for this class of fatty acids. As was observed for palmitic acid, nsL-TP has a very low affinity for C24:0, yet a 55-fold higher affinity for the CoA ester, C24:0-CoA (IC_{50} of 0.27 μM). Introduction of a double bond has a significant effect increasing the affinity for C24:1-CoA by a factor of 3. For comparison, C26:0-CoA has an IC_{50} of 0.13 μM and C26:1-CoA
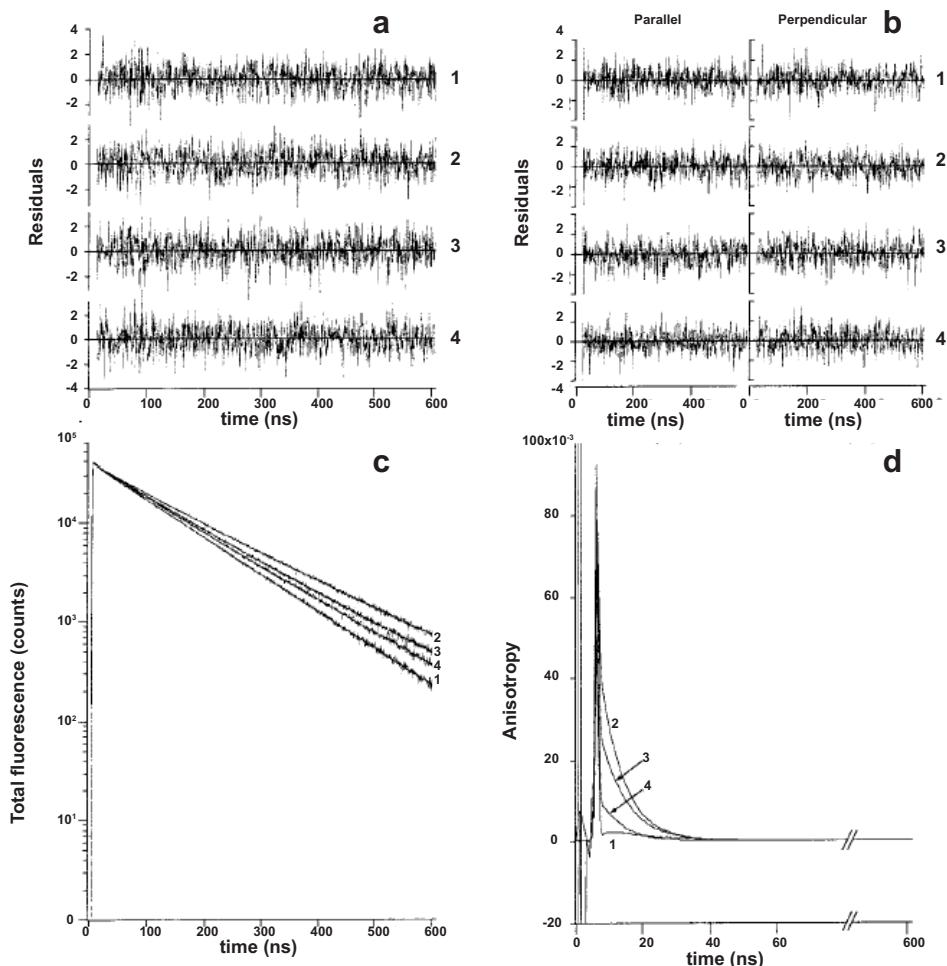
Figure 4: Time-resolved fluorescence analysis of Pyr-C12 binding to nsL-TP. a+c: Fluorescence decay analysis, **b+d**: Anisotropy decay analysis. All four experiments were carried out at room temperature in 1 ml cuvettes containing 1.5 μM Pyr-C12 bound to cyclodextrin in PBS. Subsequent additions: 1, no addition; 2: addition of 0.75 μM nsL-TP; 3: addition of 1.5 μM palmitoyl-CoA; 4: addition of 4.5 μM palmitoyl-CoA (total 6 μM). Figure **4c** shows the experimental and calculated fluorescence decays of the four experiments and the decay of POPOP in ethanol (τ=1.35 ns) that was used as a reference compound for deconvoluting the instrumental response. In figure **4a** the weighted residuals for the four fits are shown. In figure **4d**, the anisotropy decays of the four experiments are shown. For reasons of clarity, only the calculated curves are indicated. In figure **4b**, the weighted residuals for both the parallel and perpendicular experimental fluorescence decays defining the anisotropy decay are shown for all four experiments.

Table I: Fluorescence and anisotropy decay parameters for Pyr-C12 under various conditions

Exp #, Additions[a]	$<\tau>$ (ns)[b]	$\chi2$[b]	ϕ_1 (ns)[c]	(β_1)[c]	ϕ_2 (ns)[c]	(β_2)[c]	$\chi2$[c]
1: L	111.9±0.3	0.97	0.10±0.05	(0.36±0.24)	16±10	(0.003±0.002)	1.05
2: L+P	139.4±0.4	1.03	0.15±0.09	(0.24±0.17)	6.9±0.6	(0.049±0.023)	1.03
3: L+P+C (1.5 μM)	126.3±0.8	1.12	0.10±0.05	(0.34±0.25)	7.6±0.9	(0.032±0.016)	1.12
4: L+P+C (6.0 μM)	120.9±1.0	1.12	0.10±0.05	(0.4±0.3)	6.1±1.0	(0.014±0.008)	1.12

[a] L: 1.5 μM Pyr-C12 in cyclodextrin, P: 0.75 μM nsL-TP, C: Palmitoyl-CoA
[b] Parameters describing the fluorescence decay analysis.
[c] Parameters describing the anisotropy decay analysis.
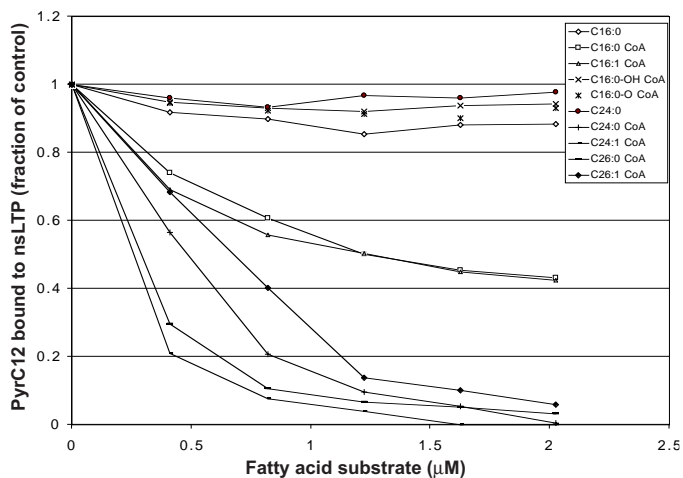
Figure 5: Displacement of Pyr-C12 bound to nsL-TP by fatty acid substrates. The substrates were added to 0.6 μM nsL-TP pre-equilibrated with 1.7 μM pyr-C12. Each point is the average of at least four independent measurements. Standard deviations ranged between 0.2 – 4 % for each point.

Table 2: Relative affinity of fatty acid substrates for nsL-TP and pre-nsL-TP. The IC50-values represent the concentrations of fatty acid substrates required to displace half of the amount of Pyr-C12 from the lipid binding site of the protein. For incubation conditions, see legend to Fig. 5. Values present the mean ± standard deviation (n = 5) and were estimated from representative fits through the points indicated in Fig. 5.

fatty acid substrate	nsL-TP IC_{50} (μM)	pre-nsL-TP IC_{50} (μM)
C16:0	10.7 ±1.9	34.9 ±12.5
C16:0 CoA	1.28 ±0.08	3.75 ±0.37
C16:1 CoA	1.16 ±0.08	n.d.
C16:0-OH-CoA	9.8 ±2.2	n.d.
C16:0-O-CoA	7.6 ±0.9	n.d.
C24:0	14.9 ±5.0	22.4 ±7.2
C24:0 CoA	0.27 ±0.07	0.89 ±0.16
C24:1 CoA	0.10 ±0.03	0.42 ±0.04
C26:0 CoA	0.13 ±0.02	0.40 ±0.08
C26:1 CoA	0.44 ±0.11	0.90 ±0.16

of 0.44 μM. All these substrates were also tested for binding to pre-nsL-TP. As shown in Table 2, pre-nsL-TP expresses a 2-5-fold lower affinity. By using this assay nsL-TP failed to show any affinity for cholesterol supporting the idea that nsL-TP has probably no function in cholesterol metabolism (21)

Discussion

A simple and sensitive assay is presented for measuring the binding of fatty acyl compounds to nsL-TP. In this assay use is made of the presence of a single tryptophan residue and a fluorescent reporter fatty acid whose binding can be monitored directly due to the occurrence of FRET between tryptophan and the fluorescent fatty acid. The FRET signal directly represents binding of the fatty acid since this process is extremely dependent on the distance

between the fluorescent fatty acid and nsL-TP. In addition, both the time-resolved fluorescence and anisotropy analysis showed a major change in the molecular environment of Pyr-C12 when added to nsL-TP, indicative of the incorporation of the pyrene moiety in the lipid binding site of nsL-TP. The maximal entropy fit of the time-resolved fluorescence decay of Pyr-C12 in the presence of nsL-TP (curve 2, figure 4C) indicated a lifetime component The 162 ns component represents the Pyr-C12 population that is bound to nsL-TP. Hence, the quantum-yield increase of Pyr-C12 upon translocation from cyclodextrin to nsL-TP may amount to 44% which exceeds the increase of 25% as calculated from the average lifetime parameters (112 ns *versus* 139 ns). This underestimation is a consequence of the simultaneous presence of nsL-TP-bound and cyclodextrin-bound Pyr-C12 populations in the experiments. Similar quantum-yield changes have been observed for translocation of pyrene-labelled phospholipids from nsL-TP to membranes (7). The quantum yield increase greatly enhances the sensitivity of the competition binding assay as, in addition to the sensitized emission, it contributes to a net increase of pyrene fluorescence emission in the presence of nsL-TP (see figure 2).

Using this displacement assay we show that nsL-TP can specifically bind fatty acyl compounds with highest affinity for palmitoyl-CoA, palmitenoyl-CoA and VLCFA-CoA. The other substrates tested, 3-hydroxypalmitoyl-CoA, 3-ketopalmitoyl-CoA even though structurally very similar, bound with relatively low affinity suggesting that the physical constraints of the lipid binding are very distinct. It is striking that nsL-TP shows a high affinity for CoA esters and a relatively low affinity for the corresponding non-esterified fatty acids. Frolov *et al.* (11) have reported a 300-fold increase in affinity of nsL-TP for *cis*-parinaroyl-CoA as compared to *cis*-parinaric acid. Our results are in agreement with these observations. In the latter study C16:0-CoA effectively displaced *cis*-parinaric acid from nsL-TP, yet C20:0-CoA failed to do so. In contrast to the high affinities for C24:0-CoA and C26:0-CoA observed in our study, these authors conclude that nsL-TP binds saturated fatty acyl-CoAs only over a narrow acyl chain length from 10 to 18 carbons

Given the interaction of nsL-TP with acyl-CoA oxidase and the bifunctional enzyme in the peroxisomes (20) it is well possible that this protein is involved in presenting VLCFA-CoA and the enoyl derivatives to these enzymes. The finding that the binding of fatty acids is very fast when offered in the form of monomers complexed to β-cyclodextrin is in support with the idea that nsL-TP may function in the regulation of peroxisomal oxidation by transporting fatty acyl intermediates to and from the hydrophobic binding sites in oxidation enzymes. In accordance with this proposed function, the functional homologue of nsL-TP in the yeast *C. tropicalis*, PXP18, was shown to bind to peroxisomal acyl-CoA oxidase *in vitro* (34) and a novel non-specific lipid transfer protein in the yeast *S. cerevisiae* was shown to co-purify with peroxisomal acyl-CoA oxidase (35).

Since pre-nsL-TP undergoes rapid proteolytic processing to nsL-TP upon import into the peroxisome, the 20 amino acid presequence is not likely to contribute to the fatty acyl binding activity of nsL-TP. Here, we report a 2-4-fold lower binding affinity for pre-nsL-TP as compared to nsL-TP. Apparently, the presequence interferes with fatty acid binding, probably by destabilizing the tertiary structure of the hydrophobic fatty acid binding pocket and could function as an modulator for strict intraperoxisomal fatty acid binding activity.

The binding of fatty acids and CoA esters to nsL-TP has a cytosolic counterpart in the fatty acid binding protein (FABP) and acyl-CoA binding protein (ACBP) (36) The FABP

family constitutes several proteins (Mw=14-15 kDa) that differ in their substrate specificity and tissue abundance. These proteins are present in high amounts in the cytosol and show high affinity for fatty acids and in some cases (i.e. liver FABP) for fatty acyl-CoAs (37,38) A function for FABP in delivering fatty acids to the outer membrane of mitochondria (39,40) and to peroxisomes (41,42) for successive μ-oxidation has been suggested. In addition, the cytosol contains a 10 kDa ACBP with high affinity towards fatty acyl-CoA esters. ACBP is thought to bind fatty acyl-CoA esters formed by activation at the mitochondrial outer membrane and thus to "take over" the role of FABP. The ACBP-bound fatty acyl-CoA can be used for β-oxidation or the biosynthesis of phospholipids and triacylglycerols. In this respect, nsL-TP may be considered to be the peroxisomal counterpart of ACBP. The dissociation constants of the FABP's ranged from 2 to 1000 nM, depending on the FABP and the type of fatty acid used (43). The affinities reported here for nsL-TP are within this range. Interestingly, many of the features described here for nsL-TP are very comparable to those described for plant non-specific lipid transfer proteins (LTPs). LTPs (reviewed in ref. 44) have a molecular mass of about 10 kDa and basic IEP (of 8.8). Upon binding of pyrene labelled lipids to LTPs a similar pyrene quantum yield increase is observed as for nsL-TP (45). It has been shown that plant LTPs bind fatty-acyl-CoA esters in a 1:1 molar ratio (45-48). Furthermore, immunolocalization indicated that LTPs are enriched in glyoxysomes (a plant peroxisomal counterpart) and enhance acyl-CoA oxidase activity (47). This suggests that LTPs and nsL-TP have common physiological functions in both plant- and mammalian organisms irrespective of their completely different amino acid sequence. This might be a case of evolutionairy convergence similar to that proposed for yeast sec14p and mammalian phosphatidylinositol transfer protein (1,49).

Taken together, the data presented in this study support a role for nsL-TP in peroxisomal fatty acid oxidation rather than in intracellular lipid transfer and biosynthesis. In this process nsL-TP might function both by supplying the peroxisomal β-oxidation enzymes with fatty acyl-CoA esters and by removing the oxidized or chain-shortened products. Currently, we are further investigating the role of nsL-TP in the peroxisomal β-oxidation pathway.

Acknowledgments

References

(1)   Wirtz, K. W. A. (1997) Phospholipid transfer proteins revisited *Biochem. J.* **324**, 353-360.

(2)   Wirtz, K. W. A., Kamp, H. H. and van Deenen, L. L. M. (1972) Isolation of a protein from beef liver which specifically stimulates the exchange of phosphatidylcholine. *Biochim. Biophys. Acta* **274**, 606-617.

(3)   Bloj, B.& Zilversmit, D.B. (1977) Rat liver proteins capable of transferring phosphatidylethanolamine. Purification and transfer activity for other phospholipids and cholesterol *J. Biol. Chem.* **252**,1613-1619

(4)   Scallen, T. J., Srikantaiah, M. V., Seetharam, B., Hansbury, E. and Gavey, K. L. (1974) Proceedings: Sterol carrier protein hypothesis. *Fed. Proc.* **33**, 1733-1746.

(5)   Gadella, T. W. J., Jr. and Wirtz, K. W. A. (1991) The low-affinity lipid binding site of the non-specific lipid transfer protein. Implications for its mode of action. *Biochim. Biophys. Acta* **1070**, 237-245.

(6)   Nichols, J. W. (1988) Kinetics of fluorescent-labelled phosphatidylcholine transfer between nonspecific lipid transfer protein and phospholipid vesicles. *Biochemistry* **27**, 1889-1896.

(7)   Gadella, T.W.J., Bastiaens, P.I.H., Visser, A.J.W.G. and Wirtz, K.W.A. (1991) Shape and lipid-binding site of the nonspecific lipid-transfer protein (sterol carrier protein 2): a steady-state and time-resolved fluorescence study. *Biochemistry* **30**, 5555-5564.

(8)   van Amerongen, A., Demel, R. A., Westerman, J. and Wirtz, K. W. A. (1989) Transfer of cholesterol and oxysterol derivatives by the nonspecific lipid transfer protein (sterol carrier protein 2): a study on its mode of action. *Biochim. Biophys. Acta* **1004**, 36-43.

(9)   Schroeder, F., Butko, P., Nemecz, G. and Scallen, T. J. (1990) Interaction of fluorescent delta 5,7,9(11),22-ergostatetraen-3 beta-ol with sterol carrier protein-2. *J. Biol. Chem.* **265**, 151-157.

(10)   Schroeder, F., Myers-Payne, S. C., Billheimer, J. T. and Wood, W. G. (1995) Probing the ligand binding sites of fatty acid and sterol carrier proteins: effects of ethanol. *Biochemistry* **34**, 11919-11927.

(11)   Frolov, A., Cho, T. H., Billheimer, J. T. and Schroeder, F. (1996) Sterol carrier protein-2, a new fatty acyl coenzyme A-binding protein. *J. Biol. Chem.* **271**, 31878-31884.

(12)   Suzuki, Y., Yamaguchi, S., Orii, T., Tsuneoka, M. and Tashiro, T. (1990) Nonspecific lipid transfer protein (sterol carrier protein-2) defective in patients with deficient peroxisomes. *Cell Struct. Funct.* **15**, 301-308.

(13)   Gould, S. J., Keller, G. A. and Subramani, S. (1987) Identification of peroxisomal targeting signals located at the carboxy terminus of four peroxisomal proteins. *J. Cell Biol.* **105**, 1657-1664.

(14)   Keller, G. A., Scallen, T. J., Clarke, D., Maher, P. A., Krisans, S. K. and Singer, S. J. (1989) Subcellular localization of sterol carrier protein-2 in rat hepatocytes: its primary localization to peroxisomes. *J. Cell Biol.* **108**, 1353-1361.

(15)   Tsuneoka, M., Yamamoto, A., Fujiki, Y. and Tashiro, Y. (1988) Nonspecific lipid transfer protein (sterol carrier protein-2) is located in rat liver peroxisomes. *J. Biochem. (Tokyo)* **104**, 560-564.

(16)   van der Krift, T. P., Leunissen, J., Teerlink, T., van Heusden, G. P. H. and Verkleij, A. J. (1985) Ultrastructural localization of a peroxisomal protein in rat liver using the specific antibody against the non-specific lipid transfer protein (sterol carrier protein 2). *Biochim. Biophys. Acta* **812**, 387-392

(17)   Seedorf, U., Brysch, P., Engel, T., Schrage, K. and Assmann, G. (1994) Sterol carrier protein X is peroxisomal 3-oxoacyl coenzyme A thiolase with intrinsic sterol carrier and lipid transfer activity. *J. Biol. Chem.* **269**, 21277-21283.

(18)   Wanders, R.J.A., Denis, S., Wouters, F., Wirtz, K.W.A. and Seedorf, U. (1997) Sterol carrier protein X (SCPx) is a peroxisomal branched-chain beta-ketothiolase specifically reacting with 3-oxo-pristanoyl-CoA: a new, unique role for SCPx in branched-chain fatty acid metabolism in peroxisomes. *Biochem. Biophys, Res, Commun.* **236**, 565-567

(19)   Antonenkov, V.D., Van Veldhoven, P.P., Waelkens, E. and Mannaerts, G.P. (1997) Substrate specificities of 3-oxoacyl-CoA thiolase A and sterol carrier protein 2/3-oxoacyl-CoA thiolase purified from normal rat liver peroxisomes. Sterol carrier protein 2/3-oxoacyl-CoA thiolase is involved in the metabolism of 2-methyl-branched fatty acids and bile acid intermediates. *J. Biol. Chem.* **272**, 26023-26031

(20)   Wouters, F.S., Bastiaens, P.I.H., Wirtz, K.W.A. and Jovin, T.M. (1998) FRET microscopy demonstrates molecular association of non-specific lipid transfer protein (nsL-TP) with fatty acid oxidation enzymes in peroxisomes. *EMBO J.* **17**, 7179-7189.

(21)   Seedorf, U., Raabe, M., Ellinghaus, P., Kannenberg, F., Fobker, M., Engel, T., Denis, S., Wouters, F.S., Wirtz, K.W.A., Wanders, R.J.A., Maeda, N. and Assmann, G. (1998) Defective peroxisomal catabolism of branched fatty acyl coenzyme A in mice lacking the sterol carrier protein-2/sterol carrier protein-x gene function. *Genes Develop.* **12**, 1189-1201

(22)   Seubert, W., Lamberts, I., Kramer, R. and Only, B. (1968) On the mechanism of malonyl-CoA-

independent fatty acid synthesis. I. The mechanism of elongation of long-chain fatty acids by acetyl-CoA. *Biochim. Biophys. Acta* **164**, 498-517.

(23)   Rasmussen, J. T., Borcher, T. and Knutsen, J. (1990) Comparison of the binding affinities of acyl-CoA-binding protein and fatty-acid-binding protein for long-chain acyl-CoA esters. *Biochem. J.* **265**, 849-855.

(24)   Ossendorp, B. C., Geijtenbeek, T. B. H. and Wirtz, K. W. A. (1992) The precursor form of the rat liver non-specific lipid-transfer protein, expressed in Escherichia coli, has lipid transfer activity. *FEBS Lett.* **296**, 179-183.

(25)   Crain, R. C. & Zilversmit, D. B. (1980) Two nonspecific phospholipid exchange proteins from beef liver. I. Purification and characterization. *Biochemistry* **19**, 1433-1439.

(26)   Jyothirmayi, N. and Ramadoss, C. S. (1991) Soybean lipoxygenase catalysed oxygenation of unsaturated fatty acid encapsulated in cyclodextrin. *Biochim. Biophys. Acta* **1083**, 193-200.

(27)   Bastiaens, P.I.H., A. van Hoek, J.A.E. Benen, J.-C. Brochon and A.J.W.G. Visser (1992). Conformational dynamics and intersubunit energy transfer in wild-type and mutant lipoamide dehydrogenase from *Azotobacter vinelandii*. Biophys. J. **63**, 839-853

(28)   Van Hoek, A. and A.J.W.G. Visser. (1990). *Appl. Optics* **29**, 2661-2663

(29)   Van Hoek, A. and A.J.W.G. Visser (1985). *Analytical Instrumentation* **14**, 359-378

(30)   Brochon, J.C. (1994). Maximum Entropy Method of Data Analysis in Time-Resolved Spectroscopy, In: "Methods in Enzymology" 240, Numerical Computer Methods, Part B, 262-311 , Ed. M.L. Johnson and L. Brand.

(31)   Wanders, R.J.A., Denis, S. and Dacremont, G (1993) Studies on the substrate specificity of the inducible and non-inducible acyl-CoA oxidases from rat kidney peroxisomes. *J. Biochem* **113**, 577-582

(32)   Stolowich, N.J., Frolov, A., Atshaves, B., Murphy, E.J., Jolly, C.A., Billheimer, J.T., Scott, A.I., and Schroeder, F. (1997) The sterol carrier protein-2 fatty acid binding site: an NMR, circular dichroic, and fluorescence spectroscopic determination. *Biochemistry* **36**, 1719-1729

(33)   Singh, I., Moser, A.E., Goldfischer, S. and Moser, H.W., (1984) Lignoceric acid is oxidized in the peroxisome: implications for the Zellweger cerebro-hepato-renal syndrome and adrenoleukodystrophy. *Proc Natl Acad Sci U S A* **81**, 4203-4207.

(34)   Niki, T., Bun-Ya, M., Hiraga, Y., Muro, Y. and Kamiryo, T. (1994) Near-stoichiometric interaction between the non-specific lipid-transfer protein of the yeast Candida tropicalis and peroxisomal acyl-coenzyme A oxidase prevents the thermal denaturation of the enzyme *in vitro*. Yeast **10**, 1467-1476.

(35)   Ceolotto, C., Flekl, W., Schorsch, F. J., Tahonat, D., Hapala, I., Hrastnik, C., Paltauf, F.and Daum, G. (1996) Characterization of a non-specific lipid transfer protein associated with the peroxisomal membrane of the yeast, Saccharomyces cerevisiae. *Biochem. Biophys. Acta* **1285**, 71-78.

(36)   Glatz, J. F. C. and van der Vusse, G. J. (1996) Cellular fatty acid-binding proteins: their function and physiological significance. *Prog. Lipid Res.* **35**, 243-282.

(37)   Maatman, R.G., van Moerkerk, H.T., Nooren, I.M., van Zoelen, E.J. and Veerkamp, J.H. (1994) Expression of human liver fatty acid-binding protein in Escherichia coli and comparative analysis of its binding characteristics with muscle fatty acid-binding protein. *Biochem. Biophys. Acta* **1214**, 1-10

(38)   Rolf, B., Oudenampsen-Kruger, E., Borchers, T., Faergeman, N.J., Knudsen, J., Lezius, A. and Spener, F.(1995) Analysis of the ligand binding properties of recombinant bovine liver-type fatty acid binding protein. *Biochem. Biophys. Acta* **1259**, 245-253

(39)   Wootan, M. G. and Storch, J. (1994) Regulation of fluorescent fatty acid transfer from adipocyte and heart fatty acid binding proteins by acceptor membrane lipid composition and structure. *J. Biol. Chem.* **269**, 10517-10523.

(40)   Herr, F. M., Aronson, J. and Storch, J. (1996) Role of portal region lysine residues in electrostatic interactions between heart fatty acid binding protein and phospholipid membranes. *Biochemistry* **35**, 1296-1303.

(41)   Reubsaet, F. A., Veerkamp, J. H., Bruckwilder, M. L., Trijbels, J. M. and Monnens, L. A. (1990) The involvement of fatty acid binding protein in peroxisomal fatty acid oxidation. *FEBS Lett.* **267**, 229-230.

(42)   Appelkvist, E. L. and Dallner, G. (1980) Possible involvement of fatty acid binding protein in peroxisomal beta-oxidation of fatty acids. *Biochem. Biophys. Acta* **617,** 156-160.

(43)   Richieri, G. V., Ogata, R. T. and Kleinfeld, A. M. J. (1994) Equilibrium constants for the binding of fatty acids with fatty acid-binding proteins from adipocyte, intestine, heart, and liver measured with the fluorescent probe ADIFAB. *J. Biol. Chem.* **269**, 23918-23930.

(44)   Kader, J.-C., (1996), *Annu. Rev. Plant Physiol. Plant Mol. Biol.* **47,** 627-654.

(45)   Meijer, E.A., De Vries, S.C., Sterk, P., Gadella, T.W.J., Wirtz, K.W.A. and Hendriks, T. (1993) Characterization of the non-specific lipid transfer protein EP2 from carrot (Daucus carota L.). *Mol. Cell.*

Biochem. **123**, 159-166

(46)   Arondel, V., Vergnolle, C., Tchng, F. and Kader, J.-C. (1990) Bifunctional lipid-transfer: fatty acid-binding proteins in plants. *Mol. Cell. Biochem.* **98**, 49-56

(47)   Tsuboi, S., Osafune, T., Tsugeki, R., Nishimura, M. and Yamada, M., (1992) Nonspecific lipid transfer protein in castor bean cotyledon cells: subcellular localization and a possible role in lipid metabolism. *J. Biochem.* **111**, 500-508

(48)   Ostergaard, J., Vergnolle, C., Schoentgen, F. and Kader, J.-C. (1993) Acyl-binding/lipid-transfer proteins from rape seedlings, a novel category of proteins interacting with lipids. *Biochim. Biophys. Acta* **1170**, 109-117

(49)   Gnamusch, E., Kalaus, C., Hrastnik, C., Paltauf, F. andDaum, G. (1992) Transport of phospholipids between subcellular membranes of wild-type yeast cells and of the phosphatidylinositol transfer protein-deficient strain Saccharomyces cerevisiae sec 14. *Biochim. Biophys. Acta* **1121**, 120-126.
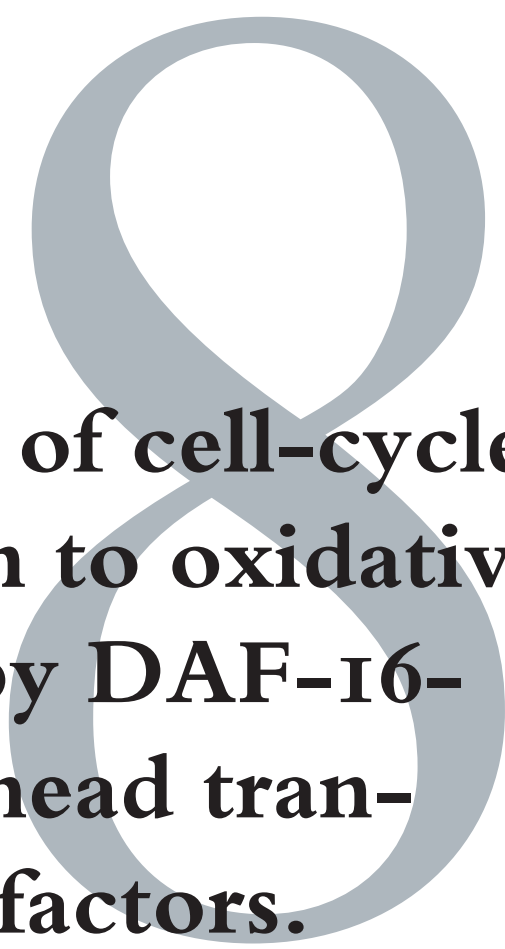
Coupling of cell-cycle regulation to oxidative damage by DAF-16-like Forkhead transcription factors.

Geert J.P.L. Kops, Tobias B. Dansen, Karel W.A. Wirtz, Paul J. Coffer, Ting-T. Huang, Johannes L. Bos, Rene H. Medema & Boudewijn M.T. Burgering. (2001) *To be submitted.*

Coupling of cell–cycle regulation and resistance to oxidative damage by DAF–16–like Forkhead transcription factors.

Geert J.P.L Kops[1], Tobias B. Dansen[2], Karel W.A. Wirtz[2], Paul J. Coffer[3], Ting-T. Huang[4], Johannes L. Bos[1], René H. Medema[5] & Boudewijn M.T. Burgering[1]

1. *Department of Physiological Chemistry and Centre for Biomedical Genetics University Medical Center Utrecht.*
2. *Department of Biochemistry of lipids, Institute of Biomembranes, Utrecht University, The Netherlands.*
3. *Department of Pulmonary Diseases, University Medical Center Utrecht.*
4. *Department of Pediatrics, University of California, San Francisco, USA.*
5. *Department of Molecular Biology, H8, Netherlands Cancer Institute, Amsterdam, The Netherlands.*

Abstract

In the absence of protein kinase B (PKB or c–Akt) activity the Forkhead transcription factors AFX, FKHR and FKHRL1, orthologues of Caenorhabditis elegans DAF–16, cause a G1/S arrest and an entry into quiescence ((1) and Kops *et al.*, submitted). Similar to anti–apoptotic signalling in proliferating cells, which involves PKB activity, quiescent cells need to be protected from damaging agents. Here we show that FKHRL1 protects the arrested cells from oxidative stress. Cells containing active FKHRL1 display increased levels of manganese superoxide dismutase. FKHRL1 directly activates the gene for manganese superoxide dismutase (SOD2) via a DAF–16 Binding Element, resulting in an increase in mRNA levels. Importantly, the increase in manganese superoxide dismutase is responsible for the Forkhead–induced enhancement of cellular anti–oxidant capacity. We propose that Forkhead transcription factors increase cellular lifespan by coupling a state of cellular quiescence with enhanced protection against oxidative damage.

The activity of the PI3K/PKB signalling pathway has been widely implicated in survival signalling (reviewed in (2)). An important component of anti–apoptotic signalling by active PKB appears to be the inhibition of the DAF–16–like Forkhead transcription factors AFX, FKHR and FKHRL1 that regulate the pro–apoptotic genes Bim and FasL (3–6). Indeed, in cell systems derived from the haematopoietic cell compartment, absence of PKB activity correlates with apoptosis partly via an increase in Bim and FasL expression (Jurkat, (4); Ba/F3, (6)). However, in many other mammalian cell types activation of the Forkheads or absence of PI3K/PKB signalling causes cell–cycle arrest and quiescence rather than apoptosis, at least in part through the regulation of p27kip1 gene expression ((1, 7, 8) and Kops *et al.*,

**Figure 1. Specific activation of FKHRL1.A3 in DL23 cells by 4OHT. a**. DL23 and DLD-1cells were transfected with the p1205Luc or p27GL2 reporter constructs containing the Forkhead-regulated promoters of the IGFBP1 or p27kip1 gene, respectively (1,3). The cells were left untreated or treated with 500 nM 4OHT for 16 hours and luciferase activity was measured. Data represent the average of three independent experiments. **b**. To show that Forkhead activation in the DL23 cells is homogeneous, DL23 cells were left untreated (-4OHT) or treated with 500 nM 4OHT (+4OHT) for 16 hours and stained for p27kip1 expression by immunofluorescence or analyzed for cell proliferation by BrdU-incorporation. Pictures were taken with identical exposure times. **c**. Total lysates of DL23 and DLD-1cells treated with or without 500 nM 4OHT were subjected to western blotting using antibodies to p27kip1 (anti-p27kip1), HA-FKHRL1.A3-ER (anti-ER) and actin as a loading control (anti-actin). WB: Western Blot.
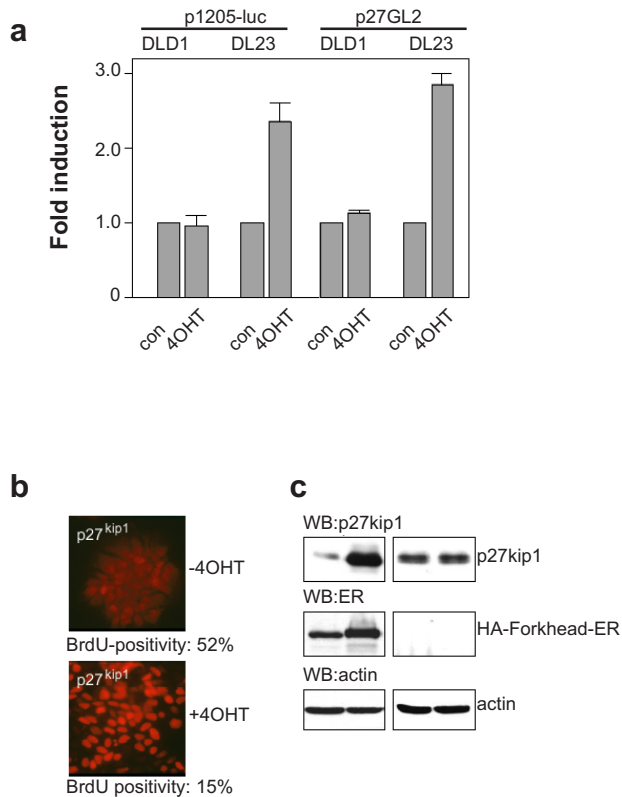
submitted). In agreement with this, in the nematode *C. elegans* the absence of AGE-1/AKT signalling and concomitant activation of DAF-16 results in longevity, not apoptosis (9-12). We set out to investigate how cells that have been driven into quiescence by the DAF-16-like Forkheads are protected from cytotoxic stress in the absence of PKB activity. Since reactive oxygen species (ROS) are a primary cause of cellular damage (reviewed in (13)), we focussed on examining the effects of Forkhead activity on cellular anti-oxidant capacity. To this end, we stably transfected a conditionally active HA-FKHRL1.A3-ER fusion (14) into DLD-1 human colon carcinoma cells. The HA-FKHRL1.A3-ER fusion protein is constitutively expressed but remains inhibited unless presented with a modified ligand for the estrogen receptor (ER), 4-hydroxy-tamoxifen (4OHT) (15). Treatment of the DL23 subclone with 500 nM 4OHT for 24 hours resulted in the specific activation of FKHRL1 as measured by previously described Forkhead activity assays including reporter assays with the promoters for the IGFBP1 and p27kip1 genes (figure 1a), a strong increase in p27kip1 protein levels and a decrease in cell proliferation (figure 1b,c) (1,3,14). Furthermore, protein levels of the p130 pocket protein were increased and pocket protein/E2F complexes shifted from p107/E2F-4 to p130/E2F-4 (Kops *et al.*, submitted). Importantly, 4OHT had no effect on the control DLD-1 cells (figure 1). To determine whether FKHRL1.A3 activation affects cellular protection against ROS, we made use of the lipophilic C11-BODIPY$^{581/591}$ probe which is suited for quantifying lipid-oxidation in single living cells (16). Upon oxidation, the fluorescence excitation/emission maxima of the C11-BODIPY$^{581/591}$ probe shift from 581/591 to 490/510

nm, facilitating the measurement of the fraction of oxidized probe versus time. DL23 cells left untreated or treated with 4OHT for 16 hours were loaded with the C11–BODIPY$^{581/591}$ probe and after addition of 200 μM H_2O_2 as a radical inducer followed in time with dual-excitation laser scanning microscopy. It is to be noted that the C11–BODIPY$^{581/591}$ probe is not oxidized by H_2O_2 itself, but by hydroxyl radicals formed in the Fenton–reaction: H_2O_2 + $O_2^{\cdot-} \rightarrow HO^{\cdot} + OH^- + O_2$ (catalyst: *metal*$^{2+}$). Fifty minutes after H_2O_2 addition the total oxidized fraction of the probe was 2-3 times lower (figure 2a) in cells containing active Forkhead compared to cells containing inactive Forkhead. Furthermore, the initial rate of oxidation of the probe in those cells was 4 times slower (figure 2b). Again, treatment of the DLD–1 control cell–line with 4OHT had no effect (figure 2b). These results demonstrate that specific activation of Forkheads increases the cellular protection against reactive oxygen species.

Next we examined whether Forkheads increase cellular anti–oxidant capacity via the regulation of anti–oxidant enzymes. The increase in protection displayed in figure 2 could be due to upregulation of either catalase or superoxide dismutase, as shown by the Fenton reaction. Superoxide dismutase was recently shown to inhibit apoptosis possibly due to an inhibition of cytochrome C release, as induced by superoxide accumulation, from the mitochon-
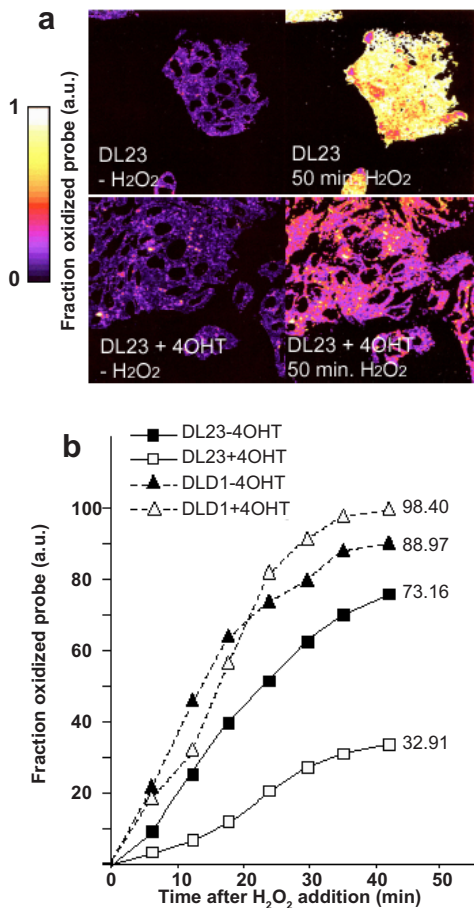
Figure 2. Forkhead transcription factors increase cellular protection against ROS. a. DL23 cells left untreated or treated with 500 nM 4OHT for 16 hours were loaded with the C11-BODIPY$^{581/591}$ probe for 20 minutes and subjected to 200 μM of the free-radical-inducing agent H_2O_2 for 50 minutes. Images of clusters of cells at timepoint 0 and 50 minutes after H_2O_2-addition were taken by confocal microscopy, and the fraction oxidized probe in arbitrary units (a.u.) was calculated as descibed in the 'Methods' section. Yellow areas represent 100% oxidation, black areas represent 0% oxidation. The circular black areas in the cell-population represent nuclei that fail to be loaded with the probe and have been ommitted from the final analysis. **b**. DL23 (solid lines) and DLD-1(dashed lines) cells were treated as in a. Images were taken at timepoints 0, 8, 16, 24, 32, 40 and 48 minutes after H_2O_2-addition. Calculations of the fraction of oxidized probe per timepoint in arbitrary units (a.u.) were performed as descibed under 'Methods'. A coulour image of figure 2a can be found at the back cover of this thesis.

dria (17). We therefore investigated whether Forkhead activity affects protein levels of superoxide dismutase. 4OHT-treatment of the DL23 cell-line for up to 24 hours showed a gradual increase in the amount of manganese superoxide dismutase (MnSOD) protein but no change in protein levels of copper/zinc superoxide dismutase (CuZnSOD) (Figure 3a). The increase in MnSOD expression was not a secondary event caused by p27kip1-induced cell-cycle arrest, since wildtype and p27kip1 -/- mouse embryo fibroblasts (MEFs) showed a similar increase in MnSOD protein upon infection with a FKHRL1.A3-expressing retrovirus
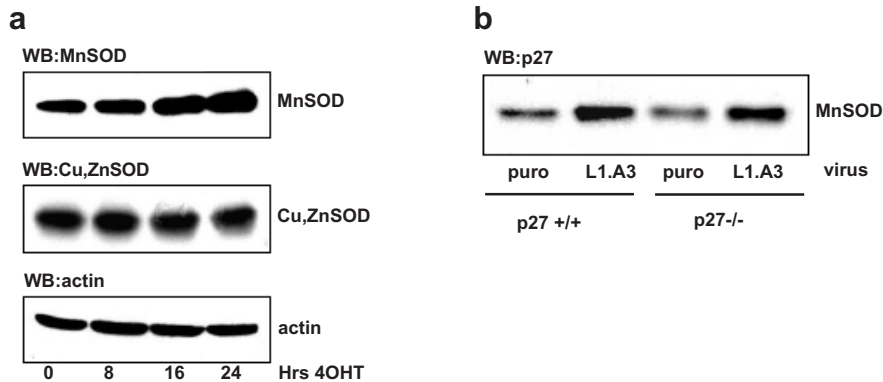
Figure 3. Forkhead activation results in upregulation of MnSOD. a. Total lysates of DL23 cells left untreated (0), or treated with 500nM 4OHT for 8, 12, 16 or 24 hours were analyzed for expression of MnSOD, Cu/ZnSOD and actin as a loading control. WB: Western Blot. **b**. Wildtype or p27kip1 MEFs were infected with a retrovirus containing a control plasmid (Con) or FKHRL1.A3 (L1.A3). Total lysates were collected 24 hours post-infection and subjected to western blotting using an antibody against MnSOD.

(figure 3b). Similar effects were seen when we used an HA-AFX-expressing retrovirus, indicating a general effect of this Forkhead subfamily (not shown).

To investigate whether the regulation of MnSOD protein levels by Forkheads is at the level of transcription, we first examined MnSOD mRNA expression in the DL23 cell-line. As seen in figure 4a, MnSOD mRNA levels are elevated between 8-16 hours of 4OHT-treatment and a ~10-fold increase is seen after 24 hours of FKHRL1 activation. Second, we investigated the effect of specific Forkhead activation on a 3340 basepair promoter fragment of the human *SOD2* gene for MnSOD using a luciferase reporter plasmid (pSODLUC-3340) (18). Luciferase expression controlled by this fragment was increased 3-4-fold upon cotransfection with the various Forkhead transcription factors in several cell-lines (data not shown) and upon 16 hours of 4OHT-addition to DL23 but not DLD-1 cells (Figure 4b). No effect was seen on a similar reporter construct lacking the sequences upstream of the transcription startsite (pSODLUC-1) (Figure 4b). Recently, the optimal DNA binding sequence for the DAF-16-like Forkhead transcription factors has been determined (19). This DAF-16 Binding Element (DBE) contains the core sequence TTGTTTAC. Point mutations in the TTGTTT sequence prevent Forkhead-binding to the DBE and transactivation of a 6XDBE reporter construct. Within the human *SOD2* promoter fragment one inverse DBE at position -1249 (GTAAACAA, DBE1) and one sub-optimal DBE at position -997 (TTGTTTAA, DBE2) are found (Figure 4c). To determine whether Forkhead-mediated increase in MnSOD gene expression is direct, we mutated single basepairs in the two DBE's. A single G to C substitution in the TTGTTT sequence of DBE2 had no effect on FKHRL1-induced luciferase activity of the *SOD2* reporter construct, but a similar substitution in the AAACAA sequence of DBE1 completely abolished FKHRL1-mediated *SOD2* gene expression (Figure 4c). This
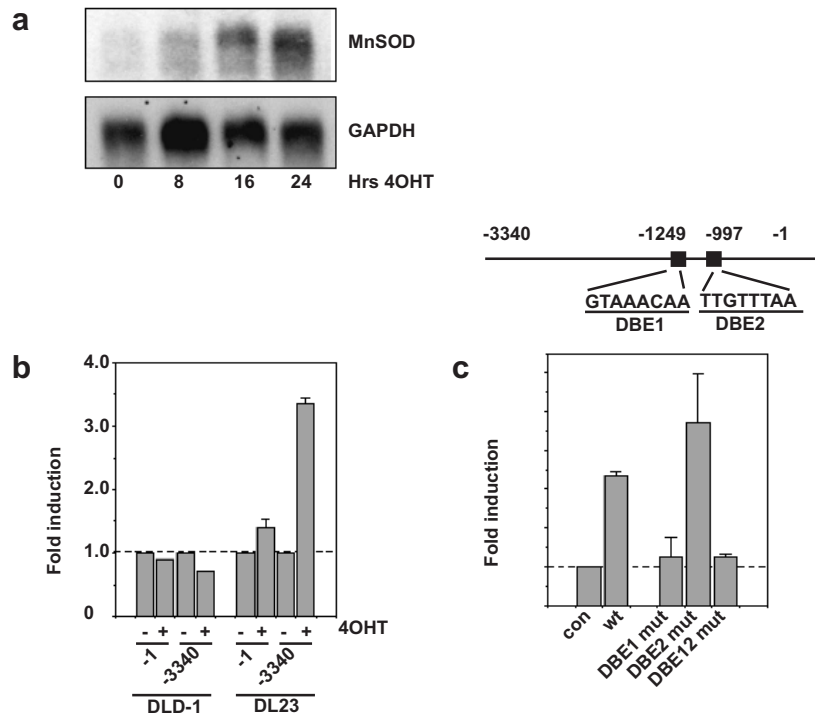
Figure 4. FKHRL1 directly regulates the MnSOD promoter via an inverse DBE. a. 2 μg mRNA isolated from DL23 cells left untreated (0) or treated with 500 nM 4OHT for 8, 16 or 24 hours were electroforesed, blotted onto a nylon membrane and probed for presence of MnSOD and GAPDH as a loading control, using radiolabelled probes. **b**. pSODLUC-3340 and pSODLUC-1 were transfected into DL23 or DLD-1cells that were subsequently left untreated or treated with 500 nM 4OHT for 16 hours after which luciferase activity was measured. Data represent the average of three independent experiments. **c**. pSODLUC-3340 carrying a point mutation at position -1246 in the first DBE (DBE1mut) or at position -995 in the second DBE (DBE2mut) or both (DBE12mut) were transfected into DL23 cells. Luciferase activity was measured after cells were left untreated or treated with 500 nM 4OHT for 16 hours. Data represent the average of three independent experiments. Drawing represents linearized *SOD2* promoter fragment containing the two DBE's.

clearly demonstrates that Forkhead transcription factors directly regulate MnSOD gene expression through a single inverse DBE.

MnSOD is a mitochondrial anti-oxidant enzyme that converts the free-radical-containing superoxide anion ($O_2^{\cdot-}$), generated as a byproduct of the electron-transport-chain, into hydrogen peroxide (H_2O_2). Some of the harmful effects of the superoxide anion such as lipid-oxidation and the induction of DNA breaks have been implicated in various diseases and aging (reviewed in (20)). By reducing the amount of superoxide anions, MnSOD can participate in the cellular protection against free radicals and thus contribute to the maintenance of cellular integrity. However, the hydrogen-peroxide formed by MnSOD is still harmful to the cell. Therefore we investigated whether the hydrogen-peroxide-metabolizing enzyme catalase is increased in cells after Forkhead activation. Indeed, DL23 cells treated with 500 nM 4OHT displayed an increase in catalase protein with kinetics similar to MnSOD upregulation (figure 5a). This indicates that the direct regulation of MnSOD by Forkheads which results in

a

WB: anti-catalase

DL23

| 0 | 8 | 16 | 24 | Hrs 4OHT |

b

c
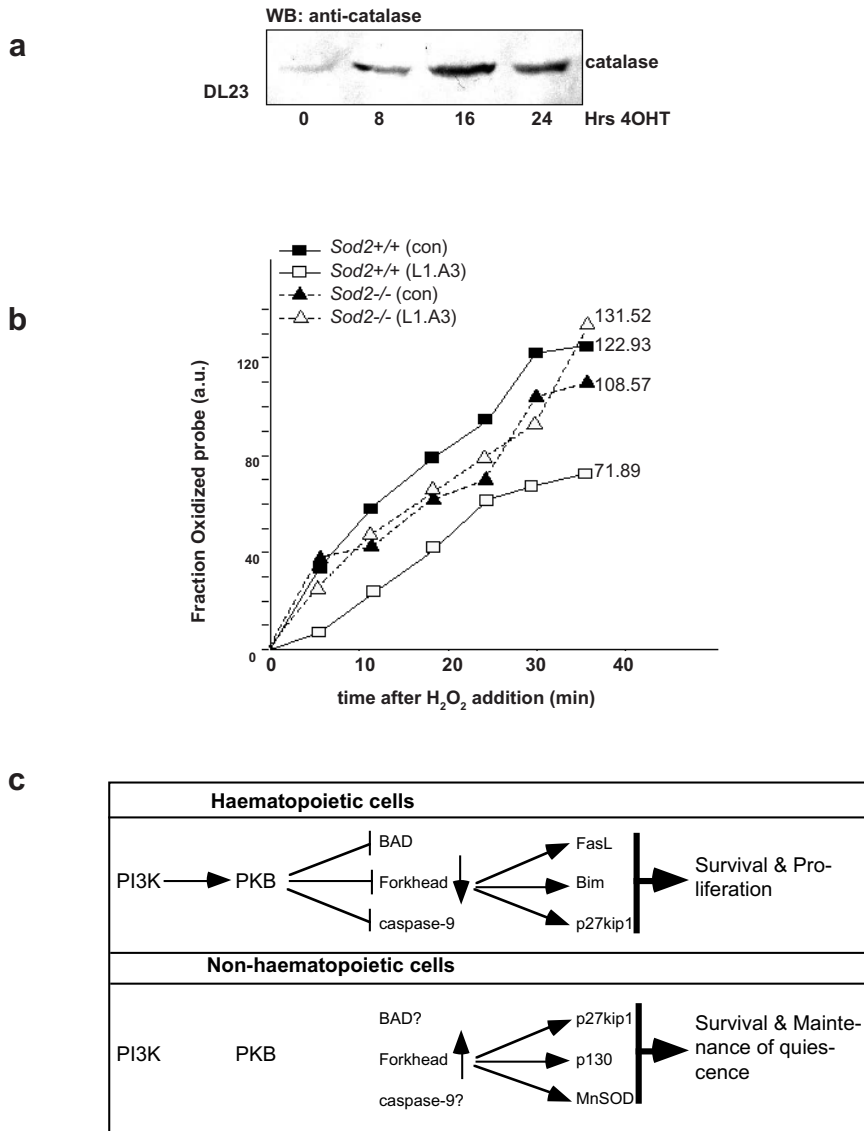
Figure 5. FKHRL1-induced protection from oxidative damage depends on MnSOD. a. Total cellular lysates from DL23 cells left untreated (0) or treated with 500 nM 4OHT for 8, 16 or 24 hours were immunoblotted for the presence of catalase. WB: western blot. **b**. Primary MEFs from wildtype (solid lines) or *Sod2* knockout (dashed lines) mice were infected with control (puro) or HA-FKHRL1.A3-expressing retrovirus. Three days post-infection, the cells were analyzed for cellular anti-oxidant capacity as in figure 2. Images were taken at 6-minute intervals after H_2O_2-addition. Calculations of the fraction of oxidized probe in arbitrary units (a.u.) per timepoint were performed as descibed under 'Methods'. **c**. Model for Forkhead-mediated cell-fate decision. In highly proliferative cell such as those from the haemaopoietic system, PKB activity induces a survival signal by inhibiting Forkheads, BAD and caspase-9. In quiescent cell types, how-ever, the absence of PKB activity does not automatically lead to apoptosis. In these cells the maintenance of quies-cence is coupled to survival through Forkhead-mediated expression of p27kip1, p130 and MnSOD.

the production of hydrogen-peroxide is coupled to the regulation of catalase which converts hydrogen-peroxide to water and oxygen. Next, we investigated whether the enhancement of cellular anti-oxidant capactiy by Forkheads as seen in figure 2 is due to a Forkhead-mediated increase in MnSOD gene expression. To this end we analyzed the effect of Forkhead expression on cellular stress in *Sod2 -/-* MEFs (21,22) using the C11-BODIPY[581/591] probe assay. Infection of primary MEFs from wildtype mice (*Sod2+/+*) with a retrovirus carrying FHKRL1.A3 resulted in a marked two-fold enhancement of cellular anti-oxidant capacity compared to infection with a control virus (figure 5b). However, in primary MEFs from *Sod2* knockout mice (*Sod2-/-*) FKHRL1.A3 expression could not protect cells from H_2O_2-induced cellular stress (figure 5b). This last results also indicates that the Forkhead-induced upregulation of catalase might be an indirect consequence of MnSOD increase, for the *Sod2-/-* cells are no longer protected. Altogether, these data clearly show that Forkhead transcription factors can decrease radical-induced oxidative damage via direct regulation of MnSOD gene expression.

In proliferating cells the activation of PKB has been associated with protection from apoptosis induced by various stimuli. Here we show that a signal equivalent to the absence of PKB activity in non-proliferating, quiescent cells can accomplish the same result. When challenged with incriminating stimuli such as H_2O_2, cells that contain active FKHRL1 are protected form oxidative damage through a Forkhead-mediated increase in MnSOD gene expression. This suggests a situation where the outcome of the activity of the PI3K/PKB/Forkhead pathway with respect to protection from cellular damage depends on the cell-system and the cell-cycle phase the cells are in (figure 5c). In *C. elegans* the DAF-2/AKT/DAF-16 pathway regulates metabolism, dauer formation and organismal lifespan (9,10,12). Restoration of DAF-2/AKT/DAF-16 signalling in different cellular compartments of DAF-2 mutants has revealed that reconstitution in neuronal cells results in rescue of all three phenotypes (11). To date, the only gene targets found for DAF-16 are the free-radical-scavenging enzymes cytosolic catalase (*ctl-1*) and MnSOD (*sod-3*) and they were shown to be required for DAF-16-induced dauer formation (23,24). The observation that *C. elegans* organismal lifespan is solely determined by DAF-16 signalling in the brain has led to the suggestion that anti-oxidant enzymes contribute to an increased cellular lifespan of neurons that deliver neuro-endocrine signals to the organism. Our results now start to define a remarkable conservation of function. Neurons are generally considered to be post-mitotic or quiescent cells. The finding that FKHRL1 expression is relatively high in the brain (19) allows us to speculate that the DAF-16 like Forkheads might be involved in the regulation of neuronal cellular lifespan through the maintenance of quiescence and protection from oxidative damage. Possibly, as in *C. elegans*, this might contribute to the control of organismal lifespan. In addition, quiescent/differentiated cells have upregulated levels of anti-oxidant enzymes, especially of MnSOD protein and mRNA (25-27), a property that is lacking in various tumor cells (reviewed in (28)). Our data suggest that the observations that certain tumors have low levels of p27kip1 and/or MnSOD (reviewed in (29)) might be a consequence of the inactivation of the DAF-16-like Forkheads by activation of the PI3K/PKB pathway and furthermore that this might contribute to the process of oncogenic transformation. Finally, it is important to note that Cu/ZnSOD is not regulated. Apparently, CuZnSOD does not need to be induced for enhanced protection during quiescence which might relate to the fact that CuZn SOD is cytosolic whereas MnSOD is mitochondrial. This points to the unique function of MnSOD and illustrates the importance of its regulation by external ques. In agreement with

this, overexpression of CuZnSOD in MnSOD deficient mouse fibroblasts cannot prevent neonatal lethality nor oxidative aconitase inactivation (30). In conclusion, we propose that the mammalian DAF–16-like Forkhead transcription factors AFX, FKHR and FKHRL1 increase cellular lifespan by coupling cell–cycle exit with enhanced protection from oxidative damage.

Methods

Cell culture, retroviral infections and stable cell-lines.
The DL23 cell–line was created as follows: linearized pcDNA3-HA-FKHRL1.A3-ER (14) was transfected into DLD-1 human colon carcinoma cells by electroporation. Transfectants were selected for two weeks on 500 μg/ml geneticin. Subsequently, clones were isolated and analyzed for expression of the fusion protein. The DL23 subclone was chosen for further study. The DLD-1 and DL23 cell–lines were maintained in RPMI-1640 with standard supplements and the appropriate selection antibiotic. Retroviral infections and maintenance of immortalized wildtype and p27kip1 –/– as well as primary wildtype and *Sod2-/-* MEFs has been described(1,22).
Cloning and plasmids. pBabe-FKHRL1.A3 was created by ligating a Klenow-blunted HindIII/BamHI fragment of pcDNA3-HA-FKHRL1.A3 into Klenow-blunted BamHI-cut pBabe-puro. pcDNA3-HA-FKHRL1.A3-ER has been described(14). pSODLUC-3340 and pSODLUC-1 were a kind gift of M. Yim (18). pSODLUC-3340.DBE1mut and pSODLUC-3340.DBE2mut were created by site-directed mutagenesis using the primers 5'-ctgacgtctgtaaagaagcccagcccttc-3' and 5'- cattcaggattgttctttaactgttgag-3', respectively. p1205luc was a kind gift of D. Powell (31). p27GL2 has been described (1). pBabe-puro used for retroviral infections of MEFs has been described (1). pGEMZ-MnSOD was a kind gift of J. Wispe (32).

Western blotting, antibodies and standard immunofluorescence.
Western blotting of total lysates was performed as descibed(3). Antibodies to MnSOD and Cu/ZnSOD were from StressGen. The antibodies to ER (C-20) and actin (I-19) were from SantaCruz. The p27kip1 antibody was from Transduction Labs. Anti-catalase has been described (33). Standard immunofluorescence using the p27kip1 antibody was performed as follows: cells were fixed in 4% paraformaldehyde, permeabilized and blocked with PBS contining 0.1% TX-100, 0.5% BSA and stained with anti-p27kip1 followed by Cy3-conjugated goat anti-mouse secondary antibody (Jackson ImmunoResearch Labs).
Northern blotting. 2 μg of mRNA (polyA-Tract, Promega) purified from 1 mg total RNA (RNAZol, TEL-TEST, Inc.) was run on a formaldehyde denaturing gel and blotted onto GeneScreen-Plus nylon membrane (NEN). The blot was hybridized using radiolabelled MnSOD (EcoRI fragment of pGEM3Z-MnSOD) and GAPDH (NotI-linearized pUC19-GAPDH) probes.

Luciferase assays.
Luciferase assays were performed as described(3).

BrdU incorporation.
BrdU incorporation was performed as described (1)

Microscopy and fluorescence ratio-imaging.

Generally, microscopy and fluorescence ratio-imaging were performed as described (16). Shortly, cells cultured on coverslips were placed in a temperature (37°C)-controlled coverslip holder in the microscope and incubated for 20 min with C11-BODIPY[581/591] (Molecular Probes). To this end, C11- BODIPY[581/591] was dissolved in fetal calf serum to a final concentration of 0.1 mgml[-1]. This stock was diluted 1000 times in PBS supplemented with 5 mM glucose, 0.5 mM $CaCl_2$ and 0.9 mM $MgCl_2$ (PBS+). After washing with fresh PBS+, images were taken with a Leica TCSNT confocal laser scanning system on an inverted microscope DMIRBE (Leica Microsystems) with an argon-krypton laser as excitation source. The green and red fluorescence of C11-BODIPY[581/591] was acquired simultaneously using double wavelength excitation (laserlines 488 and 568 nm) and detection (emission bandpass filter 530/30 nm for green and longpass 560 nm followed by a bandpass 600/30 nm for red). Oxidized and non-oxidized C11-BODIPY[581/591] are spectrally well separated and this property was used to quantify the fraction of oxidized and non-oxidized C11-BODIPY[581/591] simultaneously at any time point. Images were processed and calculated with Scion Image 1.62 on a Macintosh PowerPC. Image calculus of figure 2a was performed as followed: the red and green fluorescence of the probe was assesed at several timepoints. The fraction oxidized probe in every timepoint was calculated as the ratio of I^{green} to $I^{green}+I^{red}$, where I^{green} and I^{red} are the intensities of the green and the red fluorescent signal respectively. Images were smoothed before the algorythm was applied. The signal of the probe was filtered from the rest of the images by tresholding. The calculated fractions were averaged using the smooth filter. A false colour look-up table was applied to visualize low and high oxidation of the probe. All data are normalized, arbitrary units.

References

(1)   Medema, R. H., Kops, G. J., Bos, J. L. and Burgering, B. M. (2000) AFX-like Forkhead transcription factors mediate cell-cycle regulation by Ras and PKB through p27kip1. *Nature* **404**, 782-787.

(2)   Datta, S. R., Brunet, A. and Greenberg, M. E. (1999) Cellular survival: a play in three Akts. *Genes Dev* **13**, 2905-2927.

(3)   Kops, G.J., de Ruiter, N.D., De Vries-Smits, A.M., Powell, D.R., Bos, J.L., Burgering, B.M.(1999) Direct control of the Forkhead transcription factor AFX by protein kinase B. *Nature* **398**, 630-634.

(4)   Brunet, A., Bonni, A., Zigmond, M.J., Lin, M.Z., Juo, P., Hu, L.S., Anderson, M.J., Arden, K.C., Blenis, J., Greenberg, M.E. (1999) Akt promotes cell survival by phosphorylating and inhibiting a Forkhead transcription factor. *Cell* **96**, 857-868.

(5)   Rena, G., Guo, S., Cichy, S. C., Unterman, T. G. & Cohen, P. (1999) Phosphorylation of the Transcription Factor Forkhead Family Member FKHR by Protein Kinase B. *J Biol Chem* **274**, 17179-17183.

(6)   Dijkers, P. F., Medema, R. H., Lammers, J. J., Koenderman, L. & Coffer, P. J. (2000) Expression of the pro-apoptotic bcl-2 family member bim is regulated by the forkhead transcription factor FKHR-L1 [In Process Citation]. *Curr Biol* **10**, 1201-1204.

(7)   Li, D. M. and Sun, H. (1998) PTEN/MMAC1/TEP1 suppresses the tumorigenicity and induces G1 cell cycle arrest in human glioblastoma cells. *Proc Natl Acad Sci U S A* **95**, 15406-15411.

(8)   Nakamura, N., Ramaswamy, S., Vazquez, F., Signoretti, S., Loda, M., Sellers, W.R. (2000) Forkhead transcription factors are critical effectors of cell death and cell cycle arrest downstream of PTEN. *Mol Cell Biol* **20**, 8969-8982.

(9)   Ogg, S., Paradis, S., Gottlieb, S., Patterson, G.I., Lee, L., Tissenbaum, H.A., Ruvkun, G. (1997) The Fork head transcription factor DAF-16 transduces insulin-like metabolic and longevity signals in C. elegans. *Nature* **389**, 994-999.

(10)   Lin, K., Dorman, J. B., Rodan, A. and Kenyon, C. (1997) daf-16: An HNF-3/forkhead family member that can function to double the life-span of Caenorhabditis elegans. *Science* **278**, 1319-1322.

(11)   Wolkow, C. A., Kimura, K. D., Lee, M. S. and Ruvkun, G. (2000) Regulation of C. elegans life-span by insulinlike signalling in the nervous system. *Science* **290**, 147-150.

(12)   Paradis, S. and Ruvkun, G. (1998) Caenorhabditis elegans Akt/PKB transduces insulin receptor-like signals from AGE-1 PI3 kinase to the DAF-16 transcription factor. *Genes Dev* **12**, 2488-2498.

(13)   Beckman, K. B. and Ames, B. N. (1998) The free radical theory of aging matures. *Physiol Rev* **78**, 547-581.

(14)   Dijkers, P.F., Medema, R.H., Pals, C., Banerji, L., Thomas, N.S., Lam, E.W., Burgering, B.M., Raaijmakers, J.A., Lammers, J.W., Koenderman, L., Coffer, P.J. (2000) Forkhead transcription factor FKHR-L1 modulates cytokine-dependent transcriptional regulation of p27(KIP1). *Mol Cell Biol* **20**, 9138-9148.

(15)   Littlewood, T. D., Hancock, D. C., Danielian, P. S., Parker, M. G. and Evan, G. I. (1995) A modified oestrogen receptor ligand-binding domain as an improved switch for the regulation of heterologous proteins. *Nucleic Acids Res* **23**, 1686-1690.

(16)   Pap, E.H., Drummen, G.P., Winter, V.J., Kooij, T.W., Rijken, P., Wirtz, K.W., Op den Kamp, J.A., Hage, W.J., Post, J.A.(1999) Ratio-fluorescence microscopy of lipid oxidation in living cells using C11-BODIPY(581/591). *FEBS Lett* **453**, 278-282.

(17)   Huang, P., Feng, L., Oldham, E. A., Keating, M. J. and Plunkett, W. (2000) Superoxide dismutase as a target for the selective killing of cancer cells . *Nature* **407**, 390-395.

(18)   Kim, H. P., Roe, J. H., Chock, P. B. and Yim, M. B. (1999) Transcriptional activation of the human manganese superoxide dismutase gene mediated by tetradecanoylphorbol acetate. *J Biol Chem* **274**, 37455-37460.

(19)   Furuyama, T., Nakazawa, T., Nakano, I. and Mori, N. (2000) Identification of the differential distribution patterns of mRNAs and consensus binding sequences for mouse DAF-16 homologues. *Biochem J* **349**, 629-634.

(20)   Mates, J. M. and Sanchez-Jimenez, F. (1999) Antioxidant enzymes and their implications in pathophysiologic processes. *Front Biosci* **4**, D339-345.

(21)   Li, Y., Huang, T.T., Carlson, E.J., Melov, S., Ursell, P.C., Olson, J.L., Noble, L.J., Yoshimura, M.P., Berger, C., Chan, P.H., *et al.* (1995) Dilated cardiomyopathy and neonatal lethality in mutant mice lacking manganese superoxide dismutase. *Nat Genet* **11**, 376-381.

(22)   Huang, T.T., Yasunami, M., Carlson, E.J., Gillespie, A.M., Reaume, A.G., Hoffman, E.K., Chan,

P.H., Scott, R.W., Epstein, C.J. (1997) Superoxide-mediated cytotoxicity in superoxide dismutase-deficient fetal fibroblasts. *Arch Biochem Biophys* **344**, 424-432.

(23) Taub, J., Lau, J.F., Ma, C., Hahn, J.H., Hoque, R., Rothblatt, J., Chalfie, M.(1999) A cytosolic catalase is needed to extend adult lifespan in C. elegans daf-C and clk-1 mutants. *Nature* **399**, 162-166.

(24) Honda, Y. and Honda, S. (1999) The daf-2 gene network for longevity regulates oxidative stress resistance and Mn-superoxide dismutase gene expression in Caenorhabditis elegans. *Faseb J* **13**, 1385-1393.

(25) Oberley, L. W., Ridnour, L. A., Sierra-Rivera, E., Oberley, T. D. and Guernsey, D. L. (1989) Superoxide dismutase activities of differentiating clones from an immortal cell line. *J Cell Physiol* **138**, 50-60.

(26) Church, S. L., Farmer, D. R. and Nelson, D. M. (1992) Induction of manganese superoxide dismutase in cultured human trophoblast during *in vitro* differentiation. *Dev Biol* **149**, 177-184.

(27) Bravard, A., Beaumatin, J., Dussaulx, E., Lesuffleur, T., Zweibaum, A., Luccioni, C. (1994) Modifications of the anti-oxidant metabolism during proliferation and differentiation of colon tumor cell lines. *Int J Cancer* **59**, 843-847.

(28) Oberley, L. W. and Oberley, T. D. (1988) Role of antioxidant enzymes in cell immortalization and transformation. *Mol Cell Biochem* **84**, 147-153.

(29) Lloyd, R.V., Erickson, L.A., Jin, L., Kulig, E., Qian, X., Cheville, J.C., Scheithauer, B.W.(1999) p27kip1: a multifunctional cyclin-dependent kinase inhibitor with prognostic significance in human cancers. *Am J Pathol* **154**, 313-323.

(30) Copin, J. C., Gasche, Y. and Chan, P. H. (2000) Overexpression of copper/zinc superoxide dismutase does not prevent neonatal lethality in mutant mice that lack manganese superoxide dismutase. *Free Radic Biol Med* **28**, 1571-1576.

(31) Powell, D.R., Suwanichkul, A., Cubbage, M.L., DePaolis, L.A., Snuggs, M.B., Lee, P.D.(1991) Insulin inhibits transcription of the human gene for insulin-like growth factor-binding protein-1. *J Biol Chem* **266**, 18868-18876.

(32) Wispe, J.R., Clark, J.C., Burhans, M.S., Kropp, K.E., Korfhagen, T.R., Whitsett, J.A.(1989) Synthesis and processing of the precursor for human mangano-superoxide dismutase. *Biochim Biophys Acta* **994**, 30-36.

(33) Wiemer, E.A., Ofman, R., Middelkoop, E., de Boer, M., Wanders, R.J., Tager, J.M.(1992) Production and characterisation of monoclonal antibodies against native and disassembled human catalase. *J Immunol Methods* **151**, 165-175.
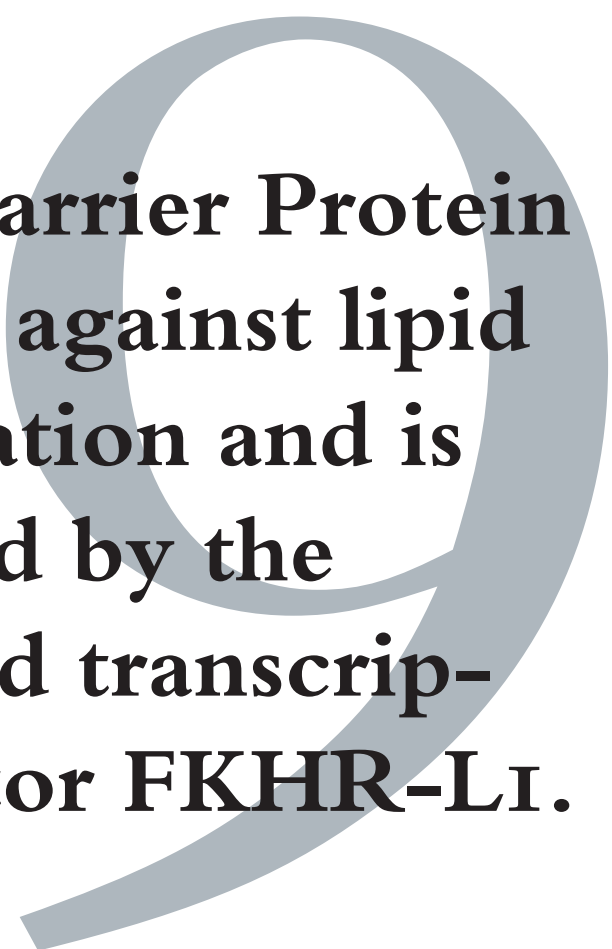
Sterol Carrier Protein protects against lipid peroxidation and is regulated by the Forkhead transcription factor FKHR-L1.

Tobias B. Dansen, Geert J.P.L. Kops, Johannes Wiekowski, Udo Seedorf, Nannette Jelluma, Johannes L. Bos, Boudewijn M.T. Burgering & Karel W.A. Wirtz. (2001) *To be submitted.*

Sterol Carrier Protein protects against lipid peroxidation and is regulated by the Forkhead transcription factor FKHR-L1.

Tobias B. Dansen[1], Geert J.P.L. Kops[2], Johannes Wiekowski[3], Udo Seedorf[3], Nannette Jelluma[1], Johannes L. Bos[2], Boudewijn M.T. Burgering[2] & Karel W.A. Wirtz[1].

1. Dept. of Biochemistry of Lipids, Institute of Biomembranes, Utrecht University, Padualaan 8, 3584 CH Utrecht, The Netherlands.
2. Dept. of Physiological Chemistry and Centre for Biomedical Genetics, University Medical Centre, Heidelberglaan 100, 3584 CG Utrecht, The Netherlands.
3. Institut für Arterioseforschung, University of Münster, Domagkstrasse 3, D-48149 Münster, Germany.

Summary

Starting from different promoter sites, the scp-gene (accession number AH004933) encodes two proteins, the 58 kDa Sterol Carrier Protein X (SCPx) and the 15 kDa precursor of Sterol Carrier Protein 2 (preSCP2). SCPx is the peroxisomal 3-keto-acyl-CoA thiolase for branched-chain fatty acids and the bile-acid precursors di- and tri-hydroxy-24-ketocholestanoyl-CoA (keto-THC-CoA). SCP2 is also peroxisomal and binds very-long chain and poly-unsaturated fatty acyl-CoA esters with high affinity. Here we show that homozygosity for a null mutation in the scp-gene leads to elevated levels of lipid peroxidation in the liver and hepatocarcinogenesis in mice. In agreement with this, isolated scp –/– hepatocytes spontaneously oxidize the fluorescent fatty acid analogue C11-BODIPY$^{581/591}$. Under conditions of oxidative stress *in vitro*, we found that C11-BODIPY$^{581/591}$ bound to SCP2 is protected from oxidative damage, indicating that SCP2 has an anti-oxidant function. By in silico screening of the *scp* gene, we identified multiple putative binding sites for the daf-16 like Forkhead transcription factors, one of which is located in the promoter site for SCP2. These Forkhead transcription factors are involved in the protection of the cell against oxidative stress by the upregulation of manganese superoxide-dismutase (MnSOD) and catalase, thereby increasing the cellular lifespan. Here we show that activation of the Forkheads leads to enhanced scp gene transcription yielding elevated levels of SCPx/SCP2. Taken together, the data presented suggest a role for SCP2 in the anti-oxidant defense mechanism of the cell.

Introduction

sterol carrier proteins SCPx/SCP2 are encoded by the *scp* gene. This gene contains two promoters; one upstream of the gene, and a second one within intron 11(1). Transcription from either promoter yields two messengers due to alternative poly-adenylation (2). When started from the first promoter, transcripts of 2.4 and 3.0 kb are formed, while the second promoter gives rise to 1.1 and 1.7 kb transcripts. Both the 2.4 and the 3.0 kb mRNAs encode the full length 58 kDa SCPx; the 1.1 and 1.7 kb mRNAs encode the 15 kDa pre-SCP2 (see figure 1). Alternatively, SCP2 can be formed by cleavage of SCPx, yielding also a 46 kDa protein (3). Both SCPx and the 46 kDa protein have been shown to be a 3-oxoacyl-CoA thiolase, that catalyzes the final step in the peroxisomal breakdown of branched-chain fatty acids (like 3-keto-pristanoyl-CoA) and in the formation of the bile-acid precursor choloyl-CoA (4, 5). The C-terminus contains a peroxisomal targeting signal of type I (AKL) which directs the SCPx/SCP2 to peroxisomes. Since SCPx is exclusively found in the peroxisome, the processing into the 46 kDa thiolase and SCP2 must take place in the matrix of this organelle (6). SCP2 has been shown to have *in vitro* lipid transfer activity (7) and to bind VLCFA- (8) and PUFA-CoA esters (9) with high affinity. Moreover it has been implicated in cholesterol trafficking and metabolism. However, *scp* null mice show no obvious defects in their cholesterol homeostasis (10). Indeed, these mice are impaired in the peroxisomal β-oxidation of BCFAs and have impaired bile-acid formation (11). Here we will show that mice carrying a null mutation in the *scp*-gene develop hepatocarcinomas and have elevated levels of lipid peroxidation products in their liver. Since SCP2 binds fatty acyl-CoA esters in a hydrophobic pocket shielded from the aqueous surroundings (12), we looked into a possible role for SCP2 in the protection of fatty acids against peroxidation. The results suggest indeed an anti-oxidant function for SCP2.

The scp gene and its products
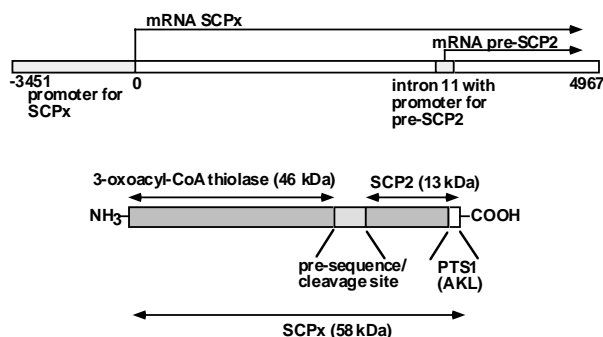
Figure 1. The scp gene has two promoters and when transcription is strated form either promoter two mRNAs are formed due to alternative polyadenylation. Transcription form the upstream promoter gives rise to mRNAs encoding the 58 kDa SCPx which consists of a N-terminal part which is the thiolase for 3-keto branched chain fatty acids and bile acid intermediates, and a C-terminal part which is SCP2. SCPx can be cleaved in the peroxisome to yield a 46 kDa thiolase and 12 kDa SCP2. Alternatively, SCP2 can be formed as a 15 kDa preSCP2 precursor when scp is transcribed form a promoter within intron 11. The presequence of 20 amino acids is cleaved off upon import in the peroxisome.

The regulation of *scp* gene products have been a matter of study, but as yet, has not been resolved. Treatment of cells with a peroxisome proliferator had no effect on its expression (13). Decreased levels of SCP2 (14) were described in *ras*- and *src*- transformed colon cells, and hepatoma cells express less SCPx/SCP2 as compared to hepatocytes (15). This could be indicative of a link between SCPx/SCP2 expression and growth factor signalling. For the following reasons, we have looked into a possible negative regulation of SCPx/SCP2 expression via phosphatidylinositol-3-OH kinase (PI3K): i) PI3K is activated in *ras* transformed cells (16); ii) PI3K is involved in the upregulation of the anti-oxidant status in *C.Elegans*

via the forkhead transcription factor daf-16 (17, 18); iii) the *scp* gene contains multiple puta-
tive binding sites for the Daf-16 like forkhead transcription factors AFX, FKHR and FKHR-
L1.

The *C. Elegans* daf-16 gene product is a Forkhead transcription factor that regulates
dauer formation via enhanced protection against oxidative stress through the upregulation of
MnSOD and catalase. Daf-16 is negatively regulated ny the Age-1 (a PI3K) and Akt (19)
pathway. In analogy, the same pathway (Pi3K/PKB(also known as Rac or Akt)) regulates the
expression of MnSOD and catalase in mammals (see also chapter 8). PKB, upon activation by
PI3K, is directed to the nucleus where it phosphorylates the Daf-16 like forkhead transcrip-
tion factors AFX, FKHR and FKHR-L1. Upon phosphorylation, these transcription factors
leave the nucleus and thus become inactive (20). In this way, PI3K siganlling decreases MnSOD
and catalase gene expression. Recently, the Daf-16 binding element (DBE) to which Daf-16
like Forkhead transcription factors bind, was identified as 5'-TTGTTTAC-3' (21). Muta-
tional analysis showed that mutations in the TTGTTT lead to impaired binding (22). We
found by *in silico* screening that the *scp* gene contains two sub-optimal DBEs (5'-TTGTTTAT-
3') at positions +451 and +2832, and one inverse DBE (5'-GTAAACAA-3') at position
+4217. The +2832 site is within the intron containing the preSCP2 promoter. Furthermore
the promoter for SCPx contains multiple 5'-TTGTTT-3' regions.

Here we describe that SCP2 can protect against lipid peroxidation. Furthermore,
upregulation of both SCPX and SCP2 on the level of mRNA and protein by the Daf-16 like
forkhead transcription factor FKHR-L1 was observed.

Results

Endogenous lipid peroxidation is higher in scp-/- mouse hepatocytes
Lipid peroxidation rates were assessed with an assay based on the oxidation of C11-
BODIPY581/591, the fluorescence emission of which shifts from red to green upon oxida-
tion. Primary hepatocytes from *scp-/-* mice and wild type mice were loaded with C11-
BODIPY581/591 and its peroxidation was monitored by calculating the fraction oxidized
probe at different time points (see figure 2). The fraction oxidized C11-BODIPY581/591 is
presented in a colour scale. At time 0 min, oxidation of the probe in the *scp-/-* mouse
hepatocytes (panel C) is already higher than in the wild type (panel A). This indicates that, in
the *scp-/-* mouse hepatocytes, oxidation of the probe occurs already during loading of cells.
It can be clearly seen that after 2.5 hrs the amount of oxidized C11-BODIPY581/591 is
substantially elevated in the *scp-/-* hepatocytes (panel D) as compared to the control (panel
B). From this we conclude that endogenous lipid peroxidation in the hepatocytes from the
scp-/- mouse is higher than in control cells. Lipid peroxidation in the liver of wild type and
knockout mice was also measured with the total barbituric acid reactive substances (TBARS)
assay (figure 2e). The results confirm that lipid peroxidation levels are higher in the livers of
scp-/- mice.

The scp knockout mouse develops liver tumors.
To evaluate long-term effects of the SCP2 gene disruption, we monitored causes of death in
male and female homozygous SCPx/SCP2 null mice (genetic background: C57Bl/6) kept
under standard laboratory conditions in a sterile incubator to minimize the risk of infections.
SCPx/SCP2 null mice of both sexes died frequently between one and two years of age,
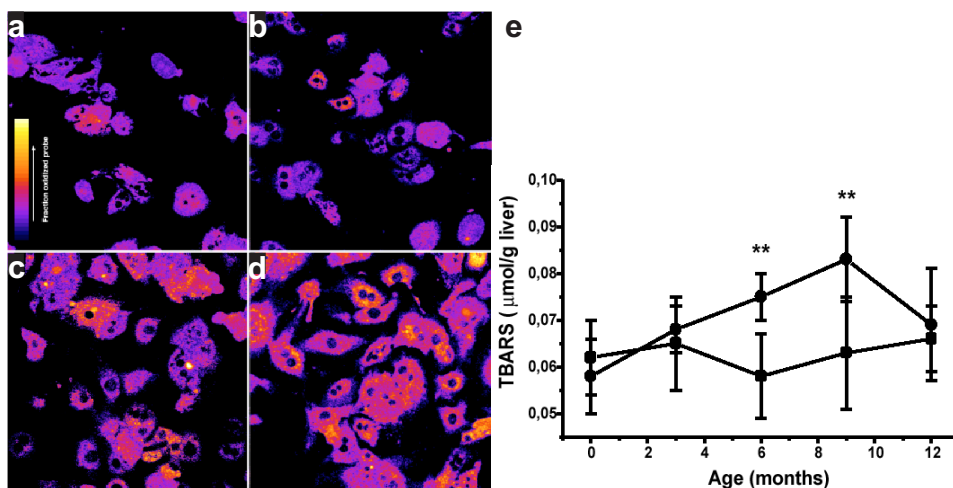
Figure 2. Isolated mouse hepatocytes form *scp* -/- mice and wild type were incubated with C11-BODIPY[581/591] in a temperature controlled life chamber in a CLSM. After 20 minutes the exces dye was washed away with PBS+. Imaging of the oxidized and intact form of C11-BODIPY[581/591] was performed during 2.5 hrs. The fraction oxidized C11-BODIPY[581/591] was calculated and depicted as a false colour scale. As can be seen, lipid peroxidation levels in the knockout mouse hepatocytes (**c**) was substantial higher after 2.5 hrs (**d**) as compared to the wild type (**a-b**). **e**. Effect of the SCP2 gene disruption on steady state concentrations of thiobarbituric acid reactive substances (TBARS) in the liver. TBARS were determined in liver homogenates at the indicated time-points from SCPx/SCP2 null mice (●) or C57Bl/6 controls (■). After extraction with n-butanol, the fluorescence was measured at 515 nm excitation and 555 nm emission. Malondialdehyde standards were prepared from 1,1,3,3-tetramethoxypropane. The data represent means ± S.D. (n = 5). Colour images of figures 2&3 can be found at the back cover of this thesis.
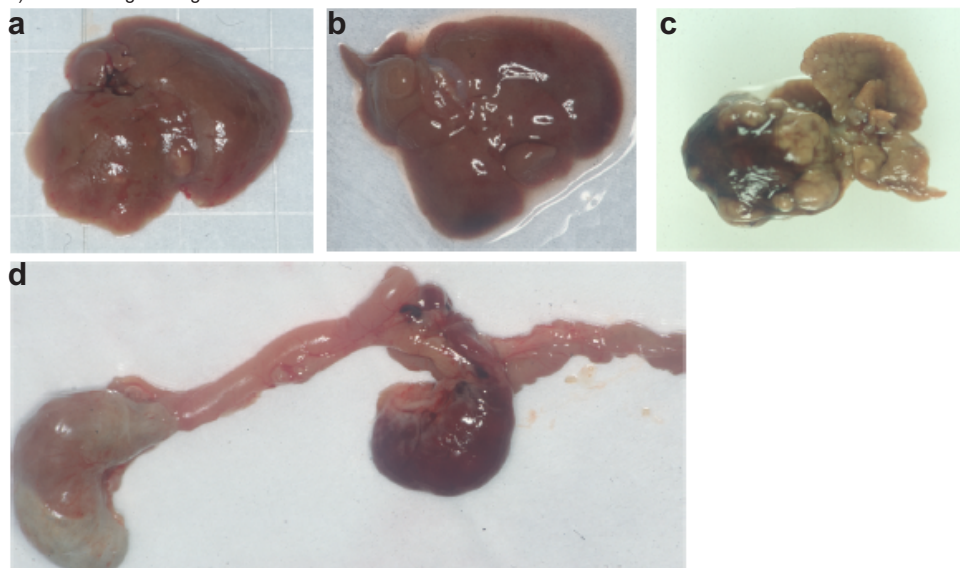
Figure 3. Hepatocarcinogenesis in SCPx/SCP2 null mice. Macroscopically evident liver alterations which are present in aged SCPx/SCP2 null mice are shown. Liver with multiple focal hepatic lesions from a 9 months old SCPx/SCP2 null mouse (**a**). Liver containing prominent hepatic cysts from a 13 months old female SCPx/SCP2 null mouse (**b**). Atrophic liver with large cavernous hemangiomas from an 18 months old female SCPx/SCP2 null mouse (**c**). (**d**) shows a prominent peritoneal liver nodule attached to the small intestine of the same mouse shown in 3c. Fig 3e (next page) shows the incidence rate of hepatocarcinogenesis in SCPx/SCP2 null mice. 24 mice (12 males, and 12 females) were examined at the indicated time-points for the presence of hepatocarcinogenic liver alterations. The presence of focal hepatic lesions and/or hepatic cysts and/or cavernous hemangiomas were used for classification as affected or non-affected. No hepatocarcinogenic liver alterations could be detected in age- and sex-matched C57Bl/6 controls.

3e
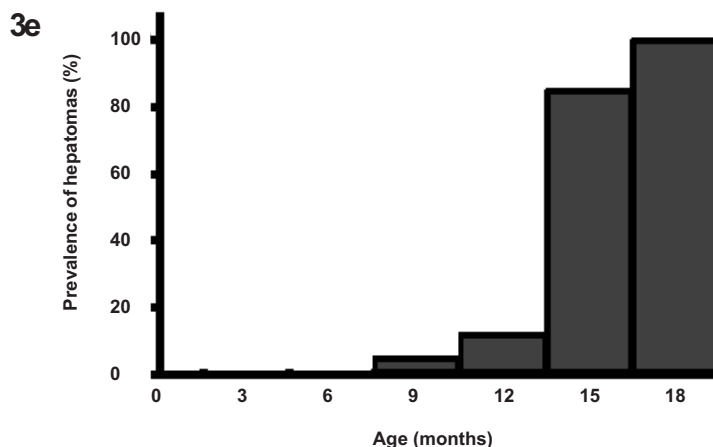
whereas the normal life-span of C57Bl/6 mice in the laboratory is ~3 years. Pathologic examination showed that the vast majority of these premature deaths related to the presence of large neoplastic liver tumors. Three representative examples for the progressive development of the abnormalities are shown in Fig. 3. Macroscopically, focal hepatic lesions were visible in a number of mice below one year of age irrespective of their sex (Fig. 3a). In contrast, prominent hepatic cysts, as exemplified in Fig. 3b, were present mostly in mice exceeding one year of age and at a later stage, large cavernous hemangiomas were visible in many mice (Fig. 3c). In addition, metastatic liver nodules were detected in a number of ~1.5 year old male and female SCPx/SCP2 null mice. Fig. 3d shows a particularly prominent peritoneal liver nodule attached to the small intestine of an 18 months old female SCPx/SCP2 null mouse. As shown in Fig. 3e, hepatomas were absent from mice younger than 9 months. However, between 12 and 15 months of age, the incidence rate of macroscopically detectable hepatomas increased steeply and all examined mice had readily detectable signs of hepatocarcinogenesis at the age of 18 months.

SCP2 protects against lipid peroxidation

Both preSCP2 and SCP2 can bind fatty acyl-CoAs with high affinity. Here we used preSCP2 to determine whether this protein is able to protect C11-BODIPY$^{581/591}$ from oxidation by hydroxyl radicals as suggested from fig. 2. As a control we used bovine serum albumin (BSA). As shown in figure 4, preSCP2 protected the fatty acid analogue four times better than an equimolar amount of BSA. BSA has five high affinity binding sites for fatty acids whereas pre-SCP2 has only one. Furthermore, fatty acid binding protein (FABP) can also protect fatty acids from oxidation, but to a lesser extent then BSA (23). Taking this into account, the anti-oxidant capacity of preSCP2 is much greater than that of BSA. The fatty acid analogue C11-BODIPY$^{581/591}$ was accommodated into the binding site of pre-SCP2 as determined by a FRET based competition assay (see **4b**) as described (chapter 7) (8).

Cell-cycle dependent expression of SCPx/SCP2

Since SCPx/SCP2 levels are low in cancers and since the observed tumor-suppressing role of the scp gene in the mouse, we studied whether growth-factor signalling contributes to scp regulation. Serum-starvation has been shown to decrease the amount of phosphorylated PKB and as a result leads to a more active Forkhead transcription factor. In agreement with this,

a

Oxidation of C11-BODIPY$^{581/591}$ bound to pre-SCP2 or BSA

b

Competition of PyrC12 binding by C11-BODIPY$^{581/591}$
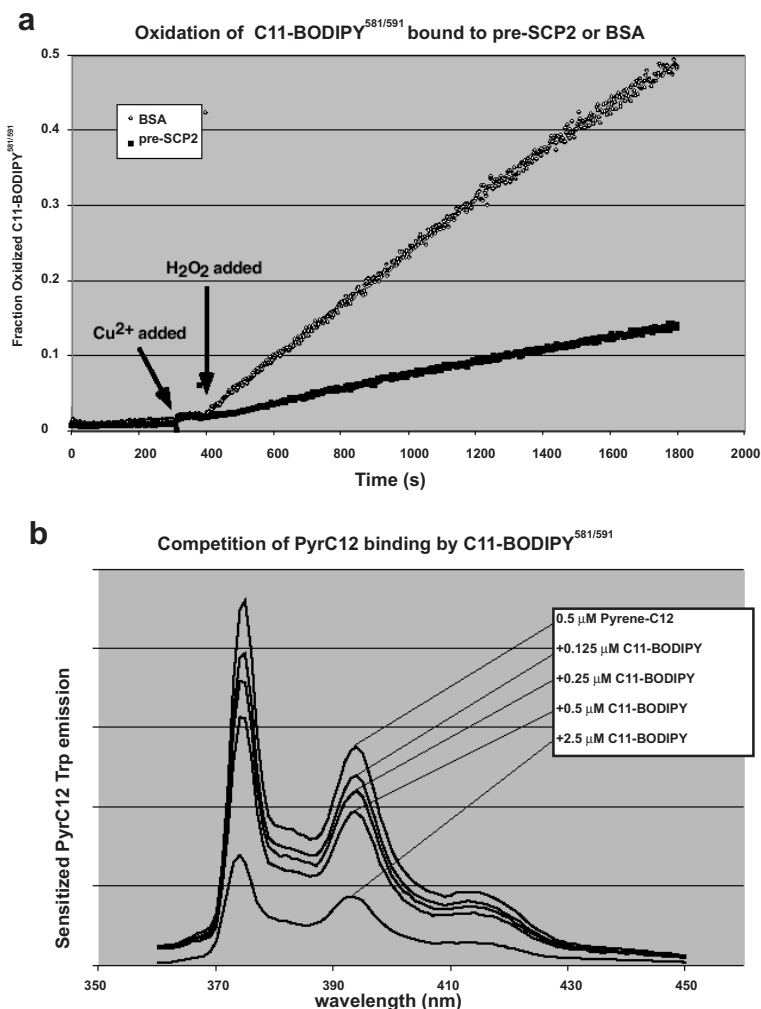
Figure 4. C11-BODIPY$^{581/591}$ bound to preSCP2 is better protected from oxidation by hydroxyl radicals formed by H$_2$O$_2$/Cu^{2+} then C11-BODIPY$^{581/591}$ bound to BSA . (**a**) PreSCP2 or BSA and C11-BODIPY$^{581/591}$ were added in equimolar amounts. The Fenton reaction catalyst copper was added at nM concentration followed by 200 µM hydrogen peroxide. The green(oxidized form) and red(intact form) fluorescence was monitored and plotted vs time as the fraction oxidized, which is the green fluorescence intensity divided by the total fluorescence intensity. (**b**) That C11-BODIPY$^{581/591}$ indeed bound to preSCP2 was checked using a FRET basewd competition assay. preSCP2 was complexed with an equimolar amount of PyrC12. The Trp residue in the binding site is excited at 280 nm and the sensitized pyrene emission spectrum is measured at 370-450 nm. Pyrene was competed out of the bindingsite by C11-BODIPY$^{581/591}$ as indicated by the decay in FRET efficiency. The affinity of preSCP2 for C11-BODIPY$^{581/591}$ was about 1.5 times lower then for PyrC12 ($\pm$ 0.36 µM)

Rat-1   **WB: anti-SCP2**

24 hrs serumstarved	+	+	+	+
24 hrs serum	-	+	-	+
24 hrs LY294002	-	-	+	+
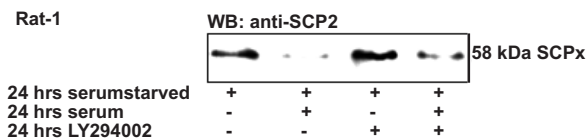
Figure 5. Serumstarved Rat-1 fibroblasts have higher protein levels of SCPx as compared to Rat-1 fibroblasts that were 24 hrs stimulated with serum. Treatment with the PI3K inhibitor LY294002 could partially prevent the decrease of SCPx upon treament with serum. Similar results were obtained for SCP2

a

b
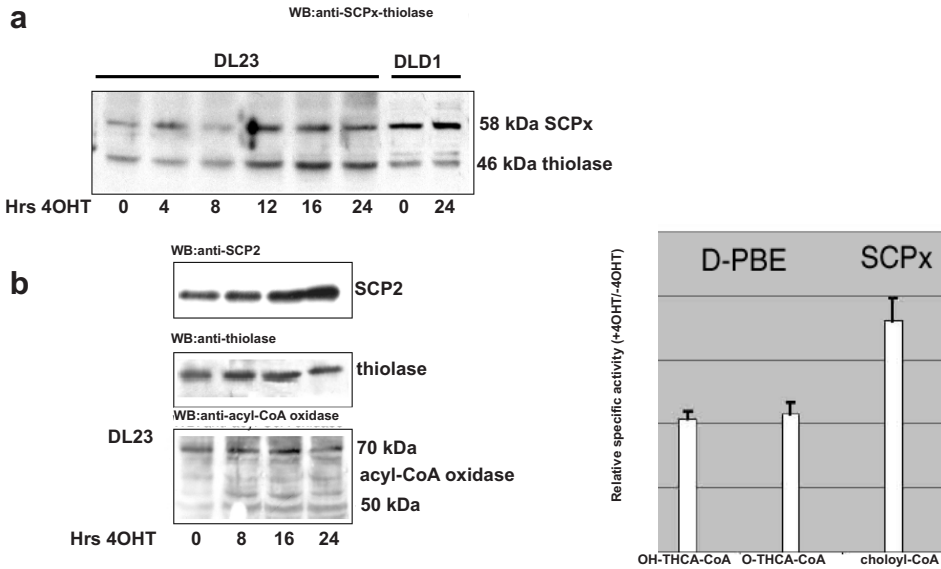
Figure 6. (**a**) The DL23 cell line expresses FKHR-L1-ER, the activity of which is fully dependent on 4OHT. Treatment of this cell line with 4OHT resulted in an increase of protein levels of SCPx, the 46 kDa fragment of SCPx and SCP2 (see also **6b**). A control cell line, DLD 1 that is not expressing the FKHR-L1 construct shows no increase in SCPx/SCP2 protein levels upon treatment with 4OHT. (**b**) Acyl-CoA oxidase and thiolase protein levels are unaffected by treatment with 4OHT. (**c**) Treatment with 4OHT led to a twofold increase of SCPx thiolase activity as monitored by the formation of bile acid intermediates from THC:1-CoA. The D-PBE activities remained unchanged.

serum–starved Rat1 fibroblasts showed high levels of SCPx/SCP2 as compared to cells that were exposed to fetal calf serum (figure 5). Treatment of the serum–starved cells with the PI3K inhibitor LY294002 showed similar levels of SCPx/SCP2 as without LY294002. However, this inhibitor reduced the observed decrease of SCPx/SCP2 upon overnight stimulation of the cells with serum: the amount of SCPx/SCP2 remaining was about twice as high as that in untreated cells. This is indicative of a role for PI3K signalling in the negative regulation of SCPx/SCP2 protein levels.
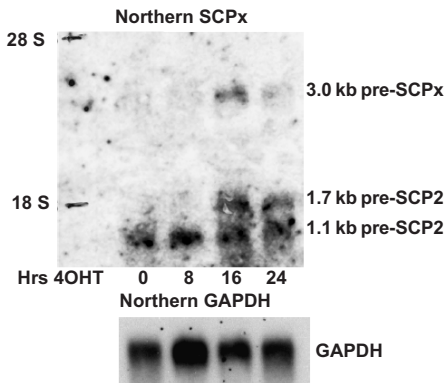
Figure 7. Treatment of the DL23 cell line with 4OHT for up to 24 hrs led to a marked increase in the 1.7 kb mRNA of preSCP2, whereas the 1.1 kb messenger remained unchanged. The 3.0 kb SCPx messenger was also induced. The 2.4 kb SCPx mRNA was not detected in these cells.

The Forkhead transcription factor FKHR-L1 regulates scp expression

To study the possible involvement of Forkheads in the PI3K-mediated regulation of SCPx/SCP2 protein levels (see Introduction), we made use of a DL23 cell-line expressing a HA-FKHRL1.A3-ER fusion protein. This protein is constitutively expressed but remains inhibited unless presented with a modified ligand for the estrogen receptor (ER), 4-hydroxytamoxifen (4OHT) (24). Treatment of the DL23 subclone with 500 nM 4OHT for 24 hours, resulted in the specific activation of FKHRL1 as measured by previously described Forkhead activity assays (22) (see also chapter 8). This activation was not observed in the control cell line DLD-1. Treatment of DL23 cells with 500 nM 4OHT for 0, 4, 8, 12, 16 and 24 hrs resulted in a time-dependent increase of SCPx, the 46 kDa protein and SCP2 (figure 6a/b). Acyl-CoA oxidase and thiolase protein levels were not increased (figure 6b). The increase in SCPx/SCP2 was specific for Forkhead activity since the DLD-1 cells did not respond to the 4OHT treatment (figure 6a).

To determine whether the increased protein levels of SCPx were functional, we measured its thiolase activity in a total cell lysate by analyzing the conversion of THC:1 CoA. The bile-acid intermediates formed by the actions of D-PBE (the enzyme catalyzing the two steps before SCPx in the β-oxidation) and SCPx in time were quantified by HPLC. Both the hydroxylation and dehydration activities of D-PBE were not influenced by 4OHT treatment, whereas the SCPx thiolase specific activity increased about two times (figure 6c).

Northern blotting of total mRNA isolated from untreated DL23 cells revealed that these cells express mainly the 1.1 kb *scp*-transcript; a very weak signal was found for the 1.7 kb and 3.0 kb transcripts. Treatment with 4OHT for 24 hrs led to an increase of the 1.7 and 3.0 kb transcripts, whereas the levels of 1.1 kb messenger remained unchanged (see figure 7). The 2.4 kb transcript was not detectable in this cell line.

Discussion

Peroxisomes produce large amounts of hydrogen peroxide and are, therefore, a site sensitive towards oxidative stress. To protect the peroxisomes from this stress, a battery of anti-oxidant enzymes is present including catalase, superoxide dismutases and glutathione peroxidase. Furthermore, anti-oxidants like glutathione and ascorbate have been detected in the peroxisomal matrix. On the other hand, hydrogen peroxide formed in the peroxisome may leak out into the cytosol (25), indicating that the anti-oxidant capacity of the peroxisome is not necessarily sufficient. Hence it may well be that hydrogen peroxide escaping the scavenging system is converted into hydroxyl radicals in the presence of $metal^{2+}$ ions. In support of this possibility, lipid peroxidation events have been reported to occur at the peroxisomal membrane (26). Fatty acids that are susceptible towards radical induced oxidation include PUFAs and intermediates of the fatty acid β-oxidation. In the first step of the β-oxidation, acyl-CoA oxidase introduces an enoyl bond at the β-position of fatty acyl-CoA esters, while generating hydrogen peroxide. Recently, SCP2 was shown to be complexed to acyl-CoA oxidase in the peroxisome (27). SCP2 has the ability to bind unsaturated fatty-acyl-CoA esters with high affinity. Here we show that this protein protects the C11-BODIPY[581/591] from oxidation by hydroxyl radicals. We therefore assume that the association of SCP2 with the β-oxidation complex is very important for the protection of unsaturated fatty acid intermediates against

attack by radicals. In support of this assumption, the lipid peroxidation in hepatocytes isolated from *scp* knockout mice was higher than in hepatocytes from the wild type mouse. Moreover, levels of lipid oxidation products as measured by TBARS were elevated in the livers of these knockout mice.

The daf-16 like Forkhead transcription factors AFX, FKHR and FKHR-L1 have been implicated in the regulation of the cellular anti-oxidant defense mechanism (see also chapter 8). Here we show that the expression of the *scp* gene products SCPx and SCP2 is positively regulated by the Forkhead transcription factor FKHR-L1. We do not know whether this regulation is direct or indirect, but the *scp* gene contains multiple putative binding elements for Forkhead transcription factors. Northern and Western blot analysis show a clear upregulation of SCPx and SCP2 protein when FKHR-L1 is active. Interestingly, the messengers that are mainly induced by FKHR-L1 are the 1.7 kb pre-SCP2 mRNA and the 3.0 kb SCPx mRNA which are the longer poly-adenylated forms. Normally, the 1.7 kb messenger is predominantly expressed in the brain (6); also one of the main sites of FKHR-L1 expression in the adult mouse (21).

In contrast to SCPx/SCP2, FKHR-L1 does not upregulate the straight chain acyl-CoA oxidase, a marker enzyme for peroxisome proliferation, or the peroxisomal straight chain thiolase. This excludes a general shift to peroxisomal lipid-metabolism by activation of FKHR-L1. In support of this, *in silico* analysis of the promoters of the latter two β-oxidation enzymes revealed no Forkhead binding sites. Also the activity of D-PBE (the enzyme that catalyzes the two steps before the thiolytic cleavage by SCPx) remains unchanged after induction of the FKHR-L1 by 4OHT in the DL23 subclone. This strongly suggests that the Forkhead induced upregulation of SCPx serves another function than the upregulation of branched fatty acid breakdown. On the other hand, SCPx can serve as a precursor of SCP2 contributing to the anti-oxidant capacity of the peroxisome.

The hepatocarcinogenesis in the *scp* knockout mouse may originate from DNA damage as a result of the elevated oxidative stress. The anti-oxidant function of SCP2 may contribute to the tumor-suppressing role of the *scp*-gene by preventing the formation of fatty acid peroxyl radicals. However, it remains to be established to what extent branched chain fatty acids, that can activate the PPARα, accumulate in the knockout mouse (28, 29). Constitutive activation of PPARα has also been implicated in hepatocarcinogenesis.

In summary, we propose that SCP2 protects (poly)-unsaturated fatty acyl-CoA esters from oxidation by reactive oxygen species in the peroxisome, and that the upregulation of SCPx/SCP2 via FKHR-L1 is in line with the regulation of anti-oxidant defense enzymes in the cell by this transcription factor.

Methods

Tissue culture and cell lines

The DL23 cell-line was created as follows (24): linearized pcDNA3-HA-FKHRL1.A3-ER was transfected into DLD-1 human colon carcinoma cells by electroporation. Transfectants were selected for two weeks on 500 μg/ml geneticin. Subsequently, clones were isolated and analyzed for expression of the fusion protein. The DL23 subclone was chosen for further study. The DLD-1 and DL23 cell-lines were maintained in RPMI-1640 with standard supplements and the appropriate selection antibiotic. 4OHT was administered at a concentration of 500 nM. Rat-1 fibroblasts were cultured in bicarbonate buffered DMEM under 5% CO_2

atmosphere. The *scp* knockout mouse has been described before (29).

Anti–oxidant capacity assay for pre–SCP2

To investigate whether preSCP2 could protect the fatty acid analogue C11–BODIPY $^{581/591}$ against oxidation by the hydroxyl radical–inducing system H2O2/Cu2+, we developed the following assay. Recombinant rat pre–SCP2 was overexpressed and purified as described by Ossendorp *et al.* (30). First, we checked whether preSCP2 could bind C11–BODIPY$^{581/591}$ by loading preSCP2 with Pyrene–C12 (PyrC12) which is a good FRET acceptor when the single Trp residue in the preSCP2 binding-site is excited at 280 nm. FRET efficiency between Trp and PyrC12 is a good indicator for binding (8). The decay of FRET upon addition of C11–BODIPY$^{581/591}$ to the preSCP2/PyrC12 complex is indicative for competition between the two fluorescent fatty acids. Equimolar concentration PyrC12 and C11–BODIPY$^{581/591}$ resulted in a FRET decay of ~35% which means that the affinity for C11–BODIPY$^{581/591}$ is about 1.5 times less than for PyrC12 which is 0.24 μM.

C11–BODIPY$^{581/591}$ dissolved in EtOH was added to PBS to a final concentration of 0.5 μM (5 μl in 1 ml PBS). The fluorescence of the oxidized (green, Ex 490 Em 510 nm) and the intact (red, Ex 570 Em 590 nm) were acquired using a PTI fluorimeter. Recombinant human preSCP2 purified from E.Coli was added to a final concentration of 0.5 μM. After equilibration of the signals, hydrogen peroxide was added, and a minute later Cu2+, a catalyst for hydroxyl radical formation from hydrogen peroxide. The green and red signal were acquired for 25 min and afterwards the fraction oxidized C11–BODIPY$^{581/591}$ was calculated in each time point by dividing the green signal by the sum of the green and red signals. The same experiment was performed using BSA as a control. Addition of a molar exces of preSCP2 could not increase the protection, indicating that all C11–BODIPY$^{581/591}$ was already bound to preSCP2.

Endogenous lipid peroxidation in isolated hepatocytes

Lipid peroxidation in living hepatocytes was measured as described by Pap *et al.* (31). Shortly, freshly isolated hepatocytes from of 6-8 months old wild type and *scp* knockout mice cultured on coverslips were placed in a temperature (37°C)-controlled coverslip holder in the microscope and incubated for 20 min with C11–BODIPY$^{581/591}$ (Molecular Probes) dissolved in fetal calf serum to a final concentration of 0.1 mgml^{-1} and diluted 1000 times in PBS supplemented with 5 mM glucose, 0.5 mM CaCl$_2$ and 0.9 mM MgCl$_2$ (PBS+). After washing with fresh PBS+, images were acquired on an inverted Leica TCSNT confocal laser scanning microscope DMIRBE (Leica Microsystems), using an argon-krypton laser as excitation source. Using dual wavelength excitation (laserlines 488 and 568 nm) and detection (emission bandpass filter 530/30 nm for oxidized C11–BODIPY$^{581/591}$ and longpass 560 nm followed by a bandpass 600/30 nm for intact C11–BODIPY$^{581/591}$, the fluorescence of C11–BODIPY$^{581/591}$ was acquired simultaneously. Image calculus with the Scion Image 1.62 computerprogram on a Macintosh PowerPC was used to quantify the formation of the oxidized form. TBARS were measured as described (32).

Northern Blotting

2 μg of mRNA (polyA-Tract, Promega) purified from 1 mg total RNA (RNAZol, TEL-TEST, Inc.) was run on a formaldehyde denaturing gel and blotted onto GeneScreen-Plus nylon membrane (NEN). The blots were hybridized using radio-labelled SCPx (BamH I and Xho I fragment of pEYFP-C1-SCPX) and GAPDH (NotI-linearized pUC19-GAPDH)

probes.

Western Blotting

SDS-Page and Western blotting were performed as described (20). Antibodies against the N-terminal thiolase of SCPx and SCP2 (6) and against acyl-CoA oxidase and straight chain thiolase were described before (27).

Activity assays

The activities of D-PBE and SCPX were measured by following the formation of bile-acid intermediates upon incubation of cell lysate with the bile-acid precursor THC:1 CoA (a substrate for D-PBE) by HPLC as described before (33). Lysates of DL23 cels that were either untreated or treated with 4OHT for 24 hrs were compared.

References

(1)   Ohba, T., Holt, J.A., Billheimer, J.T., Strauss 3rd, J.F. (1995) Human sterol carrier protein x/sterol carrier protein 2 gene has two promoters. *Biochemistry.* **34**,10660-10668.

(2)   Seedorf, U., Assmann, G. (1991) Cloning, expression, and nucleotide sequence of rat liver sterol carrier protein 2 cDNAs. *J Biol Chem.* **266**,630-636.

(3)   Atshaves, B. P., Petrescu, A.D., Starodub, O., Roths, J.B., Kier, A.B., Schroeder, F. (1999) Expression and intracellular processing of the 58 kDa sterol carrier protein-2/3-oxoacyl-CoA thiolase in transfected mouse L-cell fibroblasts. *J Lipid Res.* **40**,610-622.

(4)   Wanders, R. J., Denis, S., Wouters, F., Wirtz, K.W., Seedorf, U. (1997) Sterol carrier protein X (SCPx) is a peroxisomal branched-chain beta-ketothiolase specifically reacting with 3-oxo-pristanoyl-CoA: a new, unique role for SCPx in branched-chain fatty acid metabolism in peroxisomes. *Biochem Biophys Res Commun.* **236**,565-569.

(5)   Wanders, R. J., Denis, S., van Berkel, E., Wouters, F., Wirtz, K.W., Seedorf, U. (1998) Identification of the newly discovered 58 kDa peroxisomal thiolase SCPx as the main thiolase involved in both pristanic acid and trihydroxycholestanoic acid oxidation: implications for peroxisomal beta-oxidation disorders. *J Inherit Metab Dis.* **21**,302-305.

(6)   Ossendorp, B. C., Voorhout, W.F., van Amerongen, A., Brunink, F., Batenburg, J.J., Wirtz, K.W. (1996) Tissue-specific distribution of a peroxisomal 46-kDa protein related to the 58-kDa protein (sterol carrier protein x; sterol carrier protein 2/3-oxoacyl-CoA thiolase). *Arch Biochem Biophys.* **334**,251-260.

(7)   Bloj, B., Zilversmit, D.B. (1977) Rat liver proteins capable of transferring phosphatidylethanolamine. Purification and transfer activity for other phospholipids and cholesterol. *J Biol Chem.* **252**,1613-1619.

(8)   Dansen, T. B., Westerman, J., Wouters, F.S., Wanders, R.J., van Hoek, A., Gadella, T.W., Wirtz, K.W. (1999) High-affinity binding of very-long-chain fatty acyl-CoA esters to the peroxisomal non-specific lipid-transfer protein (sterol carrier protein-2). *Biochem J.* **339**,193-199.

(9)   Frolov, A., Cho, T.H., Billheimer, J.T., Schroeder, F. (1996) Sterol carrier protein-2, a new fatty acyl coenzyme A-binding protein. *J Biol Chem.* **271**,31878-31884.

(10)   Seedorf, U., Ellinghaus, P., Roch Nofer, J. (2000) Sterol carrier protein-2. *Biochim Biophys Acta.* **1486**,45-54.

(11)   Kannenberg, F., Ellinghaus, P., Assmann, G., Seedorf, U. (1999) Aberrant oxidation of the cholesterol side chain in bile acid synthesis of sterol carrier protein-2/sterol carrier protein-x knockout mice. *J Biol Chem.* **274**,35455-35460.

(12)   Gadella, T. W., Bastiaens, P.I., Visser, A.J., Wirtz, K.W. (1991) Shape and lipid-binding site of the nonspecific lipid-transfer protein (sterol carrier protein 2): a steady-state and time-resolved fluorescence study. *Biochemistry.* **30**,5555-5564.

(13)   Matsuo, H., Strauss, J.F. 3rd. (1994) Peroxisome proliferators and retinoids affect JEG-3 choriocarcinoma cell function. *Endocrinology.* **135**,1135-1145.

(14)   Gossett, R. E., Schroeder, F., Gunn, J.M., Kier, A.B. (1997) Expression of fatty acyl-CoA binding proteins in colon cells: response to butyrate and transformation. *Lipids.* **32**,577-585.

(15)   Lyons, H. T., Kharroubi, A., Wolins, N., Tenner, S., Chanderbhan, R.F., Fiskum, G., Donaldson, R.P. (1991) Elevated cholesterol and decreased sterol carrier protein-2 in peroxisomes from AS-30D hepatoma compared to normal rat liver. *Arch Biochem Biophys.* **285**,238-245.

(16)   Khwaja, A., Rodriguez-Viciana, P., Wennstrom, S., Warne, P.H., Downward, J. (1997) Matrix adhesion and Ras transformation both activate a phosphoinositide 3-OH kinase and protein kinase B/Akt cellular survival pathway. *EMBO J.* **16**,2783-2793.

(17)   Honda, Y., Honda, S. (1999) The daf-2 gene network for longevity regulates oxidative stress resistance and Mn-superoxide dismutase gene expression in Caenorhabditis elegans. *FASEB J.* **13**,1385-1393.

(18)   Vanfleteren, J. R., Braeckman, B.P. (1999) Mechanisms of life span determination in Caenorhabditis elegans. *Neurobiol Aging.* **20**,487-502.

(19)   Paradis, S., Ruvkun, G. (1998) Caenorhabditis elegans Akt/PKB transduces insulin receptor-like signals from AGE-1 PI3 kinase to the DAF-16 transcription factor. *Genes Dev.* **12**,2499-2498.

(20)   Kops, G. J., de Ruiter, N.D., De Vries-Smits, A.M., Powell, D.R., Bos, J.L., Burgering, B.M. (1999) Direct control of the Forkhead transcription factor AFX by protein kinase B. *Nature.* **398**,630-634.

(21)   Furuyama, T., Nakazawa, T., Nakano, I., Mori, N. (2000) Identification of the differential distribution patterns of mRNAs and consensus binding sequences for mouse DAF-16. *Biochem J.* **349**,629-634.

(22)   Kops, G. J. P. L., Dansen, T.B., Wirtz, K.W.A., Coffer, P.J., Huang, T.T., Bos, J.L., Medema, R.H., Burgering, B.M.T. (2001) Coupling of cell-cycle regulation and resistance to oxidative damage by DAF-16 like Forkhead transcription factors. *Submitted.*

(23)   Ek, B. A., Cistola, D.P., Hamilton, J.A., Kaduce, T.L., Spector, A.A. (1997) Fatty acid binding proteins reduce 15-lipoxygenase-induced oxygenation of linoleic acid and arachidonic acid. *Biochim Biophys Acta.* **1346**,75-85.

(24)   Dijkers, P. F., Medema, R.H., Lammers, J.W., Koenderman, L., Coffer, P.J. (2000) Expression of the pro-apoptotic Bcl-2 family member Bim is regulated by the forkhead transcription factor FKHR-L1. *Curr Biol.* **10**,1201-1204.

(25)   Singh, I. (1996) Mammalian peroxisomes: metabolism of oxygen and reactive oxygen species. *Ann New York Acad Sci.* **804**,612-627.

(26)   Corpas, F. J., Barroso, J.B., del Rio, L.A. (2001) Peroxisomes as a source of reactive oxygen species and nitric oxide signal molecules in plant cells. *Trends Plant Sci.* **6**,145-150.

(27)   Wouters, F. S., Bastiaens, P.I., Wirtz, K.W., Jovin, T.M. (1998) FRET microscopy demonstrates molecular association of non-specific lipid transfer protein (nsL-TP) with fatty acid oxidation enzymes in peroxisomes. *EMBO J.* **17**,7179-7189.

(28)   Ellinghaus, P., Wolfrum, C., Assmann, G., Spener, F., Seedorf, U. (1999) Phytanic acid activates the peroxisome proliferator-activated receptor alpha (PPARalpha) in sterol carrier protein 2-/ sterol carrier protein x-deficient mice. *J Biol Chem.* **274**,2766-2772.

(29)   Seedorf, U., Raabe, M., Ellinghaus, P., Kannenberg, F., Fobker, M., Engel, T., Denis, S., Wouters, F., Wirtz, K.W., Wanders, R.J., Maeda, N., Assmann, G. (1998) Defective peroxisomal catabolism of branched fatty acyl coenzyme A in mice lacking the sterol carrier protein-2/sterol carrier protein-x gene function. *Genes Dev.* **12**,1189-1201.

(30)   Ossendorp, B. C., Geijtenbeek, T.B., Wirtz, K.W. (1992) The precursor form of the rat liver non-specific lipid-transfer protein, expressed in Escherichia coli, has lipid transfer activity. *FEBS Lett.* **296**,179-183.

(31)   Pap, E. H., Drummen, G.P., Winter, V.J., Kooij, T.W., Rijken, P., Wirtz, K.W., Op den Kamp, J.A., Hage, W.J., Post, J.A. (1999) Ratio-fluorescence microscopy of lipid oxidation in living cells using C11-BODIPY(581/591). *FEBS Lett.* **453**,278-282.

(32)   Lores Arnaiz, S., Travacio, M., Monserrat, A.J., Cutran, J.C., Llesuy, S., Boveris, A. (1997) Chemiluminescence and antioxidant levels during peroxisome proliferation by fenofibrate. *Biochim Biophys Acta.* **1360**,222-228.

(33)   Ferdinandusse, S., Denis, S., van Berkel, E., Dacremont, G., Wanders, R.J. (2000) Peroxisomal fatty acid oxidation disorders and 58 kDa sterol carrier protein X (SCPx). Activity measurements in liver and fibroblasts using a newly developed method. *J Lipid Res.* **41**,336-342.

10

General Discussion.

Targeted fluorescent probes

We have shown in this thesis that polypeptides carrying a fluorescent moiety and a targeting signal can be used to measure the biophysical properties of organelles in the living cell (1-4). The synthesis of these probes involves relatively simple one- or two-step reactions (chapter 5). Purification of these probes is performed by precipitation and TLC. The uptake of the probes by the cell occurs most probably by way of spontaneous diffusion, as indicated by the low temperature experiments (chapter 6). As observed, the peptide probes still accumulate in the cell under low temperature conditions where endocytosis is blocked (5). Uptake by endocytosis would also imply that the peptides are sorted via the Golgi complex, which keeps the peptide away from the receptor for the PTS1 located in the cytosol. The signal sequences used for the Golgi and ER are also known as retention signals for the transport of proteins from the cytosol to these organelles. In conclusion, this means that all peptides used have to be cytosolic before they can be transported to their target organelle. The observation that HepG2 cells, known to overexpress a multidrug transporter that extrudes lipophilic ions, only incorporate BODIPY-PTS1 when pre-treated with verapamil, also supports the idea that diffusion over the plasma membrane is the main mode of uptake of these peptide-probes. Interestingly, although uptake is not temperature dependent, the translocation to the target organelles is. As shown in chapter 6, the different peptide probes that give similar staining patterns at low temperature, reach their target organelles only upon increasing the temperature. This observation stresses the need to use a temperature-controlled cell chamber when these peptide-probes are used. The diffusion over the plasma membrane is most likely facilitated by the hydrophobic fluorescent moiety, that in the unconjugated form is also rapidly taken up by the cell (6-8). The peptide with a nuclear localization signal of four positive charges, was not taken up by the cells. The difference in hydrophobicity between labelled and unlabelled peptides makes competition assays with unlabelled signal peptides useless. A problem with the peptide probes is the determination of their organelle specificity, as they are difficult to fix for immuno-staining. It is not unlikely that cells that are incubated with a xenobiotic like a fluorescent peptide store these probes in compartments like lysosomes or lipid droplets. Therefore, the fibroblasts from patients with peroxisome biogenesis disorders (see chapters 3 & 5) provide a useful control to confirm the specificity of the PTS1-containing peptide probes for peroxisomes. The colocalization experiment for the Golgi probe was done with the Golgi-marker NBD-ceramide, thereby omitting a fixation step. Targeted GFP and derivatives can also be very useful to study organellar properties like, for instance, organelle dynamics (9-11). The availability of GFP-analogues that change their properties depending on their environment, is increasing rapidly (12, 13). Also FRET based on donor-acceptor couples of GFP derivatives is very promising to measure biophysical properties (14). A disadvantage of GFP as compared to the peptide probes is that the use of GFP depends on the transfection of cells and is therefore relatively slow.

Peroxisomal pH and the proton gradient over the peroxisomal membrane

The peroxisomal pH ($\pm$ 8.2) was determined by ratio imaging (chapter 3). The fluorophore used, SNAFL-2 (pKa of 7.6), is a probe that shifts its emission from green to red dependent on the pH. The green and red forms have nearly identical structures and have very similar spectral characteristics in terms of quantum yields and dependence on solvent. The shift from

green to red is reversible which makes the probe very useful, because a change in the fluorescence intensity as a result of a change of the environment will most likely affect both forms equally. This can also be deduced from the dissipation experiment in chapter 3. The dissipation of the proton gradient over the peroxisomal membrane does not lead to diffusion of SNAFL-2-PTS1 out of the peroxisome, but the ratio of the red and green emissions becomes the same as that of free SNAFL-2 in the cytosol and the buffer around the cell. If the peroxisomal matrix affects the spectral properties of the two forms of SNAFL-2 unevenly, the ratio after dissipation would have been different.

The existence of a proton gradient over the peroxisomal membrane implies that under *in vivo* conditions the peroxisomal membrane is impermeable to protons. The permeability of peroxisomes has been a matter of extensive research (15-21). The paradox is that on the one hand small solutes like NAD could not spontaneously pass the membrane, but that on the other hand, completely folded proteins and even protein complexes can be imported into peroxisomes (22-24). This protein import would suggest the presence of large pores in the membrane and a protein import mechanism similar to that of the nucleus (22, 25, 26). These apparently contradictory properties of the peroxisomal membrane can be explained if one assumes that a pore is formed by the import complex only when needed, and disassembles when the protein has entered the peroxisome. In chloroplasts, folded proteins are imported by a protein translocation system using the ΔpH over the chloroplast membrane as the driving force, while maintaining the membrane integrity (27). The use of the ΔpH for the import of proteins into peroxisomes is most unlikely since the import of PTS1 proteins is normal in RCDP patients that lack a peroxisomal pH gradient (1).

The maintenance of the basic peroxisomal pH was not dependent on ATP as was determined by depleting ATP with deoxyglucose. This would exclude the involvement of an ATP-dependent proton pump to extrude protons into the cytosol as is the case in mitochondria. Most peroxisomal enzymes have a basic pI and also a basic pH optimum, suggesting an adaptation to an alkaline environment. By buffering the matrix, these basic proteins may contribute to the maintenance of the basic pH. On the other hand, the RCDP patient that lacks the proton gradient, does have almost all the matrix proteins (since only a few proteins are targeted via PTS2; the pathway defect in RCDP). Therefore, a buffering role for the basic pI of the matrix proteins could be excluded. However, it could also mean that 1) the membrane is highly permeable in this patient due to the defect in the PTS2 receptor Pex7p; 2) a metabolite accumulates in the peroxisome thereby destabilizing or even disrupting the membrane; 3) an acidic metabolite or intermediate accumulates in the peroxisome due to the lack of PTS2 proteins; 4) protons that are normally consumed by a PTS2 protein accumulate. It is very well possible that under normal conditions the combination of the basic pI of most matrix proteins and the net consumption of protons is the basis for the alkaline pH of the peroxisomal matrix. In the methylotrophic yeast Hansenula Polymorpha, an acidic peroxisomal pH has been reported (28, 29). In this case the metabolism of methanol might account for the acidic pH. We have tried to measure the pH in yeast peroxisomes with SNAFL-2-PTS1 but these experiments were unsuccessful due to the poor uptake of the probe by the yeast cells. In general, whether the pH is basic or acidic, the conclusions regarding the impermeability to protons under *in vivo* conditions are the same.

The basic pH in peroxisomes of human fibroblasts is different from the pH of other organelles like Golgi, ER and lysosomes which are acidic(30). The mitochondrial matrix has also a basic pH (13). A basic pH may be of benefit to fatty acid degrading systems, either

because most enzymes required for fatty acid β-oxidation have basic pH optima, and/or because lipid peroxidation induced by free radicals formed by complexed iron is suppressed (31). One may consider the possibility that the fatty acid β-oxidation enzymes have adapted to an alkaline pH during evolution because lipid peroxidation proceeds slower under these circumstances.

The impermeability to small solutes serves also to keep the intermediates of metabolites inside the peroxisome, close to the enzyme complexes so as to ensure their complete processing. The compartmentalization of peroxisomal functions has been shown to be essential as the lack of peroxisomes in the Zellweger patient results in early death.
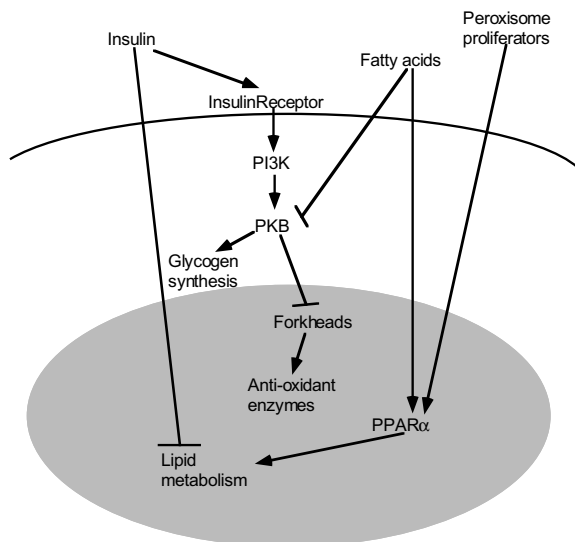
Regulation of anti-oxidant capacity via Forkheads

When PKB activity is diminished, the Daf-16 like Forkhead transcription factors AFX, FKHR and FKHR-L1 become active since these transcription factors are expelled from the nucleus upon phosphorylation by PKB(32-34). The activation of the Forkheads leads to a G0/G1 cell cycle arrest and quiescence through p27kip1(35). In proliferating cells, protection against apoptosis, amongst others via anti-oxidant enzymes, is regulated via the PI3K/PKB signalling cascade. Indeed, suppression of Forkhead activity by phosphorylated PKB leads to the concurrent suppression of the pro-apoptotic genes Bim and FasL in various cell types(34, 36). However, many cells in the human body are not proliferating and these quiescent cells need also protection against exogenous stresses. In this thesis we have shown that signalling via the Forkheads can lead to the induction of MnSOD and catalase (and SCPx/SCP2). This is in line with observations in the worm *Caenorhabditis elegans*, that uses a signalling pathway homologous to the PI3K/PKB/Forkhead pathway (Age-1/Akt/Daf-16(37, 38)) for the regulation of the MnSOD homologue sod-3 and cytosolic catalase ctl-1(39). This occurs predominantly during the so called Dauer stadium, where the worm is in a state of low metabolism in which it can prolong its lifespan up to ten times as compared to normal adult worms. It has been shown that Dauer formation does not take place when sod-3 and ctl-1 are not induced(39, 40).

In chapter 8 we describe the upregulation of MnSOD on the level of mRNA and protein via FKHR-L1. Using a fluorescence assay we showed that the induction resulted in a protection against exogenously applied oxidative stress in the form of hydrogen peroxide. Catalase protein levels were also upregulated in line with the increase of MnSOD, but we do not know whether this regulation is also directly mediated via the Forkheads. MnSOD is a predominantly mitochondrial protein that interconverses superoxide anions into hydrogen peroxide, which can decompose to the hazardous hydroxyl radicals in the Fenton reaction (see also chapter 2). Catalase decomposes hydrogen peroxide to oxygen and water, which would explain the concurrent upregulation of catalase levels with the induction of MnSOD. This is the case in *C.elegans*, where both proteins are regulated via Daf-16. However, the *C.elegans* ctl-1 is cytosolic whereas in humans catalase is peroxisomal. It is not likely that hydrogen peroxide formed by MnSOD in the mitochondrion can travel through the cytosol and over the peroxisomal membrane to be decomposed by catalase. However, MnSOD has been detected also in the peroxisomes of rat liver. It could well be that other anti-oxidant enzymes like glutathione peroxidase which is the cells other hydrogen peroxide scavenging enzyme, present in mitochondria and the cytosol, are also regulated directly or indirectly via the Forkhead transcription factors. The experiments with the *sod2 -/-* (MnSOD knockout)

mouse fibroblasts in chapter 8 show that without the induction of MnSOD the protection against the exogenous stress is diminished. This could suggest that the scavenging of hydrogen peroxide by peroxisomal catalase (or other eventually induced anti-oxidant enzymes) is not sufficient to protect the cell from exogenous applied hydrogen peroxide. As depicted in Chapter 2, the superoxide anion can facilitate the catalytic metal ion for the Fenton reaction, thereby increasing hydroxyl radicals that induce amongst others lipid peroxidation. It can be speculated that the scavenging of superoxide by MnSOD is therefore of more importance to the cells protection against exogenous oxidative stress than the scavenging of hydrogen peroxide. It has been shown in earlier studies that the prevention of the Fenton reaction is more efficiently done by lowering the amount of metal ion catalyst than by lowering the amount of hydrogen peroxide(41). This could explain the absence of protection against lipid peroxidation as measured in the *sod2 -/-* MEFS in chapter 8.

The peroxisomal localization of catalase makes it unlikely that it **can scavenge** exogenous applied oxidative stress(42). However, stress can also be formed inside the peroxisome (see chapter 2). It is not unthinkable that the protection against endogenous oxidative stress deriving from peroxisomal β-oxidation is also regulated via the Forkheads. Endogenous stress in the peroxisome derives from hydrogen peroxide formed in the first step in the β-oxidation. The Forkheads are negatively regulated by the PI3K/PKB pathway that is triggered amongst others by the insulin receptor. Insulin signalling results in glycogen synthesis. It can be speculated that when the insulin signal is absent (i.e. Forkheads are active) the cell may shift to lipid metabolism. We have shown in Chapter 9 however that acyl-CoA oxidase, a key enzyme in peroxisomal β-oxidation, is not induced by the Forkheads in the DL23 cell line. I would like to speculate that the Forkheads prepare the cell for lipid metabolism by upregulation of the anti-oxidant defense that is known to play a role in detoxification of reactive oxygen formed during mitochondrial (superoxide anion) and peroxisomal fatty acid β-oxidation (hydrogen peroxide), but that the genes that encode the β-oxidation enzymes are regulated via a different pathway (for instance the PPARs). Interestingly, it has been reported that free fatty acids inhibit PKB phosphorylation (43, 44) which would lead to induction of anti-oxidant enzymes via the Forkheads. This idea is clarified in figure 1.

Figure 1: Proposed model for the regulation of anti-oxidant enzymes via Forkheads in lipid metabolism. Phosphorylation of PKB via the insulin receptor through PI-3K leads to translocation of PKB to the nucleus and phosphorylation of the Forkheads that thereby become inactivated. Suppression of PKB phosphorylation by free fatty acids would therefore upregulate the anti-oxdant defense of the cell. Free fatty acids also activate PPARα and thereby induce lipid metabolism. When PPARα is activated via PPs like clofibrate, PKB is not affected resulting in increased lipid metabolism without induction of anti-oxidants. This might be an explanation for the carcinogenic effects of PPs. Interestingly, insulin, that as described above blocks the forkheads via PKB phosphorylation, also inhibits peroxisomal and mitochondrial fatty acid breakdown.

Other clues for interactions between these two pathways come form the observation that insulin blocks peroxisomal and mitochondrial fatty acid oxidation(45). Probably the induction of lipid metabolism is somehow dependent on the anti-oxidant capacity of the cell. Induction of lipid metabolism via PPARα can be obtained via free fatty acids or via so called peroxisome proliferators. These substances both activate PPARα, but only free fatty acids have been shown to inhibit PKB phosphorylation. Peroxisome proliferators like clofibrate have been implicated in carcinogenesis. It can be speculated that the activation of PPARα without inhibition of PKB (and thus without the induction of MnSOD and catalase (and SCP2)) leads to higher levels of oxidative stress and carcinogenesis.

Furthermore, one should keep in mind that the experiments described in chapter 8 and 9 that are performed in the DL23 cell line expressing the inducible FKHRL1-ER. In this cell line the Forkheads are switched on without activating a pathway that is normally inhibiting PKB. Therefore, it may well be that the induction of peroxisomal β-oxidation enzymes is not observed in this cell line because the induction of Forkhead activity is normally downstream of a signal that also induces the β-oxidation enzymes (chapter 9). As shown in figure 1, signalling by free fatty acids induces lipid metabolism through PPARα activation and simultaneously inhibits PKB activity resulting in the induction of anti-oxidant enzymes.

A role for SCP2 in the protection against oxidative stress

The physiological function of SCP2 has been a matter of intensive research (for a review see (46). The protein was originally characterized for its ability to transfer phospholipids and cholesterol *in vitro* and was called non-specific lipid transfer protein (nsLTP). The binding affinity of nsLTP towards lipophilic compounds like cholesterol, glycolipids and all common membrane phospholipids was low. It was reported that SCP2, which is identical to nsLTP, stimulated various steps in cholesterol metabolism. In addition, SCP2 binds fatty acyl-CoA esters (47), and as shown in chapter 7 has a high binding affinity for VLCFA-CoAs (48). SCP2 can be synthesized as pre-SCP2 and as part of SCPx, both of which proteins are encoded by the *scp* gene (see also chapter 1&7). More insight in the physiological role of SCPx/SCP2 came from the group of Seedorf that made an *scp -/-* mouse. These mice were defective in bile acid synthesis and in the breakdown of branched chain fatty acids. Subsequently, the N-terminal part of SCPx was characterized as the thiolase with specificity for branched chain 3-keto-acyl-CoAs and the bile acid intermediate 3α,7α,12α-trihydroxy-24-ketocholestanoyl-CoA. The thiolase activity is not dependent on the SCP2 segment. The *scp -/-* mouse has an apparently normal cholesterol metabolism, which strongly suggests that *in vivo* SCP2 is not a sterol carrier. The metabolism of VLCFAs was also unaffected (49-51). This was unexpected given the high affinity binding of SCP2 for these fatty acyl-CoA esters (chapter 7). Based on FRET experiments it was shown SCP2 is complexed to the β-oxidation enzymes, and especially to acyl-CoA oxidase (52). The data presented a role for SCP2 in presenting substrates to this enzyme. It was also reported that PXP-18, a yeast SCP2 homologue, was able to protect acyl-CoA oxidase from heat-inactivation at 70°C (53). The complexation of acyl-CoA oxidase to PXP-18 also suggested a role in the peroxisomal β-oxidation.

The data presented in chapter 9 suggest a new physiological function for SCP2 in that it may protect fatty acyl-CoA esters from peroxidative damage by ROS. As outlined in chapter 2, especially PUFAs with a conjugated diene system are susceptible towards oxidative damage. PUFA-CoAs bind to SCP2 with high affinity (54). Using the C11-BODIPY[581/591]

assay, it was shown that the lipid peroxidation in the hepatocytes form the *scp -/-* mouse was markedly increased as compared to the wild type. Also the total barbituric acid reactive substances (TBARS), which is a measure for oxidative stress, were increased in the livers of the knockout mice (chapter 9). In time these mice showed an increased development of hepatocarcinomas and other tumors. It is believed that liver tumors can be induced by oxidative stress (55, 56). It is to be noted that in these knockout mice SCPx thiolase activity is also absent. Hence, the liver tumors could also result from an aberrant branched chain fatty acid metabolism, or from the defects in bile acid formation. Phytanic acid is known to be a potent activator of PPARα (57). Consistent activation of this nuclear receptor has been implicated in hepatocarcinogenesis in rodents (58, 59). However, most studies describing this effect were done with peroxisome proliferators like fibrates, that are normally absent from the body (see also figure 1).

We have shown in chapter 9 that SCP2 is regulated via the Forkhead transcription factor FKHR-L1 that is negatively regulated by PI3K and PKB. It has been published that in *ras*-transformed tumors SCP2 levels are decreased (60, 61). This may be explained by the fact that the transformation of *ras* is linked to constitutive PKB phosphorylation (62) and, there-fore, to the inactivation of the Forkheads. In line with this, lower levels of the Forkhead targets MnSOD and P27kip1, have been observed in certain tumors (63-65).

In summary, we have observed that: 1) endogenous lipid peroxidation is increased in *scp -/-* hepatocytes; 2) TBARS are higher in the livers of these mice; 3) SCP2 can protect the fatty acid analogue C11-BODIPY[581/591] from oxidative damage; 4) *scp -/-* mice develop liver tumors, and 5) SCP2 is upregulated simultaneously with the anti-oxidant enzymes MnSOD and catalase via the Forkhead transcription factors. These observations strongly suggest that SCP2 fulfills an anti oxidant function *in vivo*.

As mentioned above, SCP2 shields its ligand from lipid peroxidation by hydroxyl radicals that are formed in the Fenton reaction. In the peroxisome, hydrogen peroxide is formed by acyl-CoA oxidase, the enzyme that introduces the α,β double bond. The product is an enoyl-CoA, and in the case of a PUFA might contain a conjugated diene system (see chapter 2). This means that the fatty acid β-oxidation intermediate that is most susceptible towards oxidation, is formed by the same enzyme that forms ROS. Normally, the hydrogen peroxide formed by acyl-CoA oxidase is scavenged by catalase. However, in the presence of metal ions, a very rapid conversion to hydroxyl radicals may occur (see also chapter 2). These hydroxyl radicals could then easily attack the conjugated diene in the fatty acid intermediate in the vicinity of acyl-CoA oxidase. If SCP2 interacts with acyl-CoA oxidase in a way that it shields this intermediate, the hydroxyl radicals formed cannot react with the fatty acid. This model is clarified in figure 2.

Interestingly, D-specific peroxisomal bifunctional enzyme (D-PBE), another β-oxi-dation enzyme, contains an SCP2-like domain at its C-terminus. Possibly this C-terminal SCP2 domain has the same anti-oxidant properties as SCP2. In this model, the absence of SCP2 in the *scp -/-* mouse could explain the higher susceptibility to lipid peroxidation as well as the elevated TBARS and possibly the higher incidence of liver tumors. The protec-tion against lipid peroxidation in the peroxisome would be regulated via the Forkheads by induction of both catalase and SCP2. The data in the *scp -/-* mice suggest that the hydrogen peroxide scavenging activity of catalase alone is not sufficient to prevent lipid peroxidation.
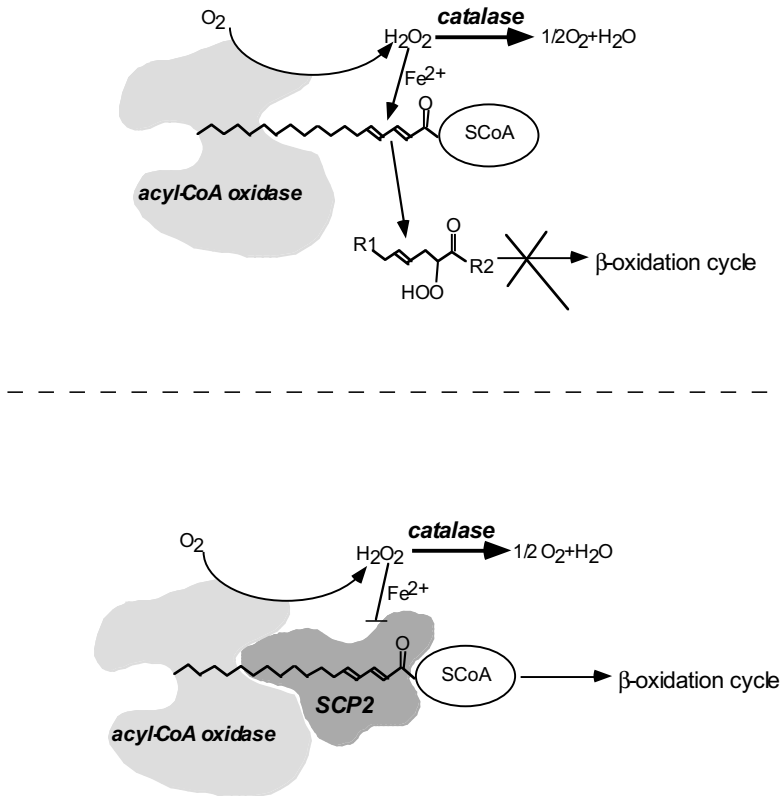
Figure 2: Proposed model for the protective role of SCP2 against oxidative damage to fatty acids during the peroxisomal β-oxidation. Especially PUFAs that are converted to the conjugated diene form during the β-oxidation are susceptible towards oxidative damage by hydroxyl radicals. These radicals may form from the hydrogen peroxide generated by acyl-CoA oxidase in the presence of metal ions. When SCP2 is present, the fatty acids are shielded from the attack by these radicals.

Summarizing conclusion

The free radical balance in the cell is of high importance for proper functioning of the cell as it is a determinant in processes like proliferation and apoptosis. In this thesis we have shown that the peroxisome probably plays a role in maintaining this delicate balance. First we have shown that the peroxisomal membrane is impermeable to protons. The impermeable membrane implies that the metabolic processes occurring inside the peroxisome are well shielded from the rest of the cell possibly protecting the cell against peroxisomal ROS. Second, SCP2 localized in the peroxisome, is an anti-oxidant protein that protects fatty acyl–CoA esters from oxidative damage. Moreover, we showed that the anti-oxidant enzymes MnSOD and catalase as well as SCP2 are regulated via the Forkhead transcripiton factors. Importantly, *scp* –/– mice showed a marked increase in the development of liver tumors, probably as a result of the elevated lipid peroxidation levels. The constitutive activation of the PI3K pathway has been implicated in cancer. The deregulation of the anti-oxidant enzymes that results from the suppressed Forkhead activity when PI3K is active, could be one of the mechanisms of carcinogenesis.

Although it is clear that peroxisomes detoxify ROS formed in the organelle, it is a matter of discussion whether the peroxisome plays a direct role in the protection of the cell against oxidative stress formed outside the peroxisome. Very little is known about oxidative stress in the peroxisome biogenesis disorders. One could speculate however, that when peroxisomal function is absent, the stress formed as a result of the β-oxidation is also absent. I would like to propose that the role of the peroxisome in the maintenance of the free radical balance in the cell is limited to scavenging ROS inside the peroxisome by anti-oxidant proteins and by ensuring the integrity of the peroxisomal membrane. In this concept, the upregulation of the peroxisomal anti-oxidant system upon activation of the Forkheads may have to be considered as a protection of the cell against radicals formed in peroxisomal fatty acid degradation.

References

(1)   Dansen, T. B., Wirtz, K.W.A., Wanders, R.J.A., Pap, E.H.W. (2000) Peroxisomes in human fibroblasts have a basic pH. *Nat Cell Biol.* **2**,51-53.

(2)   Dansen, T. B., Pap, E.H.W., Wanders, R.J.A., Wirtz, K.W.A. (2001) Targeted fluorescent probes in peroxisome function. *Histochem J.* **33**,65-69.

(3)   Pap, E. H., Dansen, T.B., van Summeren, R., Wirtz, K.W. (2001) Peptide-based targeting of fluorophores to organelles in living cells. *Exp Cell Res.* **265**,288-293.

(4)   Pap, E. H., Dansen, T.B., Wirtz, K.W. (2001) Peptide-based targeting of fluorophores to peroxisomes in living cells. *Trends Cell Biol.* **11**,10-12.

(5)   Kuismanen, E., Saraste, J. (1989) Low temperature-induced transport blocks as tools to manipulate membrane traffic. *Methods Cell Biol.* **32**,257-274.

(6)   Harris, T. E., Persaud, S.J., Jones, P.M. (1997) Pseudosubstrate inhibition of cyclic AMP-dependent protein kinase in intact pancreatic islets: effects on cyclic AMP-dependent and glucose-dependent insulin secretion. *Biochem Biophys Res Commun.* **232**,648-651.

(7)   Eichholtz, T., de Bont, D.B., de Widt, J., Liskamp, R.M., Ploegh, H.L. (1993) A myristoylated pseudosubstrate peptide, a novel protein kinase C inhibitor. *J Biol Chem.* **268**,1982-1986.

(8)   Oehlke, J., Beyermann, M., Wiesner, B., Melzig, M., Berger, H., Krause, E., Bienert, M. (1997) Evidence for extensive and non-specific translocation of oligopeptides across plasma membranes of mammalian cells. *Biochim Biophys Acta.* **1330**,50-60.

(9)   Dahm, T., White, J., Grill, S., Fullekrug, J., Stelzer, E.H. (2001) Quantitative er golgi transport kinetics and protein separation upon golgi exit revealed by vesicular integral membrane protein 36 dynamics in live cells. *Mol Biol Cell.* **12**,1481-1498.

(10)   Schrader, M., King, S.J., Stroh, T.A., Schroer, T.A. (2000) Real time imaging reveals a peroxisomal reticulum in living cells. *J Cell Sci.* **113**,3663-3671.

(11)   Tsien, R. Y. (1998) The green fluorescent protein. *Annu Rev Biochem.* **67**,509-544.

(12)   Miyawaki, A., Llopis, J., Heim, R., McCaffery, J.M., Adams, J.A., Ikura, M., Tsien, R.Y. (1997) Fluorescent indicators for Ca2+ based on green fluorescent proteins and calmodulin. *Nature.* **388**,882-887.

(13)   Matsuyama, S., Llopis, J., Deveraux, Q.L., Tsien, R.Y., Reed, J.C. (2000) Changes in intramitochondrial and cytosolic pH: early events that modulate caspase activation during apoptosis. *Nat Cell Biol.* **2**,318-325.

(14)   Wouters, F. S., Verveer, P.J., Bastiaens, P.I. (2001) Imaging biochemistry inside cells. *Trends Cell Biol.* **11**,203-211.

(15)   Van Veldhoven, P. P., Just, W.W., Mannaerts, G.P. (1987) Permeability of the peroxisomal membrane to cofactors of beta-oxidation. Evidence for the presence of a pore-forming protein. *J Biol Chem.* **262**,4310-4318.

(16)   Van Veldhoven, P., Debeer, L.J., Mannaerts, G.P. (1983) Water- and solute-accessible spaces of purified peroxisomes. Evidence that peroxisomes are permeable to NAD+. *Biochem J.* **210**,685-693.

(17)   van Roermund, C. W., Elgersma ,Y., Singh, N., Wanders, R.J., Tabak, H.F. (1995) The membrane of peroxisomes in Saccharomyces cerevisiae is impermeable to NAD(H) and acetyl-CoA under *in vivo* conditions. *EMBO J.* **14**,3480-3486.

(18)   Hettema, E. H., Tabak, H.F. (2000) Transport of fatty acids and metabolites across the peroxisomal membrane. *Biochim Biophys Acta.* **1486**,18-27.

(19)   Douma, A. C., Veenhuis, M., Sulter, G.J., Waterham, H.R., Verheyden, K., Mannaerts, G.P., Harder, W. (1990) Permeability properties of peroxisomal membranes from yeasts. *Arch Microbiol.* **153**,490-495.

(20)   Verleur N, W. R. (1993) Permeability properties of peroxisomes in digitonin-permeabilized rat hepatocytes. Evidence for free permeability towards a variety of substrates. *Eur J Biochem.* **218**,75-82.

(21)   Tabak, H. F., Elgersma, Y., Hettema, E., Franse, M.M., Voorn-Brouwer, T., Distel, B. (1995) Transport of proteins and metabolites across the impermeable membrane of peroxisomes. *Cold Spring Harb Symp Quant Biol.* **60**,649-655.

(22)   Dammai, V., Subramani, S. (2001) The Human Peroxisomal Targeting Signal Receptor, Pex5p, Is Translocated into the Peroxisomal Matrix and Recycled to the Cytosol. *Cell.* **105**,187-196.

(23)   Walton, P. A., Hill, P.E., Subramani, S. (1995) Import of stably folded proteins into peroxisomes. *Mol Biol Cell.* **6**,675-683.

(24)   Subramani, S., Koller, A., Snyder, W.B. (2000) Import of peroxisomal matrix and membrane proteins. *Annu Rev Biochem.* **69**,399-418.

(25)   Gorlich, D., Kutay, U. (1999) Transport between the cell nucleus and the cytoplasm. *Annu Rev Cell Dev Biol.* **15**,607-660.

(26)   Smith, M. D., Schnell, D.J. (2001) Peroxisomal protein import. the paradigm shifts. *Cell.* **105**,293-296.

(27)   Keegstra, K., Cline, K. (1999) Protein import and routing systems of chloroplasts. *Plant Cell.* **11**,557-570.

(28)   Nicolay, K., Veenhuis, M., Douma, A.C., Harder, W. (1987) A 31P NMR study of the internal pH of yeast peroxisomes. *Arch Microbiol.* **147**,37-41.

(29)   Waterham, H. R., Keizer-Gunnink, I., Goodman, J.M., Harder, W., Veenhuis, M. (1990) Immunocytochemical evidence for the acidic nature of peroxisomes in methylotrophic yeasts. *FEBS Lett.* **262**,17-19.

(30)   Llopis, J., McCaffery, J.M., Miyawaki, A., Farquhar, M.G., Tsien, R.Y. (1998) Measurement of cytosolic, mitochondrial, and Golgi pH in single living cells with green fluorescent proteins. *Proc Natl Acad Sci U S A.* **95**,6803-6808.

(31)   Schafer, F. Q., Buettner, G.R. (2000) Acidic pH amplifies iron-mediated lipid peroxidation in cells. *Free Radic Biol Med.* **28**,1175-1181.

(32)   Brownawell, A. M., Kops, G.J., Macara, I.G., Burgering, B.M. (2001) Inhibition of nuclear import by protein kinase b (akt) regulates the subcellular distribution and activity of the forkhead transcription factor afx. *Mol Cell Biol.* **21**,3534-3546.

(33)   Kops, G. J., de Ruiter, N.D., De Vries-Smits, A.M., Powell, D.R., Bos, J.L., Burgering, B.M. (1999) Direct control of the Forkhead transcription factor AFX by protein kinase B. *Nature.* **398**,630-634.

(34)   Brunet, A., Bonni, A., Zigmond, M.J., Lin, M.Z., Juo, P., Hu, L.S., Anderson, M.J., Arden, K.C., Blenis, J., Greenberg, M.E. (1999) Akt promotes cell survival by phosphorylating and inhibiting a Forkhead transcription factor. *Cell.* **96**,857-868.

(35)   Medema, R. H., Kops, G.J., Bos, J.L., Burgering, B.M. (2000) AFX-like Forkhead transcription factors mediate cell-cycle regulation by Ras and PKB through p27kip1. *Nature.* **404**,782-787.

(36)   Dijkers, P. F., Medema, R.H., Lammers, J.W., Koenderman, L., Coffer, P.J. (2000) Expression of the pro-apoptotic Bcl-2 family member Bim is regulated by the forkhead transcription factor FKHR-L1. *Curr Biol.* **10**,1201-1204.

(37)   Paradis, S., Ruvkun, G. (1998) Caenorhabditis elegans Akt/PKB transduces insulin receptor-like signals from AGE-1 PI3 kinase to the DAF-16 transcription factor. *Genes Dev.* **12**,2499-2498.

(38)   Ogg, S., Paradis, S., Gottlieb, S., Patterson, G.I., Lee, L., Tissenbaum, H.A., Ruvkun, G. (1997) The Fork head transcription factor DAF-16 transduces insulin-like metabolic and longevity signals in C. elegans. *Nature.* **389**,994-999.

(39)   Honda, Y., Honda, S. (1999) The daf-2 gene network for longevity regulates oxidative stress resistance and Mn-superoxide dismutase gene expression in Caenorhabditis elegans. *FASEB J.* **13**,1385-1393.

(40)   Taub, J., Lau, J.F., Ma, C., Hahn, J.H., Hoque, R., Rothblatt, J., Chalfie, M. (1999) A cytosolic catalase is needed to extend adult lifespan in C. elegans daf-C and clk-1 mutants. *Nature.* **399**,162-166.

(41)   Stohs, S. J., Bagchi, D. (1995) Oxidative mechanisms in the toxicity of metal ions. *Free radical biology & medicine.* **18**,321-356.

(42)   Antunesab, F., Cadenasa, E. (2000) Estimation of H(2)O(2) gradients across biomembranes. *FEBS Lett.* **475**,121-126.

(43)   Cousin, S. P., Hugl, S.R., Wrede, C.E., Kajio, H., Myers, M.G., Rhodes, C.J. (2001) Free fatty acid-induced inhibition of glucose and insulin-like growth factor I-induced deoxyribonucleic acid synthesis in the pancreatic beta-cell line INS-1. *Endocrinology.* **142**,229-240.

(44)   Storz, P., Doppler, H., Wernig, A., Pfizenmaier, K., Muller, G. (1999) Cross-talk mechanisms in the development of insulin resistance of skeletal muscle cells palmitate rather than tumour necrosis factor inhibits insulin-dependent protein kinase B (PKB/Akt stimulation and glucose uptake. *Eur J Biochem.* **266**,17-25.

(45)   Hamel, F. G., Bennett, R.G., Upward, J.L., Duckworth, W.C. (2001) Insulin inhibits peroxisomal fatty acid oxidation in isolated rat hepatocytes. *Endocrinology.* **142**,2702-2706.

(46)   Seedorf, U., Ellinghaus, P., Roch Nofer, J. (2000) Sterol carrier protein-2. *Biochim Biophys Acta.* **1486**,45-54.

(47)   Frolov, A., Cho, T.H., Billheimer, J.T., Schroeder, F. (1996) Sterol carrier protein-2, a new fatty acyl coenzyme A-binding protein. *J Biol Chem.* **271**,31878-31884.

(48)   Dansen, T. B., Westerman, J., Wouters, F.S., Wanders, R.J., van Hoek, A., Gadella, T.W., Wirtz, K.W. (1999) High-affinity binding of very-long-chain fatty acyl-CoA esters to the peroxisomal non-

specific lipid-transfer protein (sterol carrier protein-2). *Biochem J.* **339**,193-199.

(49)   Seedorf, U., Raabe, M., Ellinghaus, P., Kannenberg, F., Fobker, M., Engel, T., Denis, S., Wouters, F., Wirtz, K.W., Wanders, R.J., Maeda, N., Assmann, G. (1998) Defective peroxisomal catabolism of branched fatty acyl coenzyme A in mice lacking the sterol carrier protein-2/sterol carrier protein-x gene function. *Genes Dev.* **12**,1189-1201.

(50)   Wanders, R. J., Denis, S., van Berkel, E., Wouters, F., Wirtz, K.W., Seedorf, U. (1998) Identification of the newly discovered 58 kDa peroxisomal thiolase SCPx as the main thiolase involved in both pristanic acid and trihydroxycholestanoic acid oxidation: implications for peroxisomal beta-oxidation disorders. *J Inherit Metab Dis.* **21**,302-305.

(51)   Wanders, R. J., Denis, S., Wouters, F., Wirtz, K.W., Seedorf, U. (1997) Sterol carrier protein X (SCPx) is a peroxisomal branched-chain beta-ketothiolase specifically reacting with 3-oxo-pristanoyl-CoA: a new, unique role for SCPx in branched-chain fatty acid metabolism in peroxisomes. *Biochem Biophys Res Commun.* **236**,565-569.

(52)   Wouters, F. S., Bastiaens, P.I., Wirtz, K.W., Jovin, T.M. (1998) FRET microscopy demonstrates molecular association of non-specific lipid transfer protein (nsL-TP) with fatty acid oxidation enzymes in peroxisomes. *EMBO J.* **17**,7179-7189.

(53)   Bun-Ya, M., Muro, Y., Niki, T., Kondo, J., Kamiryo, T. (2000) New aspects of Sterol Carrier Protein 2 (non specific lipid-transfer protein) in fusion proteins and in peroxisomes. *Cell Biochem Biophys.* **32**,107-116.

(54)   Frolov, A., Miller, K., Billheimer, J.T., Cho, T.H., Schroeder, F. (1997) Lipid specificity and location of the sterol carrier protein-2 fatty acid-binding site: a fluorescence displacement and energy transfer study. *Lipids.* **32**,1201-1209.

(55)   Wiseman, H., Halliwell, B. (1996) Damage to DNA by reactive oxygen and nitrogen species: role in inflammatory disease and progression to cancer. *Biochem J.* **313**,17-29.

(56)   Yeldandi, A. V., Rao, M.S., Reddy, J.K. (2000) Hydrogen peroxide generation in peroxisome proliferator induced oncogenesis. *Mut Res.* **448**,159-177.

(57)   Ellinghaus, P., Wolfrum, C., Assmann, G., Spener, F., Seedorf, U. (1999) Phytanic acid activates the peroxisome proliferator-activated receptor alpha (PPARalpha) in sterol carrier protein 2-/ sterol carrier protein x-deficient mice. *J Biol Chem.* **274**,2766-2772.

(58)   Kersten, S., Desvergne, B., Wahli, W. (2000) Roles of PPARs in health and disease. *Nature.* **405**,421-424.

(59)   Rao, M. S., Reddy, J.K. (1996) Hepatocarcinogenesis of peroxisome proliferators. *Ann N Y Acad Sci.* **804**,573-587.

(60)   Gossett, R. E., Schroeder, F., Gunn, J.M., Kier, A.B. (1997) Expression of fatty acyl-CoA binding proteins in colon cells: response to butyrate and transformation. *Lipids.* **32**,577-585.

(61)   Lyons, H. T., Kharroubi, A., Wolins, N., Tenner, S., Chanderbhan, R.F., Fiskum, G., Donaldson, R.P. (1991) Elevated cholesterol and decreased sterol carrier protein-2 in peroxisomes from AS-30D hepatoma compared to normal rat liver. *Arch Biochem Biophys.* **285**,238-245.

(62)   Khwaja, A., Rodriguez-Viciana, P., Wennstrom, S., Warne, P.H., Downward, J. (1997) Matrix adhesion and Ras transformation both activate a phosphoinositide 3-OH kinase and protein kinase B/Akt cellular survival pathway. *EMBO J.* **16**,2783-2793.

(63)   Lloyd, R. V., Erickson, L.A., Jin, L., Kulig, E., Qian, X., Cheville, J.C., Scheithauer, B.W. (1999) p27kip1: a multifunctional cyclin-dependent kinase inhibitor with prognostic significance in human cancers. *Am J Pathol.* **154**,313-23.

(64)   Oberley, L. W., Oberley, T.D. (1988) Role of antioxidant enzymes in cell immortalization and transformation. *Mol Cell Biochem.* **84**,147-153.

(65)   Xu, Y., Krishnan, A., Wan, X.S., Majima, H., Yeh, C.C., Ludewig, G., Kasarskis, E.J., St Clair, D.K. (1999) Mutations in the promoter reveal a cause for the reduced expression of the human manganese superoxide dismutase gene in cancer cells. *Oncogene.* **18**,93-102.

Samenvatting voor iedereen.

Samenvatting voor iedereen

In elke cel in het lichaam vinden voortdurend duizenden chemische processen plaats. Deze processen zijn van levensbelang voor de cel en moeten op de juiste manier verlopen. Daarom is er in elke cel een aantal compartimenten (cel-organellen) aanwezig dat gescheiden is van de rest van de cel door een membraan. Op deze manier kan ieder chemisch proces netjes verlopen zonder dat het stoort bij een ander chemisch proces. Je zou de cel kunnen vergelijken met een kok die een meergangen diner aan het koken is. Als hij de chocolade-mousse probeert te maken in dezelfde pan waarin hij de biefstuk aan het bakken is, zullen zijn klanten niet graag bij hem komen eten. De membranen om de cel-organellen (en ook het membraan dat om de hele cel zit) zijn opgebouwd uit vetten en eiwitten. Een van de cel-organellen waar deze chemische processen plaatsvinden is het peroxisoom. In peroxisomen worden onder andere vetzuren afgebroken, cholesterol gemaakt, en galzoutvoorlopers gesynthetiseerd. Deze processen zijn essentieel voor het functioneren van het menselijk lichaam. Patiënten die geen peroxisomen hebben doordat een van de eiwitten die betrokken zijn bij de opbouw van peroxisomen defect is, worden meestal niet ouder dan een jaar. Bij de afbraak van vetten in het peroxisoom wordt waterstofperoxide gemaakt. Dit waterstofperoxide is schadelijk voor de cel (je kunt er niet voor niets je haar mee bleken) en wordt snel afgebroken door het enzym catalase. Toch ontsnapt er wat waterstofperoxide aan het catalase, en dit kan met ijzer-ionen worden omgezet in zeer schadelijke hydroxyl-radicalen. Deze radicalen kunnen schade toebrengen aan eiwitten, onverzadigde vetzuren en DNA. In het laatste geval kan dit leiden tot kanker. Als (meervoudig)-onverzadigde vetzuren beschadigd raken door hydroxyl-radicalen, kunnen de membranen in en om de cel hun integriteit verliezen, waardoor de cel doodgaat. Om te voorkomen dat dit gebeurt heeft de cel een aantal zogenaamde anti-oxidant eiwitten. Deze eiwitten vangen, net als catalase, radicalen weg voordat ze schade aan kunnen richten. De cel kan als het nodig is meer van deze anti-oxidant eiwitten aanmaken.

In dit proefschrift beschrijf ik een aantal studies die in meer of mindere mate te maken hebben met het functioneren van het peroxisoom. In hoofdstuk 2 wordt een overzicht gegeven van processen in het peroxisoom die bijdragen aan productie en afbraak van radicalen als het hydroxyl-radicaal. Hoofdstuk 3, 4 &5 behandelen een nieuwe methode om eigenschappen van peroxisomen in de levende cel te meten. Eiwitten die in de cel worden gemaakt en die een taak hebben in het peroxisoom krijgen een code mee in de aminozuren (de bouwstenen van het eiwit). Je kunt zo'n code een beetje vergelijken met een postcode: als een cel een nieuw eiwit aanmaakt, weet het sorteringssysteem van de cel (het postkantoor) aan de hand van die postcode waar elk eiwit hoort te zitten. De code wordt herkend door een eiwit (de postbode) in het cytoplasma (de vloeistof in de cel tussen de organellen). Dit eiwit brengt het peroxisomale eiwit dan naar het peroxisomale membraan, waarna import plaatsvindt. Bij de nieuwe techniek hebben we gebruik gemaakt van dit natuurlijke importsysteem. We hebben een fluorescent molecuul gekoppeld aan de postcode voor peroxisomen (peroxisomale target sequentie, PTS). Deze fluorescente PTS wordt door de cel vrij gemakkelijk opgenomen, en vervolgens herkend door het sorteringsmechanisme dat normaal peroxisomale eiwitten naar de juiste plek toebrengt (de postbode). Op deze manier kunnen we dus een fluorescent molecuul in het peroxisoom brengen, en dit meten met behulp van geavanceerde fluorescentie-microscopie. Een groot voordeel van deze methode is dat de cellen in leven zijn tijdens de meting. Daardoor krijg je een beter beeld van het functioneren van het peroxisoom. In hoofdstuk 3 wordt beschreven hoe we de pH hebben gemeten in het peroxisoom met behulp

van een fluorescente PTS die van kleur verandert afhankelijk van de pH van de omgeving van deze stof. De pH van het peroxisoom bleek basisch te zijn, wat betekent dat de peroxisomale membraan geen protonen doorlaat (het cytoplasma heeft namelijk een neutrale pH). In dit hoofdstuk wordt ook een patiënt beschreven die geen basische pH in de peroxisomen heeft. Wat hiervan de redenen en directe gevolgen zijn is nog onduidelijk. Hoofdstuk 4 & 5 gaan wat meer in op het gebruik van deze nieuwe techniek voor onderzoek aan peroxisomen.In hoofdstuk 6 wordt een soortgelijke techniek toegepast om andere cel-organellen zoals het Golgi en het endoplasmatisch reticulum met fluorescente signaalsequenties zichtbaar te maken.

Het niet-specifieke lipide transport eiwit (nsLTP), ook sterol-dragend eiwit (SCP2) genoemd, is een peroxisomaal eiwit. Wat SCP2 doet in de peroxisomen is niet precies duidelijk, maar het is wel bekend dat het allerlei vetten en vetzuren kan binden. In hoofdstuk 7 wordt beschreven dat SCP2 vetzuren met lange ketens van 24 koolstofatomen die gebonden zijn aan Co-enzym A zeer goed kan binden. Dit zou kunnen betekenen dat SCP2 deze vetzuren transporteert tussen de eiwitten die de vetzuren afbreken in het peroxisoom. We denken dan ook dat SCP2 een belangrijke rol speelt bij de vetzuur-afbraak.

Om goed te kunnen reageren op de omgeving, heeft een cel aan de buitenkant allerlei receptoren. Als zo een receptor geactiveerd wordt doordat er een stofje aan bindt (het ligand) geeft de receptor aan de binnenkant van de cel een seintje dat er gereageerd moet worden op dat ligand. Zo'n ligand kan bijvoorbeeld insuline zijn, waardoor de cel weet dat er voldoende suiker in het bloed zit. De cel reguleert op deze manier duizenden processen. In hoofdstuk 8 wordt een van de signaalroutes beschreven die een rol speelt bij het beschermen van de cel tegen zuurstofradicalen. Als cellen in rust zijn (dat betekent dat ze niet aan het delen zijn) worden bepaalde transcriptiefactoren actief. Transcriptiefactoren zijn eiwitten die er voor zorgen dat er meer of minder van een bepaald gen wordt afgelezen. De zogenaamde Forkhead transcriptiefactoren blijken bij verhoogde activiteit er voor te zorgen dat de cel meer van de anti-oxidant eiwitten catalase en mangaan-superoxide-dismutase aanmaakt. We hebben laten zien dat de cel dan ook beter beschermd is tegen radicaalschade.

In hoofdstuk 9 komen we weer terug op het SCP2. Het blijkt namelijk dat muizen waarbij het gen dat voor SCP2 codeert is weg gehaal (lever)kanker krijgen. Dit zou kunnen komen door radicaalschade en daarom hebben we gekeken of er meer radicalen in levercellen van deze muizen aanwezig zijn. Dit bleek het geval te zijn. Vervolgens hebben we gekeken of SCP2 een anti-oxidant eiwit zou kunnen zijn. We hebben laten zien dat een fluorescent vetzuur veel langer beschermd is tegen radicalen als het gebonden is aan SCP2. Het is niet ondenkbaar dat SCP2 dan ook als taak heeft de vetzuren in het peroxisoom te beschermen tegen de radicalen die vrij komen bij de vetzuurafbraak. Omdat we in hoofdstuk 8 hadden laten zien dat anti-oxidant eiwitten door de Forkhead transcriptiefactoren gereguleerd worden, hebben we gekeken of dat ook het geval was bij SCP2. Het bleek inderdaad zo te zijn dat als de Forkheads actief zijn, er meer SCP2 in de cel wordt aangemaakt.

In hoofdstuk 10 tenslotte wordt een model gegeven voor de regulatie van anti-oxidant eiwitten via de Forkhead transcriptiefactoren. Er wordt onder andere in gegaan op een mogelijke link tussen vet-afbraak en activiteit van deze Forkheads. Verder wordt een model besproken dat uitlegt hoe SCP2 vetzuren beschermt tegen radicalen. Tenslotte wordt een beeld gegeven van de rol van peroxisomen in het in stand houden van de balans tussen radicalen en anti-oxidant capaciteit in de cel. Er wordt gesuggereerd dat die rol beperkt is tot het binnenhouden van radicalen die in het peroxisoom ontstaan bij vet-afbraak, en dat radicalen die van een andere plek afkomen waarschijnlijk niet door peroxisomen worden weggevangen.

Dankwoord

Dankwoord

En dan nu het hoofdstukje met de meeste clichés, dat toch het meest gelezen wordt van het hele proefschrift (en dat is cliché nummer 1!). Ik weet bij voorbaat dat ik mensen ga vergeten te noemen, maar ja, dat heb ik bij deze dan van tevoren gezegd. De afgelopen vier jaar (vijf met mijn afstudeer-stage meegerekend) op de vakgroep Biochemie van Lipiden zijn omgevlogen. Ik heb het prima naar mijn zin gehad op de dan weer uitgestorven en dan weer door hordes studenten overspoelde westvleugel op de zesde etage van het Kruyt. Ik wil graag een aantal mensen bedanken die in meer of mindere mate hebben bijgedragen aan het tot stand komen van dit proefschrift. Allereerst wil ik mijn co-promotor bedanken. Eward, bedankt voor je begeleiding de eerste drie jaar van mijn promotie. Je enthousiasme was altijd erg aanstekelijk. Onder het motto 'een goed idee is het halve artikel' hebben we samen aardig wat voor elkaar gekregen. Ik zou graag aan dat motto toe willen voegen: 'een goede controle is de andere helft'. Erg jammer dat je hebt gekozen voor het bedrijfsleven. Ik denk dat de vakgroep daardoor een flinke klap heeft gehad. Ik hoop dat je het naar je zin hebt in Duitsland, en veel geluk met Andrea, Leonie en Gustav. En nog bedankt voor je compliment toen je afscheid nam. Mijn promotor, Karel Wirtz, wil ik bedanken voor een aantal dingen. Ten eerste voor de vrijheid die ik heb gekregen om alles te proberen waar een beetje muziek in leek te zitten. Mede daardoor, denk ik, zijn hoofdstuk 8 & 9 tot stand gekomen. Ten tweede voor het geduld dat je met me gehad hebt bij het samen doorlezen van manuscripten. Ik ben geloof ik niet zo goed in het verbergen van ongeduldigheid. Ten derde voor alle congressen (2x Spetses!) waar jij altijd wel ergens een beurs voor wist te vinden. Ronald Wanders, jou wil ik bedanken omdat je altijd veel interesse toonde in mijn onderzoek, en altijd cellen en chemicaliën ter beschikking stelde. Ik vond het altijd erg prettig om bij jou op de vakgroep in het AMC langs te gaan, omdat ik dan vaak weer met nieuwe ideeën terugkwam.

De studenten die ik tijdens mijn promotie begeleid heb: bedankt voor jullie hulp en gezelligheid! Siestke, je was mijn eerste studente, en inmiddels ben je zelf al bijna klaar met je promotie. Jammer dat we nooit meer iets gedaan hebben met de data van de ALS patiënten. Dat was best veel werk met al die Bligh & Dyers. Ik wil wel nog een keer revanche met tennis, en dan spring ik niet meer over het net. Lonneke, ook jij bent inmiddels al aardig op weg met je eigen promotie. Helaas liep het project met de peroxisomen in rattenlongen wat minder rooskleurig dan gehoopt. Elke keer weer die infecties in de cellen, maar je gaf het niet op. Marco, bedankt voor al die probes die je hebt gemaakt... nu weten we eindelijk hoe het moet. Hardstikke goed dat je door die zeven rondes bent gekomen bij Unilever, en ik hoop dat je het leuk blijft vinden. Ook bedankt voor de gezelligheid buiten het lab: in de kroeg, in tivoli of op de nodige feestjes. Nannette (zie ook verderop in dit hoofdstuk), toen je begon op de vakgroep had je al na twee weken een EYFP-PTS1 construct voor elkaar en werd je al gauw de 'cloning-queen'. Helaas voor jou kon je ook goed blotten en dat heb je dan ook tot in den treure gedaan. Bedankt voor je hulp op het lab, ik hoop dat we nog tijd hebben om een artikeltje te schrijven van jouw data, en natuurlijk bedankt voor de peroxisoom foto op de voorkant, en het nakijken op spelfouten.

De mensen van buiten het lab met wie ik samen heb gewerkt. Udo Seedorf: Dear Udo, thank you very much for your help the last four years. Your knock-out mouse data have become a quite important part of this thesis, and I'm very happy that you let me use them. I would also like to thank you for the discussions by phone and e-mail and of course in

Utrecht. I would also like to thank Johannes Wiekowski, from Udo Seedorfs group. Johannes, although we never met, thank you for the data! Carlo van Roermund: Carlo, we hebben aardig wat uurtjes achter de confocale doorgebracht om de pH van gist-peroxisomen te meten, maar zonder succes. Tegen de tijd dat ik dit proefschrift verdedig hoop ik van je gehoord te hebben wat de FACS data opgeleverd hebben! Geert Kops: Mr G! echt heel tof dat de wilde plannen die we raaskalden na teveel zon, bier en ouzo uiteindelijk de hoofdstukken 8 & 9 van dit proefschrift (en tevens een hoofdstuk van jouw proefschrift) zijn geworden. Op die manier zou ik altijd wel wetenschap willen bedrijven. Nu nog even zorgen dat een of ander blad de boel ook nog publiceert, en dan is het feest helemaal compleet. Laten we daar in California fijn mee doorgaan. Ook de andere mensen op jouw lab waar ik mee te maken had: Boudewijn, Rene, Hans, bedankt voor de samenwerking! Jorrit, Marieke, Nancy en al die andere kamergenoten van Geert, bedankt voor het 3 maal daags de telefoon opnemen en het 1000 x Geert zoeken. Dorus Gadella: bedankt voor je hulp met de tijdopgeloste fluorescentie-metingen van hoofdstuk 7!

De collega's: Dennis, bedankt voor de gezelligheid als huisgenoot, congresgenoot (Israel en Spetses!) en kamergenoot, en natuurlijk als fietsmaatje op onze barre tocht door het oververhitte Griekse en Italiaanse binnenland. Voor jou duurt het ook allemaal niet zo lang meer, succes met de laatste loodjes. Arjan, we hebben elkaar aardig lopen dollen af en toe, en dat heb ik altijd zeer op prijs gesteld. Ik hoop dat je het naar je zin hebt in Nijmegen. Bedankt ook voor de diverse gebrande CDs! Ook succes met het lay-outen van je proefschrift. Claudia, bedankt voor alle hulp met protocolletjes voor het DNA werk, en de gezelligheid op de AiO kamer, en natuurlijk de Bouble Trouble en Maelstrom competitie. Jan W, je maakte altijd tijd om even een meting voor me te doen, en had altijd wel een waardevol advies, niet alleen over werk, maar over van alles en nog wat. Bedankt daarvoor, en doe het rustig aan! Rineke, succes in Canada. Misschien nog een keer de Amstelgold? Greg, je hebt geloof ik iedereen gemaild de laatste tijd behalve mij! (haha) Ik hoop dat je weer een beetje de oude bent en binnenkort weer aan de slag kunt. Barend, wat was ik altijd trots als ik 100 km in jouw wiel kon blijven. En wat waren die overige kilometers altijd zwaar als beek dat ik weer te lang achter je aan had geprobeerd te fietsen. Het tafeltennis-eskader: Ben (ideale dubbel-partner!) Albert (sla's als een vent), Yvette, Bahram (laatste), Martijn, Wim, Arjen, Arjan, en al die anderen die wel eens tegen het balletje mepten in de pauze: bedankt voor de ontspanning! De rest van de collega's: Diana, Dick, Dimitri, Erik den H., Floortje, Fred, Fridolin, Gerry, Grzegorz, Hester, Jan B, Jos, Meta, Ton, Wouter B, bedankt voor de gezelligheid op het lab. Alle studenten die op west 6 hebben gewerkt (voor zover ik die allemaal nog weet)... Bas (Kato), Ton, Marten, Taco(infiltracie), Lydia, Ilse, Susanne (bacterial girl), Ginette, Victor (denk om de clue), Wouter, Ruben, Hanneke, Selma, Martha (doet je netwerk het nog?), Jolein (weet je al waar je AiO wordt?) Loesje (Der Jan wint misschien wel dit jaar!).

Mensen op Noord, Oost en Zuid 6: succes verder! Iban, Lenia and Maria, thank you for creating a Southern European atmosphere in Utrecht. Op de vijfde etage, Mika(cool down, you hyperactive fool! have fun in Heidelberg!), Petra, Wendy, Elsa, Renate, Paul vB&H, Robert, Cees (volgend jaar weer 255 km?) en al die andere mensen waarmee je altijd als laatste overbleef in Lunteren of op AiO avonden.

En verder Michael Schrader, thank you for our peroxisome discussions, arranging the trip to Marburg and the company in York and Utrecht! Fred Wouters, bedankt voor de introductie op de vakgroep, en voor de e-mails over van alles en nog wat. Op het AMC: Sacha Ferdinandusse, Simone Denis, Petra Mooijer, en al die anderen die mij de spullen

gaven die Ronald me beloofde. Op het Hubrecht: Willem & Fons, bedankt voor al jullie hulp bij het werken met de confocale. Bij diergeneeskunde: Coos: voor de hulp bij de begeleiding van Lonneke. Bart: voor de tips over microscopie. Frits: voor de gezelligheid in Kopenhagen.

Dan de mensen waar ik veel aan heb gehad buiten het lab. Allereerst de mensen van de karate-club, met name Frans, Bauke & Hans en al die anderen die me fijn hebben afgemat al die uren in de dojo: bedankt voor alle blauwe plekken die m'n aandacht even afleidden van dit proefschrift! Van het kook-clubje: Annelies, Susan en Cindy: bedankt voor al die avonden met nieuwe gerechten, en de nachten in Tivoli. Coolacanth, het best-bewaarde jazz-funk-pop-rock geheim van Utrecht en omstreken: Steven, Gijs en Rikkert, echt zeer zeer cool om met jullie samen te jammen! laten we daar zo lang mogelijk mee doorgaan. Ook bedankt voor jullie vriendschap natuurlijk. De hele rits mensen met wie ik meer of minder contact had, en die ik vaak in de kroeg tegenkwam: Geert H, Helene, Jorrit, Esther, Roel, Hanneke, Ilse, Paula, Frederic, Jurjen, Jelka, MJ, Roos en al die anderen. Annemieke, bedankt voor de tijd samen. Bart Borghuis: heel erg bedankt dat ik je kamer en computer mag gebruiken om onder andere dit dankwoord te schrijven en het proefschrift te lay-outen. Die brand had bijna roet in het eten gegooid.

Joost J, bedankt voor een stabiele vriendschap sinds de brugklas, en natuurlijk de trip naar Frankrijk (insane in the membrane!). MN, bedankt voor alle anagrammen, het reisgezelschap naar Helsinki en de jaren als huisgenoot. Martijn de K., tof dat je m'n paranymph wilt zijn. Bedankt voor al die jaren vriendschap, de trip in de eend naar Rome, goeie gesprekken enzovoorts. Maarten, met jou heb ik (vrijwel) alles gedeeld de laatste 7-8 jaar. Echt geweldig dat ik altijd op je kan rekenen voor goeie gesprekken, maar ook voor flauwe woordgrappen, argeloze slemp-partijen, onbezonnen acties, (ongevraagd) advies, en eigenlijk alles dus. Ik vind het fijn dat je mijn paranymph wilt zijn! Bedankt voor alles!

Mijn ouders en aanhang: Paula & Wiebe, Koos & Antoinette: bedankt voor al jullie steun en interesse in wat ik deed/doe. Ik ben heel blij dat jullie altijd achter me stonden. Bedankt voor alles. Mijn broers, ooms & tantes (Tjits & Rob en Diny & Wino, bedankt voor alle e-mails!), neven & nichten en aanverwante artikelen: bedankt!

Tenslotte dan: Lieve Nannette, bedankt voor de geweldige tijd de laatste maanden! Zonder jou was ik vast af en toe vergeten dat het schrijven van een proefschrift slechts bijzaak is.

Curriculum Vitae

Tobias Dansen werd geboren op 6 november 1973 in het Dijkzigt ziekenhuis in Rotterdam. In 1992 werd het VWO-diploma behaald aan het Nederrijn College in Arnhem. In datzelfde jaar werd begonnen met de studie Scheikunde aan de Universiteit Utrecht. Het propaedeutisch examen werd afgelegd in 1994. Het plan om de bovenbouw-studie milieukunde te gaan doen was inmiddels van de baan en er werd gekozen voor de richting biochemie. Bij de faculteit Biologie werd een onderzoeksstage van 9 maanden doorlopen bij de vakgroep Moleculaire Celbiologie onder begeleiding van Dr. Sanne van Delft en Dr. Paul van Bergen en Henegouwen. Bij de vakgroep Biochemie van Lipiden werd het onderzoeksjaar afgerond onder begeleiding van Dr. Fred Wouters en Prof. Dr. Karel Wirtz. In augustus 1997 werd het doctoraal diploma Scheikunde behaald. Het promotie-onderzoek dat in dit proefschrift wordt behandeld is uitgevoerd van 1 september 1997 tot 1 september 2001 onder begeleiding van Dr. Eward Pap en Prof. Dr. Karel Wirtz bij de vakgroep Biochemie van Lipiden van de faculteit Scheikunde, Universiteit Utrecht .

Publications

Dansen, T. B., Westerman, J., Wouters, F.S., Wanders, R.J.A., van Hoek, A., Gadella, T.W.J., Wirtz, K.W.A. (1999) High-affinity binding of very-long-chain fatty acyl-CoA esters to the peroxisomal non-specific lipid-transfer protein (sterol carrier protein-2). *Biochem J.* **339**,193-199.

Biermann, J., Gootjes, J., Humbel, B.M., Dansen, T.B., Wanders, R.J.A., van den Bosch, H. (1999) Immunological analyses of alkyl-dihydroxyacetone-phosphate synthase in human peroxisomal disorders. *Eur J Cell Biol.* **78**,339-348.

Dansen, T. B., Wirtz, K.W.A., Wanders, R.J.A., Pap, E.H.W. (2000) Peroxisomes in human fibroblasts have a basic pH. *Nat Cell Biol.* **2**,51-53.

Pap, E. H.W., Dansen, T.B., Wirtz, K.W.A. (2001) Peptide-based targeting of fluorophores to peroxisomes in living cells. *Trends Cell Biol.* **11**,10-12.

Pap, E. H.W., Dansen, T.B., van Summeren, R., Wirtz, K.W.A (2001) Peptide-based targeting of fluorophores to organelles in living cells. *Exp Cell Res.* **265**,288-293.

Dansen, T. B., Pap, E.H.W., Wanders, R.J.A., Wirtz, K.W.A. (2001) Targeted fluorescent probes in peroxisome function. *Histochem J.* **33**,65-69.

Dansen, T. B., Wirtz, K.W.A. (2001) The peroxisome in oxidative stress. *Accepted for publication in IUBMB Life.*

Dansen, T. B., Kops, G.J.P.L., Wiekowski, J., Seedorf, U., Jelluma, N., Bos, J.L., Burgering, B.M.T., Wirtz, K.W.A. (2001) Sterol carrier protein protects against lipid peroxidation and is regulated by the Forkhead transcription factor FKHR-L1. *To be submitted.*

Kops, G. J. P. L., Dansen, T.B., Wirtz, K.W.A., Coffer, P.J., Huang, T.T., Bos, J.L., Medema, R.H., Burgering, B.M.T. (2001) Coupling of cell-cycle regulation and resistance to oxidative damage by DAF-16 like Forkhead transcription factors. *To be Submitted.*

Steenbergen, R. H. G., Struik, M.L., Bunte, H., Dansen, T.B., Koster, A.S., Post, J.A., Verkleij, A.J., Op den Kamp, J.A.F. (2001) Lipid peroxidation, ATP, pHi and intracellular calcium during PE redistribution in cardiomyocytes.A comparison to ischemia. *submitted.*

Wirtz K.W.A, Dansen T.B., Wouters F.S., Westerman J., Bastiaens P.I., Wanders R.J., Seedorf U., Jovin, T.M., (1999)Non-specific lipid transfer protein (sterol carrier protein 2) and fatty acid β-oxidation). In:" *Molecular Mechanisms/ Transcellular Signalling*" (J.P.Thiery ed.); **309,** 332-338. IOS Press Amsterdam.